Cape Peninsula
University of Technology

THERMODYNAMIC STUDY OF THE BIODEGRADATION OF CYANIDE IN WASTEWATER

by

ENOCH AKINBIYI AKINPELU

Thesis submitted in fulfilment of the requirements for the degree

Doctor of Engineering: Chemical Engineering

in the Faculty of Engineering

at the

Cape Peninsula University of Technology
Cape Town, South Africa

May 2017

Supervisors

1. Prof. Seteno Karabo Obed. Ntwampe (EngD; HDHET*)
   Associate Professor and Head of Bioresource Engineering Research Group (*BioERG*)
   Head of Department: Biotechnology and Consumer Sciences
   Faculty of Applied Sciences
   Cape Peninsula University of Technology
   Cape Town

2. Prof. Tunde Victor Ojumu (PhD)
   Associate Professor and Head of Programme: Chemical Engineering
   Department of Chemical Engineering
   Faculty of Engineering
   Cape Peninsula University of Technology
   Cape Town

DECLARATION

I, **ENOCH AKINBIYI AKINPELU**, know the meaning of plagiarism and declare that all the work in this thesis, save for that which is properly acknowledged, is my own unaided work, both in concept and execution, apart from the normal guidance of my supervisors. This thesis represents my own opinions and not necessarily those of the Cape Peninsula University of Technology.

Furthermore, the thesis has not been submitted for any degree or examination in any other university.

The intellectual concepts, theories, methodologies and mathematical derivations, including model developments used in this thesis and published in various scientific journals were derived solely by the candidate and first author of the published manuscripts. Where appropriate, the intellectual property of others was acknowledged by using appropriate references.

Enoch Akinbiyi. Akinpelu — **Signed**

May 1st, 2017 — **Date**

ABSTRACT

The high rate of industrialisation in most developing countries has brought about challenges of wastewater management especially in the mineral processing industry. Cyanide has been used in base metal extraction processes due to its lixiviant properties thus, its presence in wastewater generated is inevitable. Furthermore, partial and/or the use of unsuitable treatment methods for such wastewater is a potential hazard to both human and the environment. There are several reports on biotechnological treatments of cyanide containing wastewater but few mineral processing industries have adopted this approach. Hence, the thermodynamic study of biodegradation of cyanide containing wastewater was undertaken. The primary aim of this study was to explore the application of bioenergetic models and biological stoichiometry to determine the functionality and thermodynamic requirements for cyanide degrading isolate (*Fusarium oxysporum* EKT01/02), grown exclusively on *Beta vulgaris,* for a system designed for the bioremediation of cyanidation wastewater. Chapter 2 reviews some of the applicable thermodynamic parameters such as enthalpy, entropy, heat of combustion, heat capacity, Gibbs energy, including stoichiometry models in relation to their applicability for microbial proliferation in cyanidation wastewater. The chapter places emphasis on the application of agro-industrial waste as a suitable replacement for refined carbon sources for microbial proliferation in bioremediation systems because such systems are environmentally benign. The choice of using agro-industrial waste is due to organic waste properties, i.e. agro-industrial waste is rich in nutrients and is generated in large quantities. Chapter 3 presents the materials and various standardised methods used to address the research gaps identified in chapter 2.

For an organism to degrade free cyanide in wastewater, it must be able to survive and perform its primary function in the presence of such a toxicant. Chapter 4 exemplifies both molecular and biochemical characteristics of *Fusarium oxysporum* EKT01/02 isolated from the rhizosphere of *Zea mays* contaminated with a cyanide based pesticide. The molecular analyses confirmed the fungal isolate to be *Fusarium oxysporum* EKT01/02 and the nucleotide sequence of the isolates were deposited with National Centre for Biotechnology Information (NCBI) with accession numbers KU985430 and KU985431. The biochemical analyses revealed a wide substrate utilisation mechanism of the isolate dominated by aminopeptidase including nitrate assimilation capabilities. A preliminary investigation showed free cyanide degradation efficiency of 77.6% (100 mg CN^-/L) after 5 days by the isolate. The excess production of extracellular polymeric substance (EPS) was attributed to the isolates' strive to protect itself from cyanide toxicity. The limiting substrate concentration of the isolate was found to be 300 mg/L for both refined carbon (glucose) and agro-industrial waste (*Beta vulgaris*). Furthermore, different operating conditions – temperature, pH and agro-industrial waste concentration were optimised for optimum free cyanide biodegradation using response surface

methodology (RSM). The optimum conditions using numerical optimisation techniques were found to be at a temperature of 26.50 ˚C, pH 10.77 and agro-industrial waste concentration of 310.89 mg/L (Chapter 5).

Furthermore, aerobic growth of *Fusarium oxysporum* EKT01/02 in synthetic gold mine wastewater under different substrates was examined using biological stoichiometry and thermodynamic models in batch systems. On average, the dry biomass had a molecular weight of 27.74 g/C-mol, with an elemental formula of $CH_{1.788}N_{0.062}O_{0.818}$, including a degree of reduction of 3.966. The microbial growth model indicated the highest biomass yield of 0.69 g dry cell/g substrate in *Beta vulgaris* with ammonia (BA) than in both glucose with ammonia (GA) – 0.39 g dry cell/g substrate and *Beta vulgaris* with cyanide (BCN) cultures – 0.38 g dry cell/g substrate. The bioremediation processes were found to be both exothermic and spontaneous with mean values for thermodynamic parameters for *F. oxysporum* growth in cyanidation wastewater being; -379.34 kJ/C-mol for ΔH_f^{cell}, -385.16 kJ/C-mol for ΔH_{RX}^o, -376.22 kJ/C-mol for ΔG_{RX}^o and -0.03 kJ/C-mol for ΔS_{RX}^o.

Additionally, the total Gibbs energy dissipated increased steadily over time and the metabolic functionality of the *F. oxysporum* EKT01/02 was not adversely affected by the cyanidation wastewater as shown by the unitary respiratory quotient for all substrates used (Chapter 6). The heat capacity of the lyophilised mycelia of *F. oxsporum* EKT01/02 was measured on a modulated differential scanning calorimeter. The heat capacity was found to be 0.572, 0.978 and 0.772 J K^{-1} g^{-1} with corresponding changes in entropy of 0.384, 0.792 and 0.547 J K^{-1} g^{-1} for fungal biomass grown on *B. vulgaris* with ammonia (BA), glucose with ammonia (GA) and *B. vulgaris* with cyanide (BCN), respectively at 298.15 K. There was no glass transition observed on the total heat flow profiles including the non-reversible heat flow profiles except on the reversible heat flow in the endothermic direction – Chapter 7.

This study showed that the exclusive utilisation of agro-industrial waste as a sole carbon and/or energy source for bioremediation of cyanidation wastewater is as feasible as when refined carbon sources are used. The bioenergetics parameters support this observation especially at optimum process conditions.

Keywords: Agro-industrial waste; *Beta vulgaris*; Biodegradation; Bioenergetics; Cyanide; *Fusarium oxysporum*; Stoichiometry; Thermodynamics

ACKNOWLEDGEMENTS

I wish to thank:

- God for making this vision a reality, though it tarried, I waited for it and it came to pass. To Him alone be all the glory,
- My supervisors, Prof. S. K. O. Ntwampe and Prof. T. V. Ojumu for their assistance, guidance and technical input throughout the duration of this study,
- My wife and children, for their love, support and holding forth in my absence,
- My parents and the entire Akinpelu family, for their encouragement and support towards this vision,
- My friends at home and abroad, who have contributed in different ways to this success,
- The technical staff of the Department of Chemical Engineering – particularly Hannelene Small and Alwyn Bester, for their support during the experimental set-up,
- The technical staff at the Agrifood station, particularly Ndumiso Mshicileli and Rose Gwanpu for their support during experimental set-up for biochemical tests,
- Staff and fellow students of the Bioresource Engineering Research Group (Bio*ERG*) for their support,
- Cape Peninsula University of Technology, University Research Fund (URF) for their financial support, without which this project would not have been possible.

Enoch A. Akinpelu

May, 2017

DEDICATION

To my Treasure – Oladunni

And our lovely children –

Akinwale and Akintayo

RESEARCH OUTPUT

The following research outputs represent candidate's contribution to scientific knowledge and development during his doctoral candidacy (2015-2017):

Publications

Published

Akinpelu, E. A., Ntwampe, S. K. O., Mekuto, L. & Itoba Tombo, E. F. Optimizing the bioremediation of free cyanide containing wastewater by *Fusarium oxysporum* grown on beetroot waste using response surface methodology. *In:* Ao, S. I., Douglas, C. & Grundfest, W. S., eds. Lecture Notes in Engineering and Computer Science: Proceedings of the World Congress on Engineering and Computer Science, ISBN: 987-988-14048-2-4, 19-21 October 2016 San Francisco, USA. Newswood Limited, 664-670.

Akinpelu, E. A., Adetunji, A. T., Ntwampe, S. K. O., Nchu, F. & Mekuto, L. 2017. Biochemical characteristics of a free cyanide and total nitrogen assimilating Fusarium oxysporum EKT01/02 isolate from cyanide contaminated soil. *Data in Brief,* 14, 84-87 DOI: 10.1016/j.dib.2017.07.023

Accepted

Akinpelu, E.A., Ntwampe, S.K.O & Bing-Hung Chen. Biological stoichiometry and bioenergetics of *Fusarium oxysporum* EKT01/02 proliferation using different substrates in cyanidation wastewater. *The Canadian Journal of Chemical Engineering* DOI:10.1002/cjce.22935

Submitted

Akinpelu, E.A., Adetunji, A.T, Ntwampe, S.K.O, Nchu, F & Mekuto, L. Characterisation of *Fusarium oxysporum* EKT01/02 Isolate associated with cyanide biodegradation system. Submitted to *Biology* (Manuscript ID: biology-216360)

Akinpelu, E.A., Ntwampe, S.K.O, Mekuto, L & Itoba-Tombo, E.F. Thermodynamics of microbial growth in cyanidation wastewater. Submitted to *Environmental Science and Pollution Research*. (Manuscript ID: ESPR-D-17-00974).

Akinpelu, E.A., Ntwampe, S.K.O, Mekuto, L & Ojumu T.V. Heat capacity measurements of lyophilised biomass of *Fusarium oxysporum* associated with cyanidation wastewater from temperatures 130 to 305 K. Submitted to *Chemical Engineering and Technology* (Manuscript ID: ceat.201700359)

Akinpelu, E.A., Ntwampe, S.K.O., Mekuto, L & Ojumu, T.V. Thermodynamic data of Fusarium oxysporum using different substrates in gold mine wastewater. Submitted to *Data* (Manuscript ID: data-214190)

TABLE OF CONTENTS

LIST OF FIGURES

LIST OF TABLES

LIST OF SYMBOLS

Nomenclature

Symbol	Description	Units
α_o	Constant	------
α_i	Linear coefficient	-------
α_{ii}	Quadratic coefficient	--------
α_{ij}	Interactive coefficient	--------
CN_B^-	Biodegraded cyanide	mg/L
CN_R^-	Residual cyanide	mg/L
CN_S^-	Initial cyanide	mg/L
CN_V^-	Volatilized cyanide	mg/L
CN_{IC}^-	Initial cyanide in control	mg/L
CN_{FC}^-	Final cyanide in control	mg/L
R^2	Goodness of model fit	------
X_i	Coded independent variables	Units not defined
Y	Response variable	Units not defined
$Y_{i/j}$	Yield of *i* versus *j*	C-mol/C-mol
$f_{i=O,C,H,N,ash}$	Percent fraction of constituent in dry biomass	------
A	Electron acceptor	-------
S	Energy source, electron donor	---------
ND	Nitrogen donor	--------
X	Dry biomass	mg
P	Reduced electron acceptor	------
M_W	Molecular weight	g/C-mol
m	Sample mass	mg
γ_i	Degree of reduction of *i*th compound	-------
ΔH_f^{cell}	Enthalpy of formation of biomass	kJ/C-mol
ΔH_{rx}^o	Heat of reaction of formation of a unit C-mole of dry biomass	kJ/C-mol
ΔH	Change in enthalpy	kJ/C-mol
C_p	Heat capacity	kJ K^{-1} g^{-1}
T_g	Transition temperature	K
$\delta Q/dt$	Heat flow rate	kJ/s
dT/dt	Heating rate	K/s
S	Entropy	kJ C-mol^{-1} K^{-1}

$S_{T_{low}}$	Absolute entropy at low temperature	kJ K^{-1} g^{-1}
a	Empirical constant	--------
ΔG^{o}_{cat}	Standard Gibbs energy of catabolic reaction	kJ/C-mol
ΔG^{o}_{ana}	Standard Gibbs energy of anabolic reaction	kJ/C-mol
ΔG^{o}_{rx}	Standard Gibbs energy of overall growth reaction per unit C-mole of dry biomass	kJ/C-mol
ΔG	Free energy change	kJ/C-mol
ΔS	Change in entropy	kJ C-mol^{-1} K^{-1}
n	Number of moles	mol

Greek symbols

Symbol	Description	Units
ε	Error	Units not defined

Subscripts

Symbol	Description	Units
A	Temperature	° C -
B	pH	
C	Substrate concentration	mg/L

GLOSSARY

BA	*Beta vulgaris* with Ammonia
BCN	*Beta vulgaris* with cyanide
CCD	Central composite design
EPS	Extracellular Polymeric Substances
F-CN	Free cyanide
GAN	GenBank Accession number
GA	Glucose with ammonia
HCN	Hydrogen cyanide
ICMC	International Cyanide Management Code
ICMI	International Cyanide Management Institute
KCN	Potassium cyanide
NaCN	Sodium Cyanide
NH_4^+-N	Ammonium-nitrogen
NO_3^--N	Nitrate-nitrogen
PCR	Polymerase chain reaction
RSM	Response surface methodology

CHAPTER 1

INTRODUCTION

CHAPTER 1
INTRODUCTION

1.1 Introduction

Thermodynamics has been identified as an instrument in physical science for determining feasibility of any reaction and conditions under which the reaction can occur. However, in bioprocessing, thermodynamic analysis is rarely applied (von Stockar et al. 2006). This is most likely due to the complex nature of biological processes characterised by diverse phases and numerous driving forces, including a large number of physical, chemical and biological processes occurring under rigorously irreversible conditions (von Stockar & van der Wielen 2003). In biochemical engineering, thermodynamic analysis can be used to predict feasibility of metabolic reactions and the conditions under which they can occur, including to provide an opportunity for a rough estimate of key parameters of the cultures, thus address the economic viability of the process (Duboc et al. 1999a, Liu et al. 2007, Heijnen 2010, von Stockar 2010). The thermodynamic predictions based on preliminary experimental results could serve as a benchmark for the improvement of process performance both on a laboratory scale and industrial scale.

A biodegradation system can be said to be a thermodynamic process since there is energetic changes within the system associated with changes in temperature, biological stoichiometric parameters and metabolic biomass functions, including metabolic heat generation and other kind of heat transfer (Avalos Ramirez et al. 2008, Finley et al. 2009, Yeddou et al. 2010). Arrhenius model's prediction has been used by several researchers to describe the microbial growth rate but this has been limited to a narrow temperature range under normal physiological range, for the estimation of activation energy for microbial proliferation (Parolini & Carcano 2010, Liu et al. 2015, Akinpelu et al. 2016). Cellular metabolic processes use different pathways in response to varying environmental conditions for nutrient processing, energy accession and conversion. These pathways are known as anabolic and catabolic pathways. The catabolic pathway is a process that breakdown molecules into smaller components. Cellular respiration takes place via the catabolic pathway whereby energy is released and converted into a useful form –adenosine triphosphate (ATP), to drive the anabolism process. The anabolic pathway is an energy demanding process, responsible for the synthesis of complex molecules from monomers, which are used to form cellular structures (Russell & Cook 1995, Heijnen 2002, Parolini & Carcano 2010). The energy released through the hydrolysis of ATP, known as the Gibbs energy, is believed to be the driving force for microbial growth processes.

The performance of microorganisms as it relates to growth and bioprocessing can be understood via thermodynamic analysis. Different thermodynamic models have been developed for microbial growth to explain the relationship between Gibbs energy dissipation as the driving force for growth and the biomass yield (von Stockar et al. 2006). Generally, Gibbs energy dissipation per C-mol of biomass grown is used to achieve a balance between growth efficiency and metabolic rates, such that observed biomass yields can be elaborated and predicted (von Stockar et al. 2008). Besides, other kinetic growth parameters such as the specific growth rate and cellular maintenance coefficient have been analysed thermodynamically using the Herbert-Pirt relation (Tijhuis et al. 1993, Heijnen 2002, Heijnen 2010, Braissant et al. 2013). In addition, due to the irreversible nature of microbial growth which occurs spontaneously, a non-equilibrium thermodynamical approach has been used to elucidate the energy conservation and conversion process for well-defined microbial systems (Larsson & Gustafsson 1999, Demirel & Sandler 2002).

Presently, thermodynamic analysis of microbial systems in which microorganisms such as bacteria (*Lactococcus lactis* and *Escherichia coli*) (Duboc et al. 1999a, Kabanova et al. 2009), algae (Rocan BUV 2 and *Scenedesmus obtusiusculus*) (Duboc et al. 1999a), yeast (*Saccharomyces cerevisiae* and *Candida utilis*) (Battley 1998, von Stockar & Liu 1999) and fungi (*Penicillium roqueforti* and *P. camemberti*) (Wadsö et al. 2004), have been carried out successfully using a direct and an indirect approach. All these studies employed refined carbon sources such as glucose, ethanol and acetate, among others, for microbial growth assessment under both aerobic and anaerobic conditions using thermodynamic analysis (Battley 1998, Xiao & VanBriesen 2006, Xiao & VanBriesen 2008). However, it is unclear as to what extent the use of renewable sources as a carbon source can affect a thermodynamic analysis study, particularly that of an environmental engineering nature, such as wastewater treatment focusing on a highly toxic compound.

Likewise, various studies have also reported on thermodynamics for microbial growth in an ideal environment, without accounting for inhibition or competing substrate utilisation due to the complexity associated with yield estimation including the laborious extensive experimental work required for such a quantification (VanBriesen 2001, McCarty 2007). Therefore, a need for an empirical approach in biomass yield prediction, computation of stoichiometric equation for the growth process, estimation of free energy, enthalpy, change in entropy and kinetic growth parameters using thermodynamic analysis is required in biodegradation processes involving an inhibitor such as cyanide in order to determine the feasibility of such a process at an industrial scale.

1.2 Research questions

In order to achieve the aims of this research, it is important to provide answers to the following questions:

- Does *Beta vulgaris* agro-industrial waste has adequate nutrients for microbial growth to support free cyanide biodegradation?
- Which microorganism(s) can utilise *Beta vulgaris* agro-industrial waste and free cyanide sequentially without supplementation with refined nutrients?
- What is the effect of process parameters (temperature, pH, and agro-waste concentration) on free cyanide biodegradation?
- What is the mechanism of microbial growth thermodynamics using *Beta vulgaris* agro-industrial waste?
- What is the effect of *Beta vulgaris* agro-industrial waste on bioenergetics parameters (enthalpy, entropy and free energy) of a microorganism used for the free cyanide biodegradation process?

1.3 General aim of the study

Sequel to previous research findings and the challenges mentioned above, the aim of this research was to isolate and characterise a cyanide tolerant microorganism capable of utilising *Beta vulgaris* agro-industrial waste, optimise the operating conditions for free cyanide biodegradation, and determine the feasibility of this process using thermodynamic tools in a bioenergetics study whereby a suitable microorganism(s) will be used for the bioremediation of synthetic gold mine wastewater containing cyanide.

1.4 Specific objectives

1. To isolate and characterise a cyanide tolerant microorganism, capable of utilising *Beta vulgaris* agro-industrial waste as a sole carbon source for growth and degradation of free cyanide,
2. To optimize the conditions for maximum free cyanide biodegradation by studying the effects of process parameters such as temperature, pH and agro-waste concentration using response surface methodology,
3. To study the mechanism of microbial growth thermodynamics in *Beta vulgaris* agro-industrial waste, ascertaining that the kinetics of the process are studied in detail using

existing models and developed stoichiometric growth models which must be verified using an enthalpy balance,

4. To study and/or quantify heat capacity and entropy of lyophilised biomass of the isolated microorganism at both low and optimum temperatures, for complete thermodynamic property of the isolate.

1.5 Delineation of the study

The following were not investigated in this study:

- Economic evaluation of the feasibility study.
- Scale up of the experiments to a large scale.
- Enzyme identification and activities within the biodegradation process.
- Environmental impact of free cyanide.

PREFACE TO THE THESIS

The research work presented in this thesis was conducted at the Bioresource Engineering Research Group (*BioERG*) Laboratory, Department of Biotechnology and Chemical Engineering Department –all on the Cape Town campus of the Cape Peninsula University of Technology, South Africa.
The thesis is made-up of seven chapters.

Chapter 1 is a brief introduction to the thesis, research questions and the objectives of the study, including a preface to the thesis.

Chapter 2 presents a review on the feasibility of microbial growth in environmental engineering applications using thermodynamic tools. It highlights some of the constraints of microbial growth in polluted environments and the likely solution to these challenges.

Chapter 3 highlights the materials, methods, and procedures used for experimentation including some result analyses techniques.

Chapter 4 contains the isolation, molecular characterisation and biochemical properties of the fungal isolate. It further analyses the fungal isolate using bioinformatic methods, and finally examines the suitability of the isolate for a heavy metals and free cyanide biodegradation system.

Chapter 5 elucidates the substrate utilisation and performance of the isolate on both refined carbon (Glucose) and a selected renewable source (*Beta vulgaris*). The chapter also presents the optimisation of free cyanide biodegradation by *Fusarium oxysporum* EKT01/02 grown exclusively on *Beta vulgaris* (Beetroot) using Response Surface Methodology using a design expert software.

Chapter 6 focuses on the bioenergetics and stoichiometric of *Fusarium oxysporum* EKT01/02 growth using different substrates in wastewater contain free cyanide. It presents the microbial growth equations using both material and energy balances of the constituent elements.

Chapter 7 discusses the heat capacity and change of entropy in the lyophilised biomass of *Fusarium oxysporum* EKT01/02 in a modulated DSC, including the usefulness and/or application of such information.

Chapter 8 contains the summary of the research and general remarks.

CHAPTER 2
LITERATURE REVIEW

Akinpelu, E.A., Ntwampe, S.K.O, Mekuto, L & Itoba-Tombo, E.F. Thermodynamics of microbial growth in cyanidation wastewater. Submitted to *Environmental Science and Pollution Research*. (Manuscript ID: ESPR-D-17-00974).

CHAPTER 2
THERMODYNAMICS OF MICROBIAL GROWTH IN WASTEWATER

2.1 Introduction

Annually, more than two million tons of wastewater are generated globally, with industrial processes accounting for a larger percentage (Corcoran 2010). Most of the industrial wastewater contains heavy metals such as copper, arsenic, lead, and iron as well as nitrogenous compounds such as free cyanide, including its complexes, by-products, i.e. ammonium-nitrogen and others. If the wastewater is untreated, its discharge into freshwater bodies can be deleterious to both the environment and human health. Conventionally, wastewater treatment can be performed using physical and chemical methods such as chemical precipitation, dissolved air flotation, electrochemical precipitation, electrodialysis, nanofiltration, membrane electrolysis, alkaline chlorination, ion exchange, and reverse osmosis among others (Acheampong et al. 2010, Ahluwalia & Goyal 2007, Kurniawan et al. 2006, Lazaridis et al. 2002). A conventional sequence of wastewater treatment is shown in Fig. 2.1. However, owing to various challenges associated with these methods, including high capital and/or operational costs associated with the maintenance of various equipment including components within the wastewater treatment plant (WWTP), high energy requirements, a large plant footprint and secondary pollution due to chemical usage within the WWTP, there is a paradigm shift from conventional to biological treatment methods.

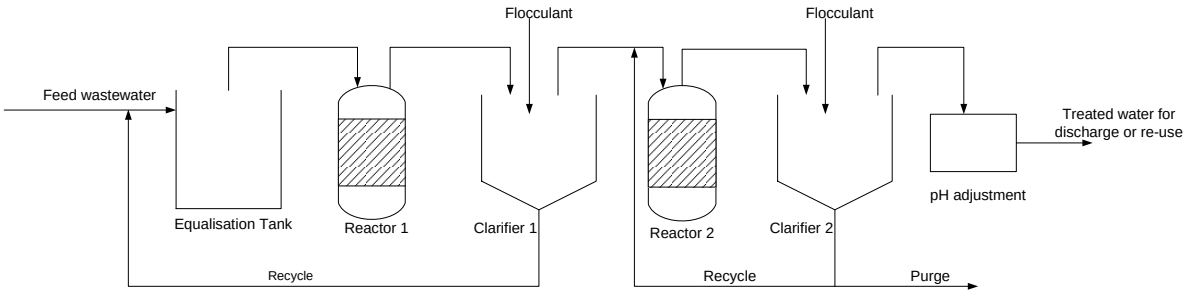

Figure 2. 1: A schematic flow diagram of wastewater treatment plant

Biological treatment methods involve the application of suitable microorganisms and/or their components, i.e. enzymes, which effectively bioremediate the wastewater using different metabolic pathways to transform the pollutants into benign by-products and nullifying even the toxicity of heavy metals via biochelation and adsorption. Such treatment methods are favoured as they are environmentally benign and cost effective, and can be applied feasibly in situ using a variety of microbial species such as bacteria, fungi, algae and yeast; although, there is still a predilection for refined carbon source usage albeit at laboratory scale (Srivastava et al. 2015,

Vargas-García et al. 2012, Gupta et al. 2010, Vijayaraghavan & Yun 2008) deemed unsuitable for environmental engineering applications at an industrial scale.

Despite these advantageous attributes, most treatment plants have not aligned their future operational strategies to this method because of the perceived unsustainability of nutrient requirements for microbial sustenance on a large scale, which can be mitigated by the large quantity of agro-industrial waste generated annually from processing of agricultural produce (Gustavsson et al. 2011). Agro-industrial waste can be used as the sole nutrient and/or carbon source for microbial proliferation in wastewater treatment processes owing to the presence of micro- and macro-nutrients such as proteins, soluble sugars, and minerals contained within such waste which can promote microbial metabolic activity (Mussatto et al. 2012). The agro-industrial waste can further be used for bioaugumentation processes to further reduce environmental and/or soil degradation (Oso et al. 2015, Gadd 2010), thus improving the ecological viability, including minimizing the exertion of anthropogenic activities on environmental health. Additionally, for such wastewater bioprocesses to be understood, elementary and thermodynamic analyses are required. Such analyses can be used to gauge process performance, which can culminate in appropriately designed and well understood processes.

Thermodynamic analysis has been identified as a useful tool for the analysis of microbial performance as it is directly related to the success of bioprocesses. The microbial proliferation can also be directly described by the stoichiometric coefficients that relate the growth efficiency of a specific microbial strain and/or consortia in a biological process such as those used in wastewater. In such applications, process performance, including the resultant concentrations of expected by-products, can be estimated in relation to biomass concentration and thus microbial activity including metabolism at cellular level, even when agro-industrial waste is used. For example, Gibbs energy dissipation per C-mol of biomass grown has been used to directly link growth efficiency and metabolic rates using different thermodynamic models, with outcomes of such an analysis emphatically suggesting that Gibbs energy dissipation is the driving force of biomass performance (von Stockar et al. 2006, von Stockar et al. 2008). In view of the importance of assessing the feasibility of wastewater remediation using such an approach, this literature review sought to review thermodynamic tools used to predict the feasibility of microbial processes, with a proposal of how such an analysis could be used in microorganism/agro-industrial waste/wastewater systems to address the economic viability of such a process on a large scale.

2.2 Associating microbial growth with thermodynamic analysis

Growing cells are thermodynamically defined as open systems; however, since cells are infinitesimally small, they are treated as aggregates in the form of biomass – a product emanating from a growth process (Battley 1999b). Previous reports have shown that batch cultures are the most preferred reactors for the study of thermodynamics in microbial systems, as these type of reactors best replicate what occurs naturally (von Stockar et al, 2006, Battley, 2013, da Silva et al, 2016). A microbial growth process starts from a thermodynamically well-defined initial state to a final state in a system, consisting of a single organic substance that serves both as an electron donor and nutrient source, providing macronutrients such as $NH_{4(aq)}^{+}, H_2PO_{4(aq)}^{-}, SO_{4(aq)}^{2-}$, among others, including micronutrients $Cu_{(aq)}^{2+}, Cl_{(aq)}^{-}, Fe_{(aq)}^{3+}, Zn_{(aq)}^{2+}$ and other trace elements, components readily available in wastewater and some agro-industrial waste. The growth of biomass can be defined by the coupling of catabolism and anabolism, whereby the nutrient source is broken down to release energy in a useful form (catabolism) and whereby energy is utilised for the synthesis of new biomass (anabolism) – see Fig. 2.2.

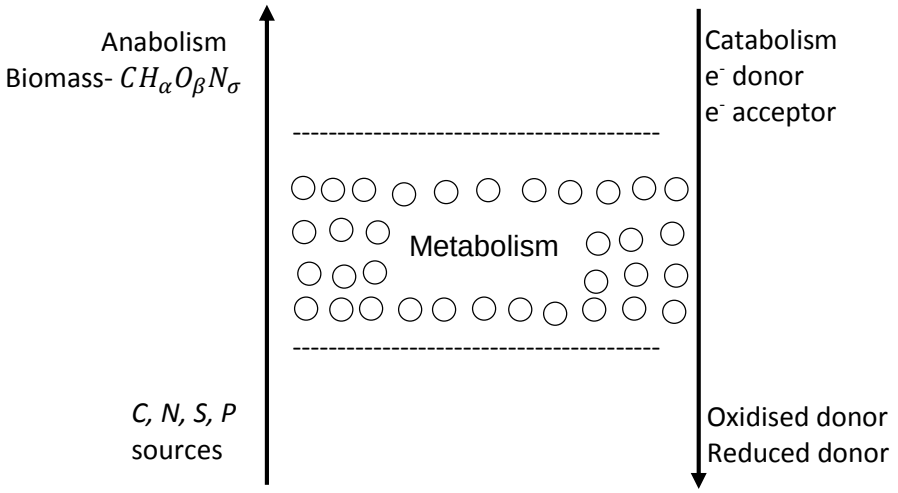

Figure 2. 2: Coupling of anabolism and catabolism in the microbial growth process

Presently, reports on thermodynamic analyses of biomass growth constituting bacterial (*Lactococcus lactis* and *Escherichia coli*) (Kabanova et al. 2009, Duboc et al. 1999b), algal (*Rocan BUV 2* and *Scenedesnus obtusiusculus*) (Duboc et al. 1999b), yeast (*Saccharomyces cerevisiae* and *Candida utilis*) (Battley 1998, von Stockar & Liu 1999) and fungal (*Penicillium roqueforti* and *P. camemberti*) (Wadsö et al. 2004) cells, using refined carbon sources such as glucose and acetate under both aerobic and anaerobic conditions, have been published. It is unclear what impact the utilisation of agro-industrial waste as a nutrient source will have on the thermodynamic properties of such biological processes, i.e. whether the process outcomes

will differ substantially from those in which refined carbon sources are used. Operationally, a minute quantity of cells, i.e. a loopful of microorganism and/or 10 % (v/v) inoculum, is used during the initial state of the process to initiate the bioremediation process, thus making it easier to define the initial state of the system. Furthermore, to effectively elucidate thermodynamic parameters, environmental factors such as temperature, pH, and dissolved oxygen (for aerobic cultures) should be at an optimal level to ensure that the primary carbon source, even if it is agro-industrial waste, is the only limiting factor in the growth process. For optimal process performance, cellular yield must be maximized with cells growing exponentially until all the growth-limiting substrate is exhausted. For a successful thermodynamic analysis, care should also be taken to ensure sterile process conditions from an initial state to the final state in order to limit the destabilisation of the process and to pivotally attribute thermodynamic changes to the organism and/or biomass being studied. Ideally, the cells are assumed to be free of glutinous by-products such as extracellular polymeric substances (EPS) which occur during biomass aggregation under excessive nutrient conditions, presence of toxicants and when cells are growing exponentially, as this can result in molecular mass transfer limitations which can further complicate process dynamics for thermodynamic analysis. Overall, when the primary assimilation rate of the carbon source is not directly related to the growth rate, the microbial yield and elemental composition computations of the cells can be distorted, effectively leading to an ineffectual analysis. Therefore, where feasible, the contributory role of EPS must be quantitatively determined and appraised during analysis, to ascertain its role even on the mass of cells grown (Battley 2013, Battley 1999b).

2.2.1 Analysis of microbial growth

The microbial growth process can be described by the stoichiometric equation representing the material balance of the system in compliance with the *Law of Conservation of Mass*. The initial and final states of the system are represented by the left and right sides of a generalized stoichiometric reaction, as shown in Eq. 2.1. Different techniques have been used to develop such a microbial growth equation. The first is an oxidation-reduction (O-R balance) approach, whereby the molecular composition and quantity of each reactant and product, are required. However, research has shown that once the quantity of one of the reactants, in particular the carbon source is known, the stoichiometric distribution of other reactants and products can be easily determined using an elemental balance analysis (Heijnen 2002). Secondly, the concept of the degree of reduction, which focuses on the number of available electrons per gram atom C, as being equivalent to the quantity of electrons transferred to the electron acceptor, usually dissolved oxygen in an aerobic system. The higher the degree of reduction, the lower the

degree of oxidation of the electron donor. Subsequently, the degree of reduction of the primary substrate can thus be estimated using elemental balances of constituents such as carbon (*C*), Nitrogen (*N*) species, and available electrons.

$$\frac{1}{Y_{X/S}} S + Y_{A/X} A + Y_{N/X} ND \rightarrow X + Y_{P/X} P + Y_{C/X} CO_2 \quad (2.1)$$

where *S, A, ND, X*, and *P* represent growth limiting carbon source, electron acceptor, nitrogen donor, dry biomass and reduced electron acceptor –product, respectively. In all cases of aerobic growth, electron acceptor, *A* is dissolved oxygen and *P* is water. For anaerobic growth, *A* is absent during the bioremediation process, while in respiratory systems such as in denitrification, *A* is any inorganic compound other than the dissolved oxygen and *P* is the nitrogen gas produced (Liu et al. 2007).

2.2.2 Analysis of the electron acceptor using elemental analysis

For the elemental analysis of harvested biomass, it has been recommended that after lyophilisation, the biomass should be held at 100 °C for 24 h to completely remove moisture prior to further experimentation (Battley 1999b, Heijnen 2002). The biomass elemental composition can be obtained using different elemental analysers via repeated combustion analysis for determination of the percentages of *C, H,* and *N* in a given mass of dried biomass, while the quantity of *O* can be estimated by the difference from the total dry weight after accounting for ash as illustrated in Eq. 2.2.

$$f_O = 1 - (f_C + f_H + f_N + f_{ash}) \quad (2.2)$$

where $f_O, f_C, f_H, f_N,$ and f_{ash} are fractions of oxygen, carbon, hydrogen, nitrogen, and ash respectively, on a dry biomass basis.

The percentage ash can be determined by combustion in a furnace using a temperature between 550 and 600 °C, given a known weight of the biomass. There are divergent views on the constituents of ash, ranging from oxides or salts of residual inorganic substances in the biomass such as *P, K, Ca, Mg, Na, S, Si*, and *Fe,* to salts of cations such as *Cl* embedded within individual cells. Chemical analysis of the ash can therefore be used to determine the ash composition, especially in studies in which agro-industrial waste/wastewater are studied. Generally, ash is not considered as part of the thermodynamic analysis because it is energetically a non-functional fraction in the cellular dry weight (Cordier et al. 1987). The percent remaining as ash subsequent to combustion is determined by the difference in weight

between the dry biomass weight and the ash-free dry weight of the biomass. However, Battley (Battley 1995a) noted an anomaly with this approach, arguing that *P* and *S* contribute significantly to the ash in the form of oxides, including salts when compared to the total ash-free dry biomass of *E. coli* K-12, suggesting that the total dry weight should be used (Battley 1995b).

Once the composition of the biomass is known, products and substrates can be stoichiometrically quantified using an elemental balance for the biological reaction. Cellular elemental compositions of different microorganisms are shown in Table 2.1.

Table 2. 1: Elemental composition of several microorganisms

Microorganisms	Composition (% by weight)					Elemental Formula	M_w	γ_b
Bacteria	**C**	**H**	**N**	**O**	**Ash**			
[a]*Aerobacter aerogenes*	48.70	7.30	13.90	21.10	8.90	$CH_{1.78}N_{0.24}O_{0.33}$	22.5	4.4
[b]*B. flavum*	38.54	5.78	8.47	16.98	30.23	$CH_{1.80}N_{0.19}O_{0.33}$	31.15	4.57
[b]*Bacillus cereus*	46.05	5.73	11.98	26.26	9.98	$CH_{1.49}N_{0.22}O_{0.43}$	26.06	3.97
[b]*Escherichia coli*	47.83	6.95	12.30	21.65	11.27	$CH_{1.74}N_{0.22}O_{0.34}$	25.05	4.40
Yeast								
[c]*Saccharomyces Cerevisiae*	45.88	6.21	8.47	34.03	8.62	$CH_{1.63}N_{0.16}O_{0.56}$	24.83	4.03
[b]*Candida utilis*	45.97	6.39	3.76	34.20	9.68	$CH_{1.66}N_{0.07}O_{0.56}$	26.10	4.33
[b]*Debaryomyces hansenii*	44.41	6.36	5.27	35.22	8.74	$CH_{1.71}N_{0.10}O_{0.60}$	27.02	4.21
[b]*D. nepaliensis*	45.67	6.78	4.74	38.30	4.51	$CH_{1.77}N_{0.09}O_{0.63}$	26.27	4.24
Algae								
[b]*Chlamydomonas*	53.26	7.34	7.25	27.95	4.20	$CH_{1.65}N_{0.12}O_{0.39}$	22.53	4.52
[b]*Chlorella Spain sp.*	53.90	8.00	7.75	26.04	4.31	$CH_{1.78}N_{0.12}O_{0.36}$	22.26	4.79
[b]*Rocan BUV 2*	44.52	5.78	2.84	35.19	11.67	$CH_{1.56}N_{0.05}O_{0.59}$	26.95	4.21
[b]*Rocan I*	51.18	5.96	2.66	34.05	6.15	$CH_{1.40}N_{0.04}O_{0.50}$	23.45	4.26
Fungi								
[b]*Aspergillus niger*	46.18	6.17	5.16	33.72	8.77	$CH_{1.60}N_{0.10}O_{0.55}$	25.98	4.22
[b]*Mucor rouxii*	50.35	7.52	3.91	28.65	9.57	$CH_{1.79}N_{0.07}O_{0.43}$	23.83	4.74
[b]*Neurospora crassa*	48.17	7.22	7.14	28.99	8.48	$CH_{1.80}N_{0.13}O_{0.45}$	24.91	4.52
[b]*Penicillium chrysogenum*	51.14	7.95	4.78	15.00	21.13	$CH_{1.87}N_{0.08}O_{0.22}$	23.47	5.18
Standard deviation	3.84	0.77	3.44	7.00	6.61	-	2.25	0.31

M_w : molecular weight, γ_b : degree of freedom of biomass, [a]adapted from (Atkinson & Mavituna 1983), [b]adapted from (Duboc et al. 1999a), [c]adapted from (Battley 1999b)

The elemental components of organisms were determined to vary considerably from one strain to another, with an exception for carbon, hydrogen and nitrogen components (standard deviation range from 0.8 to 3.85). Statistically, the oxygen content varied greatly from one

species to another (standard deviation of 7), which can be attributed to the effect of oxides or inorganic substances being considered in the computations. The ash content variation is also directly influenced by purported trace element constituents embedded via absorption in the biomass as a result of media composition.

Considering a unit carbon mole of a substrate including ammonium-nitrogen as a nitrogen donor in an aerobic system in which minute extracellular products, besides water and carbon dioxide are formed, Eq. 2.1 can be linked illustratively to a stoichiometric reaction using an elemental analysis approach as shown in Eq. 2.3:

$$CH_sO_t + bO_2 + cNH_3 \rightarrow dCH_\alpha O_\beta N_\sigma + eH_2O + fCO_2 \quad (2.3)$$

where $CH_\alpha O_\beta N_\sigma$ represents the molecular formula of the biomass as determined by the conservation of mass equations (Eq. 2.4) based on an elemental balance.

C conservation	$1 = d + f$	(2.4)
H conservation	$s + 3c = d\alpha + 2e$	
O conservation	$t + 2b = d\beta + e + 2f$	
N conservation	$c = d\sigma$	
and		
the respiratory quotient (*RQ*) is	$RQ = f/b$	

2.2.3 Analysis for the degree of reduction for an electron acceptor

The degree of reduction is used in proton-electron balances since the elemental analysis provides minimal information in respect of energetics of the reactions being studied. The degree of freedom, γ, is defined as the number of available electrons (AE) that can be transferred to oxygen per gram atom *C* upon oxidation of an organic compound, even biomass. The degree of reduction of an element for an organic compound is equivalent to its valence value. Generally, the degree of reduction can be estimated as follows (Battley 2013):

$$\gamma = (4nC + nH - 2nO - 3nN)/nC \quad (2.5)$$

where *n* represents the number of atoms of elements in the molecular formula of the organic compound or biomass. For instance, γ of glucose and methane is 4 and 8 respectively,

meanwhile for carbon dioxide, water and ammonia, it is zero. Similarly, the degree of reduction for substrate (γ_s) and that of biomass (γ_b) can be estimated relative to ammonia using Eq. 2.6 & 2.7:

$$\gamma_s = 4 + s - 2t \tag{2.6}$$

$$\gamma_b = 4 + \alpha - 2\beta - 3\sigma \tag{2.7}$$

Since water is used in excess, the quantity of water being formed is difficult to quantify for an aerobic system, thus the available electron balance can be written as Eq. 2.8, provided that the molar yield coefficient and other remaining coefficients are known.

Available electron: $\gamma_s - 4b = d\gamma_b$ (2.8)

2.3 Quantifying thermodynamic properties for microbial systems

Cells generally multiply and metabolise nutrient sources in aqueous, including semi-liquefied environments. Theoretically, some processes are considered to be reversible; however, for microbial growth, it is impractical to have such a hypothesis, as biomass generation is irreversible. Although this may not be a valid assumption for all nutrient components, as some may dissociate in the aqueous solution, they are mostly consumed and become transformed to other constituents, i.e. as by-products, resulting in an equilibrium being reached, particularly under a steadied environment. Since cells cannot be un-grown, and there are no equilibrium constants for either anabolism or catabolism, any concept of equilibrium or near-equilibrium thermodynamics in microbial systems is largely theoretical and not practicable. Once the thermodynamic properties of participating reactants and products in an aqueous form are known, the energy requirements in the process can be estimated using Hess's law, i.e. determining the difference between the energies of the initial and final states (Battley 2013, Battley 2011).

2.3.1 Estimating the heat of combustion for biomass

The energy capacity of a dry biomass is largely dependent on its composition. To obtain the enthalpy of formation for biomass (ΔH_f^{cell}), it is essential to quantify the heat of combustion for the dry biomass using calorific methods and to model the combustion using a unit mass of the dry biomass. Thornton's (Thornton 1917) model indicates that the molar heat of combustion for most organic compounds is directly proportional to the oxygen atoms consumed during combustion as described in Eq. 2.9.

$$CH_\alpha O_\beta N_\sigma + \left(1 + \frac{\alpha}{4} - \frac{\beta}{2}\right) O_2 \rightarrow CO_2 + \frac{\alpha}{2} H_2O + \frac{\sigma}{2} N_2 \quad (2.9)$$

The biomass sample can be prepared as described in elemental analysis experiments with the moisture content being known. Such a determination is done in an adiabatic calorimeter using analytical grade oxygen. A mass of the dry biomass will thus be introduced into a crucible with an ignition wire looped over it prior to filling the vessel with pure oxygen; the vessel must be allowed to equilibrate subsequent to loading the sample into the calorimeter. A complete guide to such a measurement is available in Cordier (Cordier et al. 1987) and Battley (Battley 1999a). Thereafter, the heat of combustion (kJ/g) of the biomass can be used in conjunction with the predetermined molecular mass of the dry biomass, i.e. as a product of the multiplication between these two parameters, to get the enthalpy of formation for the biomass (kJ/mol). Alternatively, Thornton's rule can be used to estimate the heat of combustion directly once the molecular formula of the organic substance is known using Eq. 2.10.

$$\Delta H_c^o = -108.99 \frac{kJ}{eq} X\ (eq.transferred\ to\ oxygen\ during\ bomb\ calorimetric\ combustion) \quad (2.10)$$

Where the number of equivalents (eq) transferred to oxygen can be quantified using Eq.2.11.

$$eq = 4nC + nH - 2nO - 0nN \quad (2.11)$$

Consequently, the heat of reaction involved in the synthesis of a unit carbon mole of the biomass can be estimated using Hess's Law (Eq. 2.12).

$$\Delta H_{rx}^o = \sum n\left(\Delta H_{products}\right) - \sum n\left(\Delta H_{reactants}\right) \quad (2.12)$$

2.3.2 Quantifying the heat capacity and absorbed thermal energy in biomass

There are numerous studies reporting on the heat capacity of biological materials such as proteins, including their monomeric amino acids, and carbohydrates such as glucose, including starch amongst others, based on the application of a method developed to be used at low temperature in an adiabatic calorimeter (AC) with the subsequent determination of absolute entropy (Boerio-Goates 1991, Oja & Suuberg 1999, Pyda 2001, Pyda 2005, Kabo et al. 2013). However, to date, there are few reports focusing on the heat capacity and entropy of dry biomass (Battley et al. 1997), particularly from analyses applying a low temperature AC. The challenge in the use of such an analytical instrument is largely based on its complexity, unavailability of comparable experimentation standards which results in uncertainty, irreproducibility of the outcomes achieved, operational expenses, and a lack of adequately

trained personnel, unlike with conventional calorimeters. Currently, a broader study of thermodynamic properties for microbial systems can enhance and address limitations to assess the sustainability of designed bioprocesses in order to improve their performance.

Recently, research has shown that a standard differential scanning calorimeter (DSC) can be used to quantitatively estimate the heat capacity of biological materials with subsequent estimation of the entropy (Leyx et al. 2005, Pyda 2005). However, for such a calorimeter to operate optimally, biomass must be prepared using an appropriate protocol, as lyophilised biomass has poor thermal relaxation and thus misleading results may be attained. For the DSC, the heat capacity measurement can be performed using repeated runs at a heating rate of 10 K/min (Leyx et al. 2005, Pyda 2005). To do this, a baseline measurement is required with both pans in the calorimeter being empty to minimise system bias. Thereafter, a reference test involving the use of a standard material with a well-defined heat capacity, such as a sapphire, can be used for calibration, with one pan being empty subsequent to the analysis of the lyophilised biomass. For accuracy, the mass of the lyophilised biomass used should be equivalent to the mass of the sapphire. Variations with temperature differences are produced by the glass transition temperature (T_g). The heat capacity can then be directly calculated using heat flux obtained directly from the DSC curve, using Eq. 2.13:

$$C_p = \frac{1}{m}\frac{\delta Q}{\Delta T} = \frac{1}{m}\frac{(\delta Q/dt)}{(dT/dt)} \tag{2.13}$$

where $(\delta Q/dt)$ is the heat flow from the DSC curve, m is the sample mass and (dT/dt) is the heating rate of the sample.

There is no basis for comparison for Battley's (1997) results, since it is the only report for dry biomass heat capacity, although biological materials such as starch and glucose have been explored (Boerio-Goates 1991, Pyda 2005, Kabo et al. 2013). For instance, the heat capacity results of D-glucose by Kabo et al. (2013) using AC concurred with those obtained by Pyda (2001) using a DSC, but do not agree with the AC results from both Pyda (2001) and Boerio-Goates (1991). The AC results from these reports differ greatly for the same type of sample. This explains the reason for Pyda's (2001) preference for results obtained using a DSC over those of an AC, although both systems operated within the same temperature range. Subsequently, by knowing the heat capacity of a material, the third law of entropy for materials as a function of temperature can be estimated. Since entropy is the measurement of the disorder of a system, biomass is treated as being insoluble, and thus the entropy of the lyophilized biomass can be obtained (Battley & Stone 2000), i.e. quantifying the heat capacity

of the biomass from absolute zero to higher than ambient temperature (298.15 K) as shown in Eq. 2.14:

$$S = \int_0^{298.15} C_p \, d\ln T \tag{2.14}$$

where C_p is the heat capacity at a constant pressure of 1 bar for a given mass of dry biomass.

Therefore, since the heat capacity of the biomass is rarely quantifiable at absolute zero, Debye (T^3) law (Eq. 2.15) can be used for the extrapolation of data to 0 K and the subsequent integration defining the heat capacity data – see Eq. 2.16 (Leyx et al. 2005). Alternatively, the third law of thermodynamics is also suited to the determination of absolute entropy, in particular by using a graphical illustration whereby the ratio C_p/T is compared with the independent variable (T), with the area under the curve between 0 K and a final temperature (T) being estimated to be equivalent to the absolute entropy of that material.

$$C_p = aT^3 \tag{2.15}$$

where *a* is an empirical constant, for which the absolute entropy at low temperature can be quantified (Eq. 2.14).

$$S_{T_{low}} = \int_0^{T_{low}} \frac{aT^3}{T} \, dT = \frac{aT_{low}^3}{3} \tag{2.16}$$

2.3.3 Gibbs free energy in microbial systems

The exchange of energy in microbial systems can be assumed to proceed spontaneously from its initial to final states as described by the Gibbs free energy Eq. 2.17:

$$\Delta G = \Delta H - T\Delta S \tag{2.17}$$

where $\Delta G, \Delta H,$ and ΔS represent the free energy, enthalpy and entropy changes respectively that accompany the biomass growth under adiabatic and isobaric conditions.

The Gibbs energy has been adjudged the primary driving force in microbial proliferation, particularly under suitable conditions with sufficient nutrients; thus the importance of biomass metabolism in environmental engineering applications, as this will determine the biomass proficiency in toxicant remediation. According to thermodynamic laws, the Gibbs free energy associated with such a process must be negative. Once the thermodynamic properties of the constituents involved in the process are known, although via the quantification of other

associate parameters, the Gibbs energy can be estimated. The Gibbs energy is generated from the catabolic reaction, for which it is hypothetically assumed that the free energy of the overall reaction must be minutely negative when compared with the free energy of catabolism for systems in which the biomass yield is large. For this, catabolic and anabolic reactions can be independently analysed in order to simplify the metabolic reaction based on the assumption that the electron donor is first completely catabolised and a fraction of catabolism products is used to synthesise new biomass (Eq. 2.18 & 2.19) (Liu et al. 2007).

$$\textbf{Catabolism}: S + Y_A^{cat} A \rightarrow Y_P^{cat} P + Y_C^{cat} CO_2 \qquad (\Delta G_{cat}^0) \tag{2.18}$$

$$\textbf{Anabolism}: Y_p^{ana} P + Y_C^{ana} CO_2 + Y_N^{ana} NS \rightarrow X + Y_A^{ana} A \qquad (\Delta G_{ana}^0) \tag{2.19}$$

For process sustainability, a decrease in the ΔG_{cat}^0 is desirable, as this will be the driving force of the biosynthesis of sufficient biomass to carry-out detoxification and/or bioremediation processes. The Gibbs energy associated with biomass growth can be summed as the Gibbs energy for anabolism and catabolism (Eq. 2.20).

$$-\Delta G_{rx}^o = \Delta G_{cat}^o + \Delta G_{ana}^o \tag{2.20}$$

Since biomass yields will vary from one organism to another depending on the carbon source used, different models of Gibbs energy dissipation can be developed to predict process yields prior to the performance of actual experiments. These models must be expressively defined, as this is needed to perform an appropriate experiment. The widely used model only requires a black box information which predicts the quantity of Gibbs energy dissipated for synthesis of a carbon mole of biomass, as it is dependent on the degree of reduction of the carbon source (γ_s) and the carbon atoms of the substrate (C) – see Eq. 2.21 (Heijnen & Van Dijken 1992, Heijnen & van Dijken 1993).

$$-\Delta G_{rx}^o = 200 + 18(6 - C)^{1.8} + \exp[(3.8 - \gamma_s)^{0.32} . (3.6 + 0.4C)] \tag{2.21}$$

Therefore, even if there is unavailability of suitable equipment, including time to perform such experiments, the Gibbs free energy for both biomass generation and the process can be estimated using appropriate thermodynamics properties of the reactants and products involved as shown in Table 2.2 for some substances of biological importance. However, this can be complicated when dealing with wastewater or constituents that are not well defined such as agro-industrial waste.

Table 2. 2: Thermodynamic parameters of selected substances of biological importance at 298.15 K and 1 atm

Substance	Conditions	ΔG^o (KJmol^{-1})	ΔH^o (KJmol^{-1})	ΔS^o (JK^{-1}mol^{-1})
[a]Potato starch	Anhydrous	-670.4	-974.1	182.2
[b]α-D-Glucose	Crystal	-910.56	-1274.45	-1220.48
[b]Glycine	Crystal	-377.69	-537.22	-535.07
[b]Chymotrypsinogen A	Crystal	-26.88	-67.87	-139.96
[b]Potassium oxide	Crystal	-321.84	-363.15	-138.55
[b]Calcium oxide	Crystal	-604.04	-635.09	-104.14
[b]Magnesium oxide	Micro crystal	-565.97	-597.98	-107.36
[b]Zinc oxide	Crystal	-318.32	-348.28	-100.48
[b]Palmitic acid	Crystal	-315.05	-890.77	-1930.97
[b]L-Methionine	Crystal	-508.35	-761.07	-847.63
[b]L-Valine	Crystal	-358.99	-617.98	-868.66
[b]Water	Liquid	-237.18	-285.83	-163.17
[c]*S. cerevisiae*	Anaerobic, growth on glucose	-210.41	-105.40	352.20
[c]*S. cerevisiae*	Aerobic, growth on glucose	-1996.95	-1976.27	69.36
[c]*S. cerevisiae*	Aerobic, growth on ethanol	-827.42	-883.72	-188.83
[c]*S. cerevisiae*	Aerobic, growth on acetic acid	-562.66	-601.86	-131.47
[d]*D. desulfuricans*	Anaerobic, sulphate-limited	- 1012.5	- 809.2	691.93
[d]*M. thermoautotrophicum*	Anaerobic, hydrogen-limited	-802	-3730	-9823.91
[d]*M. thermoautotrophicum*	Anaerobic, iron-limited	-3049	-7141	-13724.63
[d]*Ms. acetivorans*	Anaerobic, acetate-limited	-745.1	201.5	3174.91

[a]Adapted from (Kabo et al. 2013), [b]adapted from (Battley 1999a), [c]adapted from (Battley 1999b), [d]adapted from (Duboc et al. 1999a)

2.4 Elucidation of agro-industrial waste and thermodynamic parameter interaction in bioprocesses

2.4.1 Prospect of using agro-industrial waste to support microbial growth

Agro-industrial waste consists of residues from agricultural and food industries which in their totality account for over nine million tonnes of waste per annum in South Africa alone (Oelofse & Nahman 2013). The potential and application of biotechnological principles allow this waste

to be seen as a resource of great value. Although several agricultural residues are disposed of safely into the environment owing to their biodegradable nature, the quantity generated necessitate their utilisation in other processes as carbon and/or energy sources to support bioprocesses. Agro-industrial wastes are generated during industrial processing of agricultural produce, post-harvest handling, distribution and consumption, with each stage contributing to the waste generated (Gustavsson et al. 2011). Agro-industrial wastes are rich in proteins, reducible sugars and minerals essential for microbial growth. As a result, there are numerous reports on the application of these wastes, including in wastewater treatment (Brunner & Rechberger 2015, ElMekawy et al. 2015, Pham et al. 2015). Most concerns are related to the notion that some of the agro-industrial wastes contain compounds with a toxic potential which when used and/or disposed off, might result in leachate generation into the process or water bodies culminating in process failure or ecological contamination. However, the economical perspective is based on the notion that such waste being a low-cost raw material, it can be utilised with the expectation of reducing production and/or operating cost in industrial processes and environmental health applications. Most of these agro-industrial wastes are made of lignin, cellulose and hemicellulose, which constitute a large portion of the materials.

Microorganisms, especially bacteria and fungi, are capable of multi-enzyme production in order to break down lignocellulosic constituents in agro-industrial waste. These enzymes use hydrolytic and/or oxidative functions in the decomposition of lignocellulose materials to simple sugars and further to some value-added products (Leiva-Candia et al. 2014, Uçkun Kiran et al. 2014). For instance, cellulase, which includes exoglucanase, endoglucanase, and β-glucosidase enzymes, can hydrolyse cellulose to simple sugars which are fermentable for the microorganisms. These agro-industrial wastes may be subjected to diverse pre-treatments – see Table 2.3.

Table 2. 3: Pre-treatment of agro-industrial waste

Pre-treatment	Examples	Effect of pretreatment	References
Physical	Milling	Reduces to fine particles	(Li et al. 2009)
	Steam explosion	Alters lignin structure and removes hemicellulose	(Menon & Rao 2012)
	Hydrothermal	Hydrolysis of hemicellulose	(Brebu & Vasile 2010)
Chemical	Alkaline exposure	Removal of lignin and hemicellulose	(Jin et al. 2009)
	CO_2 explosion	Removal of hemicellulose and decrystallisation of cellulose	(Menon & Rao 2012)
	Minerals acid	Hydrolysis of cellulose and hemicellulose	(Menon & Rao 2012)
Biological	White-rot fungi	Degradation of lignin	(Dias et al. 2010)

Several bioprocesses have been reported to be supported on agro-industrial waste using either submerged or solid state fermentation to remediate and/or produce value-added products as shown in Table 2.4.

Table 2. 4: Recent microbial growth on agro-industrial waste

Microorganisms	Agro-industrial waste	Process supported	References
Fungi			
Arbuscular mycorrhizal	Sugar beet	Phytoremediation of copper	(Meier et al. 2015)
Aspergillus awamori	Orange, carrot, onion, apple	Biodegradation of free cyanide	(Ntwampe & Santos 2013)
Aspergillus niger	Apple pomace	Production of citric acid	(Dhillon et al. 2013)
Aspergillus niger	Potatoe peel	Production of enzymes	(dos Santos et al. 2012)
Aspergillus niger	Sugar beet	Recovery of contaminated soil	(Azcón et al. 2009)
Aspergillus niger, Glomus mosseae	Sugar beet	Bioremediation of Cadmium	Medina et al. (2005)
Aspergillus niger, Glomus mosseae	Sugar beet	Phytoremediation of zinc	Medina et al. (2006)
Aspergillus niveus	Sugar cane bagasse	Production of enzymes	(Guimarães et al. 2009)
Aspergillus sojae	Orange peel	Production of enzymes	(Buyukkileci et al. 2015)
Fusarium moniliforme	Mango peel	Production of enzymes	(Kumar et al. 2010)
Fusarium oxysporum	Beetroot	Biodegradation of free cyanide	(Akinpelu et al. 2015)
Trichoderma harzianum	Rice straw	Production of fertilizer	(Chen et al. 2011)
Mucor rouxii	Rice bran, soy bean, malt grain	Production of γ-linolenic acid	(Jangbua et al. 2009)
Penicillium sp.	Soybean bran	Production of enzymes	(Wolski et al. 2009)
Bacteria			
Bacillus sp.	Whey	Biodegradation of free cyanide	(Mekuto et al. 2013)
Bacillus amyloliquefaciens	Rice straw	Production of surfactin	(Zhu et al. 2013)
Bacillus licheniformis STK 01	Beetroot	Production of biosurfactant	(Amodu et al. 2014)
Bacillus subtilis	Mushroom residue	Production of γ-glutamic acid	(Tang et al. 2015)
Burkholderia sp.	Tomato	Bioremediation of cadmium	(Dourado et al. 2013)
Escherichia coli	Sugar cane bagasse	Production of ethanol	(Geddes et al. 2011)
Lactobacillus sp.	Banana, potato, orange peel	Production of lactic acid	(Liang et al. 2016)
Pseudomonas aeruginosa	Jatropha curcas seed cake	Degradation of phorbol esters	(Joshi et al. 2011)
Pseudomonas aeruginosa	Wheat bran	Production of enzymes	(Meena et al. 2013)
Pseudomonas fluorescens	Areca husk and sheath	Production of enzymes	(Shashidhar et al. 2013)
Pseudomonas putida	Coconut shell	Biosorption of cyanide and phenol	Singh and Balomajumder (2016)
Rhodococcus	Yeast extract	Biodegradation of cyanide	Maniyam et al. (2013)

Serratia odorifera	Coconut shell	Biodegradation of cyanide and phenol	Singh and Balomajumder (2016)
Streptomyces	Coffee pulp	Production of polyphenol	(Orozco et al. 2008)
Yeast			
Candida lipolytica	Molasses	Production of biodiesel	(Karatay & Dönmez 2010)
Candida tropicalis	Molasses	Production of biodiesel	(Karatay & Dönmez 2010)
Baker yeast AF37X	Sweet sorghum	Production of ethanol	(Yu et al. 2008)
Saccharomyces cerevisiae	Mahula flowers	Production of ethanol	(Behera et al. 2011)
Rhodotorula glutinis	Palm oil mill effluent	Production of lipids/biodiesel	(Saenge et al. 2011)
Cryptococcus curvatus	Beet molasses and Cheese whey	Production of acid and esters	(Takakuwa & Saito 2010)
Pichia stipitis	Rice straw	Production of ethanol	(Srilekha Yadav et al. 2011)
Trichosporon cutaneum	Corn	Saccharification	(Liu et al. 2012)
Monascus anka	Guava leaves	Production of polyphenol	(Wang et al. 2016)
Pichia kudriavzevii	Orange peel	Production of ethanol	(Koutinas et al. 2016)
Yarowia lipolytica	Dry olive cake, sugar beet	Improvement of soil properties	Medina et al. (2004)

Medina et al. (2005, 2006) in their report, using *Aspergillus niger* and *Glomus mosseae* grown on sugar beet agro-industrial waste as a sole carbon source for the removal of cadmium and zinc in contaminated soil, showed that the sugar beet agro-industrial waste promoted microbial growth and enzymatic activities, thus promoting the nutrient uptake in the phytoremediation process (Medina et al. 2005, Medina et al. 2006). Similarly, *Aspergillus awamori* (Ntwampe & Santos 2013), *Fusarium oxysporum* (Akinpelu et al. 2015), *Bacillus* sp. (Mekuto et al. 2013), *Psuedomonas putida* (Singh & Balomajumder 2016b), *Rhodococcus* sp. (Maniyam et al. 2013) and *Serratia odorifera* (Singh & Balomajumder 2016a) grown on orange, beetroot, whey, coconut shell, yeast extract and coconut shell agro-industrial waste respectively, have shown capability to degrade cyanide using different enzymatic pathways (Ebbs, 2004, Gupta, 2010). The organisms' enzymatic pathway has been found to be dependent on environmental conditions, mostly absence/presence of toxins, pH, and temperature. The use of agro-industrial waste as a sole carbon source has been observed to promote biofilm formation, thus sustaining microbial growth in bioremediation processes. Thermodynamic analysis of microbial proliferation in the bioremediation process utilising agro-industrial waste as a sole carbon source would aid the understanding of the process in a large-scale application.

Additionally, a majority of microorganisms easily ferment reducible sugars, resulting in high microbial yield – a necessity in bioprocessing. Thus the need for delignification to separate hemicellulose and cellulose from the cell wall is paramount (Singh nee' Nigam et al. 2009, Anwar et al. 2014). The utilisation of agro-industrial waste in microbial growth will not only

serve as a carbon source and nitrogen source, it can also provide minerals ($NO^{3-}, Cl^{-}, Ca^{2+}, SO_4^{2-}, Na^{+}$, etc.) and trace elements ($Cu^{2+}, Zn^{2+}, Fe^{2+}, Ni^{2+}$, etc.) for biomass sustenance (Wruss et al. 2015) when used to support microbial growth in wastewater treatment, thus having a direct influence on the thermodynamic analysis of such processes.

2.4.2 Thermodynamic parameter analysis in agro-industrial waste-supported microbial systems

There is no doubt of the veracity of microbial growth in wastewater treatment systems, owing to sufficient research available; yet, this approach has not been adopted by most large-scale wastewater treatment industries owing to the cost of sustaining microbial growth. The utilisation of agro-industrial waste can be ascertained using appropriate thermodynamic tools. The agro-industrial waste should be subjected to a pre-treatment procedure depending on bioreactor configuration and for optimum operability. A generalized stoichiometry for microbial growth on agro-industrial waste can thus be written as Eq. 2.22, an expression modified from Eq. 2.1(Liu et al. 2007).

$$\frac{1}{Y_{X/S}}\, n(CH_2O) + Y_{A/X}A + Y_{N/S}\, ND \rightarrow X + Y_{P/X}P + Y_{C/X}CO_2 \qquad (2.22)$$

where $n(CH_2O)$ represents the number of carbohydrate monomers in the agro-industrial waste available for microbial growth. The stoichiometry coefficient (*n*) can be found using elemental analysis as described previously, once the dry biomass yield is known via experimentation. For thermodynamic property assessment, the agro-industrial waste must be dried and pulverised to less than 100 µm prior to analysis. The heat of combustion can then be determined in an adiabatic calorimeter using pure oxygen, with the subsequent determination of the heat of reaction. Also, for the heat capacity of agro-industrial waste estimation, the use of standard DSC is proposed. A slurry of pulverised agro-industrial waste can be prepared in a sample pan using a ratio of 1:3 i.e. waste:water, and allowed to stand for less than 1h at ambient temperature prior to loading on to the DSC as described by Pyda (Pyda 2005) for heat capacity measurements and subsequent entropy estimation. With this, the Gibbs free energy of an agro-industrial waste-supported microbial wastewater treatment system can be estimated.

2.5 Summary

The large volumes of wastewater generated from sewage, industrial and agricultural waste contribute to environmental pollution. Bioremediation of wastewater should be designed to

accommodate high influent throughput rates at minimal cost. The application of microorganisms is an alternative to the traditional physical and chemical methods used. Microbial wastewater treatment processes have been found to be robust, environmentally benign and cost effective. However, the future of such bioremediation strategies is dependent on the sustainability of nutrient requirements for microbial growth. Hence, this literature review proposes the utilisation of agro-industrial waste as a nutrient source for microbial growth, to reduce ecological contamination and minimise costs in environmental engineering applications. Nevertheless, there is a need for research to focus on thermodynamic analysis for operations in which agro-industrial waste-supported microbial systems are used, particularly for wastewater treatment facilities – a strategy which will be accepted for industrial applications, and which can provide information on the feasibility of such processes on a large-scale.

The research gaps which will be addressed in this thesis are as follows:

- There has been minimal reports on cyanide biodegradation using agro-industrial waste as a sole carbon and/or an energy source.
- Also, most research on bioenergetics and stoichiometry of microbial growth have been without inhibition and in systems using various refined carbon sources – processes not applicable on an industrial scale.
- There is no report on heat capacity of microorganisms except for *Saccharomyces cerevisiae* in published science related literature.

CHAPTER 3

MATERIALS AND METHODS

CHAPTER 3
MATERIALS AND METHODS

3.1 Materials

3.1.1 Microorganism isolation and identification

Isolates of *Fusarium oxysporum* were obtained from the rhizosphere of *Zea mays* saturated with cyanide based pesticides using a culture based technique. The isolates were sub-cultured on Potato Dextrose Agar (PDA) plates in order to obtain pure colonies, subsequent to incubation for days (n = 5) at 25 ± 1 °C, alternating exposure to light and darkness at 12 h intervals for optimum growth (Leslie et al. 2006). The fungal identification was based on microbial morphological characteristics. The initial identification was done by submersion in a lactophenol cotton blue staining reagent on glass slides containing the fungal isolates followed by observations under a light microscope (Olympus CX21 model CX21FS1, Olympus corp., Tokyo, Japan) at X 100 magnification (Ajay Kumar 2014, Jiménez-Fernández et al. 2010).

3.1.2 Wastewater constituents

A synthetic gold mine wastewater containing metals similar to a previous report by Acheampong et al. (Acheampong et al. 2013) was used. The wastewater had the following constituents (per litre): 47 mg $CuSO_4.5H_2O$, 42 mg $Fe_2(SO_4)_3.H_2O$, 278 mg $(NH_4)_2SO_4$, 27 mg KH_2PO_4, 3 mg $ZnSO_4.7H_2O$, 0.9 mg $PbBr_2$, and 40 mg $Na_2HAsO_4.7H_2O$.

3.1.3 Reagents used

All chemical reagents were of analytical grade and were obtained from Merck (South Africa) and Sigma-Aldrich (South Africa). *Beta-vulgaris* agro-industrial waste was obtained from a fruit and vegetable processing facility close to the Cape Peninsula University of Technology, Cape Town campus, South Africa

The summary of the experimental procedure for the study is shown in Fig. 3.1.

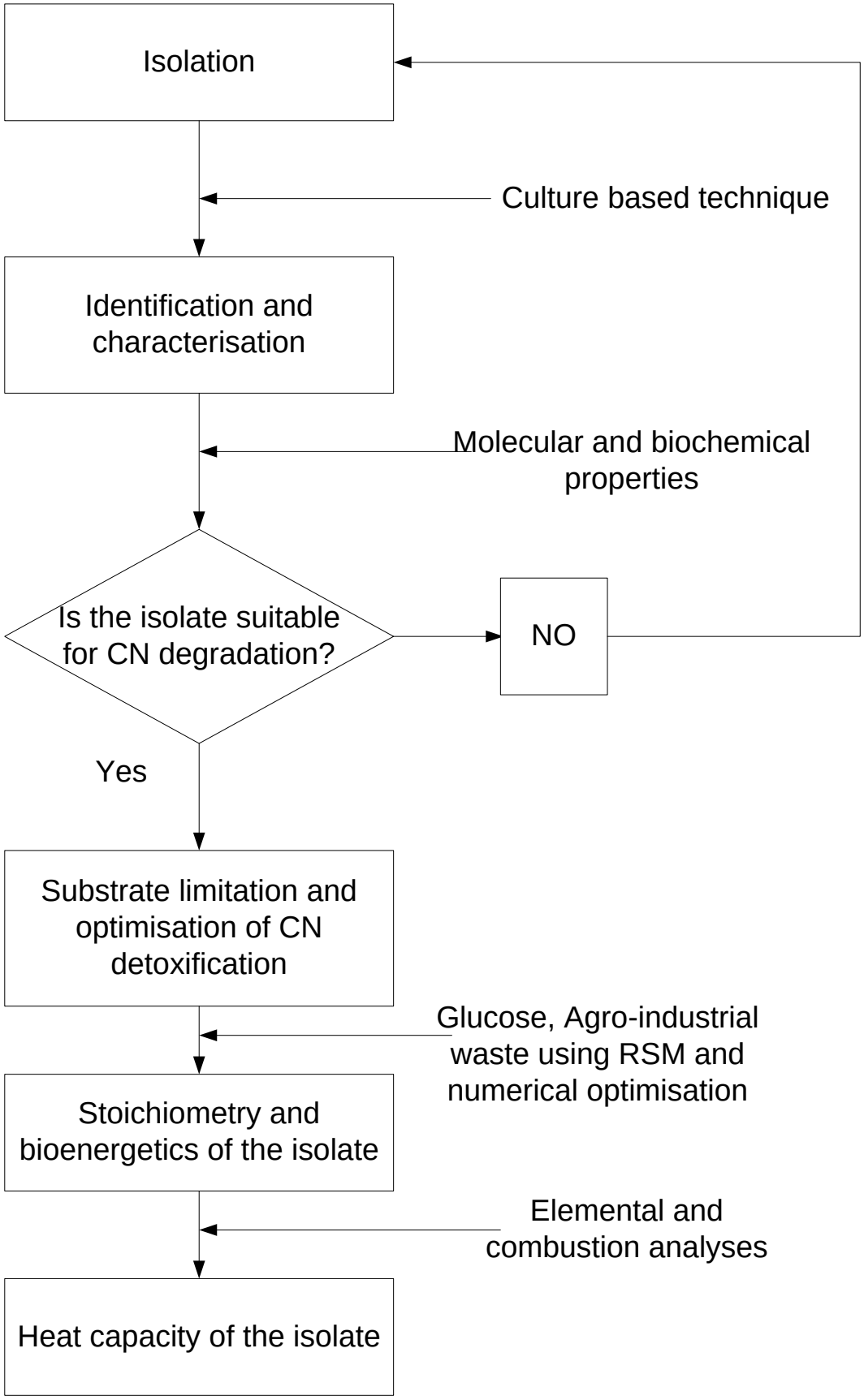

Figure 3. 1: Flow chart showing the summary of experimental procedure for the study

3.2 Materials and procedures

3.2.1 Isolation, DNA extraction and sequencing of isolated microorganism

The fungal isolate was identified both morphologically and by structural ribosomal deoxyribonucleic acid (rDNA) sequence analysis. The genomic DNA was extracted using a PowerBiofilm DNA kit (MOBIO Laboratories, Inc., CA- USA) according to the manufacturer's instructions. The Polymerase Chain Reaction (PCR) amplification and sequencing was done using the approach described earlier (Itoba Tombo et al. 2015). For complete identification, translation elongation factor 1-alpha (TEF1-α) and internal transcribe spacer (ITS) rDNA sequences were amplified using universal primers EF1F/EF1R (EF1F: 'ATGGGTAAGGARGACAAGAC' and EF1R: 'GGARGTACCAGTSATCATGTT') and ITS1/ITS4 (ITS1: ITS 'TCCGTAGGTGAACCTGCGG' and ITS4: ITS 'TCCTCCGCTTATTGATATGC'), respectively (O'Donnell et al. 1998). The PCR amplicons were purified using a QIAquick PCR purification kit (Qiagen, Hilden, Germany). PCR amplicons from TEF 1-α gene were denoted EKT01 while those of ITS were denoted EKT02. Sequences were analysed using a CLC Main Workbench 7 followed by a search in the National Centre for Biotechnology Information (NCBI, www.ncbi.nlm.nih.gov) database. Alignment of 16 nucleotide sequences from the NCBI database and obtained sequences was done using the MAFFT online server (MAFFT version 7, http://mafft.cbrc.jp/alignment/server/). The aligned sequences were imported into the Molecular Evolutionary Genetics Analysis (MEGA) software version 6 (Tamura et al. 2013), which was used for sequence analyses.

The evolutionary history was done both individually and collectively for the dataset obtained. The Maximum Likelihood method based on the Kimura 2-parameter model with 1000 bootstrapped data sets was used (Kimura 1980). The tree with the highest Log Likelihood (-1606.48) is shown in Fig. 4.1a for the combined dataset. The percentage of trees in which the associated taxa are clustered together are shown next to the branches. Initial tree(s) for the heuristic search were obtained by applying the Neighbour-Joining and BioNJ algorithms to a matrix of pairwise distances estimated by using the Maximum Composite Likelihood (MCL) approach, followed by selecting a topology with a superior log likelihood value. Evolutionary rate differences among sites (5 categories) were modelled using a discrete Gamma distribution. Maximum Parsimony method was used to further analyse the TEF 1-α genes using the Max-mini branch-and-bound algorithm with 1000 replications of parsimony bootstrap for clade stability assessments (Felsenstein 1985, Purdom Jr et al. 2000). All positions < 95% site coverage were eliminated. All trees are drawn to scale, with branch lengths measured in the number of substitution per site. Table 3.1 presents the accession numbers. The nucleotide sequences (EKT01 and EKT02) of the fungus were converted to corresponding amino acid sequences using the NCBI translation tool. The corresponding amino acid sequences were

aligned with *Fusarium oxysporum* isolates F72, FUS1, FSY0829, FSY0812, CCF4362, WM04.490 and FOI48 genes using ClustalX version 2.1.

Table 3. 1: Accession number of genes used for alignment and phylogenetic analysis

Genes	Accession number
TEF 1-α	
ATCC90245	KP964890.1
A28	KP964859.1
FUS1	KP964876.1
A8	KP964908.1
S1	DQ837657.1
F72	KF574859.1
FSY0829	JQ965438.1
FSY0812	JQ965435.1
ITS	
SK 1649	HE974453.1
Sa/1/2	JN624908.1
CCF4362	HE974454.1
WM04.490	KP132221.1
FOI48	EU839398.1
FOI18	EU839370.1
FOI43	EU839394.1
Ecu311	KF472154.1

3.2.2 Nucleotide sequence homogeneity test

The homogeneity of substitution patterns between the nucleotide sequences was measured using the disparity index (Kumar & Gadagkar 2001). These tests assessed the probability of rejecting the null hypothesis that sequences have evolved with the same pattern of substitution, as judged from the extent of differences in base composition biases between sequences. A Monte Carlo test (500 replicates) was used to estimate the P-values. P-values smaller than 0.05 are considered significant (marked in bold –Table A2). The estimates of disparity index per site are shown for each pair above the diagonal. The analysis involved 18 nucleotide sequences, with 1st, 2nd, 3rd, and noncoding codon positions. All positions with less than 95% site coverage were eliminated. There were a total of 378 positions in the final dataset. The composition distance (D_C) between aligned DNA sequences was estimated using Eq. (3.1):

$$D_C = \frac{1}{2}\sum_i (x_i - y_i)^2 \tag{3.1}$$

where x_i is the i^{th} type of nucleotide ($i = A, C, G, T$) in sequence X and y_i is the corresponding count in *Y*. When the evolutionary substitution pattern is homogeneous at individual sites between lineages, the expected composition distance (D_C) is equivalent to the expected number of differences (N_d), i.e. Eq. (3.2):

$$E(D_C) = E(N_d) \tag{3.2}$$

All evolutionary analyses were conducted in MEGA v6 (Tamura et al. 2013).

3.2.3 Extraction of extracellular polymeric substance (EPS) from the isolate

The isolate was incubated in two different media: initially in nutrient broth and subsequently in gold mine wastewater containing CN^- and heavy metals as shown in Akinpelu et al. (2016) with glucose as a carbon source for 48h at 140 rpm, 28 °C and pH of 10. After incubation, the culture was centrifuged at 10,000 rpm for 10 min at 4 °C in an Avanti® J-E centrifuge (Beckman Coulter, Inc., USA). To the recovered supernatant, cold ethanol (96% v/v, Merck, USA) at 4 °C was added using a ratio of 1: 2, i.e. supernatant: ethanol, and incubated overnight at 4 °C. The mixture was swirled and centrifuged at 10,000 rpm for 10 min at 4 °C. The EPS was rinsed twice in sterile distilled water (SDW) and dialysed in SDW overnight at 4 °C. The recovered EPS was lyophilised using a Duran® desiccator (Dlangamandla et al. 2016). The EPS was used to ascertain the influence of the isolate's EPS on the maintenance of microbial activity in wastewater containing CN^- and heavy metals.

3.2.4 Biochemical tests

Tests were done using colorimetric reagent cards; GN (Gram negative), GP (Gram positive), BCL (Gram positive spore-forming bacilli), and YST (Yeast and yeast-like organisms) of the VITEK® 2 Compact 30 system (BioMérieux, France). The inoculum was prepared from a culture of the isolate incubated at 35 °C for 18 to 24 h on Potato Dextrose Agar (Merck, USA). A sterile stick was used to transfer a sufficient number of morphologically similar colonies into a 3.0 ml sterile saline (aqueous 0.4 to 0.5% NaCl) in a clear plastic test tube (12 x 75 mm). The turbidity was adjusted to a McFarland standard (0.5 to 0.63) for each card using a DensiLameter®. All cards were incubated on-line at 35.5 ± 1.0 °C. Periodically (15 min), each card was removed from the incubator carousel and inserted into the optical system for reaction readings at different wavelengths. The generated data were analysed using the VITEK® 2 software version 7.01, according to the manufacturer's instructions. Test reaction results are shown as "+", "-", "(+)", or "(-)" in Table A3. Results in parentheses indicated reactions which are weak and too close to the test threshold (Pincus 2006). This test was used to assess the ability of the isolate to utilise various substrates (mainly carbohydrate and amino acid assimilation), and identify prominent enzymes expression by the isolate.

3.2.5 Microbial growth in free cyanide and heavy metals

Heavy metal salts of $CuSO_4$, Na_2HAsO_4, $PbBr_2$, $Fe_2(SO_4)_3$, $ZnSO_4$, and CN^- in the form of KCN (Merck, USA), each at 1mM were prepared in 50 mL nutrient broth, and inoculated with a loopful of the isolate and incubated at 28 °C for 24 h. Nutrient broth containing the isolate without CN^- and heavy metals served as a control. Then, 1 mg of the isolate's EPS was added to the inoculated nutrient broth and further incubated at 28 °C overnight. The microbial growth was observed in a microplate reader; SpectraMax® M2 (Molecular Devices, California, USA) based on optical density at a wavelength of 300nm. All experiments were in triplicate.

3.2.6 Inoculum preparation

The isolated *Fusarium oxysporum* was re-cultured on potato dextrose agar (PDA) plates, covered with parafilm and incubated at 25°C for 5 days. Sterile distilled water (SDW) was added to each plate and spatula was used to harvest the spores and mycelium from the plate. The spore-mycelium suspension was filtered through a glass wool using 20 mL syringes to entrap the mycelium unto the glasswool and the filtrate containing spores was collected and stored at 4 °C. The procedure was repeated for each plate. Furthermore, spore concentration was quantified by a series of dilution using sterile distilled water and spore solution. A Jenway 6715 UV/Visible spectrophotometer was used at varying wavelength to determine the maxima absorbance for the spore dilution. The absorbance was found at a maximum of 300 nm. The spore concentration and absorbance of each of the spore dilutions was determined in duplicate using both a direct counting system in a Marienfeld Neubauer cell-counter and a Nikon Eclipse E2000, phase contrast 1 and 100 x magnification.

3.2.7 Agro-industrial waste preparation

The *Beta-vulgaris* (Beetroot) was dried at 80°C for seven days and milled to less than 100 µm using a grinder (Bosch MKM 7000, Germany). The agro-waste was mixed with distilled water and autoclaved at 116°C for 15 minutes and then cooled to ambient temperature.

3.2.8 Substrate limiting growth of *Fusarium oxysporum* EKT01/02

A volume of 79 mL synthetic wastewater with 1 mL spore concentration of 1.25 % (v/v) was used in a multiport flask of 200mL. The wastewater constituents are listed in section 3.1.2. The

growth of the isolate was observed on both refined carbon source (glucose) and agro-industrial waste i.e. *Beta vulgaris* (Beetroot) at a feed rate of 0.05 g L^{-1} h^{-1}. The cultures were incubated in a rotary shaker (ZHICHENG® model ZHWY-200D, Shanghai, China) at 25°C, pH of 11 and 160rpm. The uninoculated bioreactors served as a control. Samples were taken hourly for optical density measurements in a Jenway 6715 UV/Visible spectrophotometer at a wavelength of 300nm. All experiments were in triplicate. Experimental error was determined using the standard deviation obtained from sets of data (n=3).

3.2.9 Bioremediation of free cyanide containing wastewater

The isolate *F. oxysporum* EKT01/02 (1 mL spore solution) was inoculated in 49 mL of wastewater and incubated in an orbital shaking incubator at 70 rpm at various pH, temperature and concentrations for *B. vulgaris* waste specified in Table 5.1 for 48 h. Afterwards, free cyanide (as KCN) at concentration of 300 mg CN^-/L was added to the culture subsequent to further incubation for 72 h in the rotary shaking incubator (ZHICHENG® model ZHWY-200D, Shanghai, China) at 70 rpm. An uninoculated culture served as a control at various specified conditions. The pH of the samples was adjusted using 1 M NaOH or 1 M HCl, accordingly.

3.2.10 Stoichiometry and bioenergetics of *Fusarium oxysporum* EKT01/02 in cyanide containing wastewater

The cultivation was carried out in a 1 litre stirred tank reactor at ambient temperature i.e. 25 ± 2 °C. A 10% (v/v) *F. oxysporum* culture (48 h old), was inoculated in synthetic wastewater containing 300 mg glucose as refined carbon source, followed by experiments on 300 mg pulverized *B. vulgaris* agro-waste and subsequently on 300 mg pulverized *B. vulgaris* with 100 mg CN^-/L in the form of KCN that was added to the synthetic wastewater. An overhead stirrer fitted with a four blade impeller at 250 rpm provided mixing and aeration was at 0.4 L/min. Biomass was harvested once the carbon source was exhausted and/or when the stationary microbial growth phase has been reached. Harvested biomass was centrifuge at 10,000 rpm for 10 min at 4 °C in an Avanti® J-E centrifuge (Beckman Coulter, Inc. USA). Recovered biomass was washed thrice in sterile distilled water, dried in a Duran® vacuum desiccator (DURAN Group GmbH, Germany), and stored at -20 °C for further analyses. All procedures were repeated until a suitable quantity of dry biomass was obtained.

3.2.11 Sample preparation for heat capacity measurements

A loopfull of *Fusarium oxysporum* was cultured in different substrates as described earlier under substrate limiting conditions. The recovered biomass sample was centrifuged at 10,000 rpm for 10 mins at 4 °C in an Avanti® J-E centrifuge (Beckman Coulter, Inc. USA). The cells were washed twice in sterile distilled water and dried in a vacuum desiccator. A sample of dried biomass was dissolved in sterile distilled water in a 1:1, weight: volume ratio and incubated at 25 °C for 16 h to ferment any residual carbohydrates. An aliquot of the suspension was tested for any residual carbohydrates using the Durham tube method (Battley, 1999). Once the metabolic activity has seized, the biomass was centrifuged and lyophilised (Battley, 1997).

3.3 Analytical methods

3.3.1 Photometric tests used

MERCK® cyanide (CN^-) (09701), ammonium-nitrogen ($NH_4^+ - N$) and nitrate-nitrogen ($NO_3^- - N$) kits were used to analyse the samples for residual free cyanide, ammonium-nitrogen and nitrate-nitrogen using a NOVA 60 spectroquant at absorbance of 0.010 A after incubation. The cyanide test kit measures the free cyanide using the reaction of cyanide with chlorinating agent with maximum error of ± 0.013 mg CN^-/L (Lambert et al. 1975). The nitrate test kits uses the reaction of concentrated sulphuric acid with benzoic acids derivatives to measure nitrate as nitrate-nitrogen with maximum accuracy of ± 0.6 mg $NO_3^- - N$/L (Pappenhagen 1958) while the ammonium test kit works using the Berthelot reactions among phenolic compounds, chlorine and ammonia. The ammonium is measured as ammonium-nitrogen with a maximum accuracy of ± 0.08 mg $NH_4^+ - N$/L (Patton & Crouch 1977). A Crison Basic20 pH meter, calibrated daily was used to measure and/or adjust the pH as may be required.

3.3.2 Residual glucose quantification in the culture

The glucose concentration in the culture samples were determined as reducing sugar using a modified dinitrosalicyclic (DNS) acid colorimetric method (Muller, 1959). A 1.5 mL of a DNS reagent (containing, w/v: 1% DNS; 0.2% phenol; 1% sodium hydroxide and 0.05% sodium sulphite) was added to 1.5 mL of culture samples in a capped polypropylene test tube. The mixtures were heated for 15 min in a water bath at 90 ˚C, cooled under running tap water prior to adding 0.5 mL of a 40% Rochelle salt solution (potassium sodium tartrate). The absorbance of the mixture was measured in a Jenway 6715 UV/Visible spectrophotometer (Bibby Scientific Ltd., Staffordshire, UK), at 575 nm. A standard curve of absorbance against concentration was prepared with a D(+) glucose solution across the range 0 -1000 mg/L and this was used to estimate the total sugar concentration in the culture broth.

3.3.3 Elemental and molecular weight constituent analysis of dry *F. oxysporum* EKT01/02 biomass

The biomass concentration was determined daily at 300 nm by a Jenway 6715 UV/Visible spectrophotometer (Bibby Scientific Ltd., Staffordshire, UK), and expressed in grams dried biomass per litre culture medium (g/L) using a calibration curve relating optical density (OD) to dry biomass weight. All measurements were in triplicate.

The biomass samples were dried for at least 12 h in a vacuum desiccator until the sample weight was constant. The dry samples from the desiccator were further dried at 100 °C for 24 h to remove residual moisture, subsequent to milling using a mortar and pestle prior to elemental analysis for *C*, *H*, and *N* by a Thermo Flash EA 1112 series analyser (Thermo Fisher Scientific Inc. Waltham, USA). The analyser combusts the sample with oxygen in a Helium carrier gas to produce CO_2, H_2O and N_2 which are separated in a gas chromatograph and analysed by a thermal conductivity detector. The peaks were integrated and the percentages calculated for *C*, *H*, and *N*. All measurements were in triplicate.

The heat of combustion of the biomass was determined in an e2k oxygen bomb calorimeter (Digital Data Systems Pty Ltd, South Africa) in triplicate. A pre-cut firing cotton thread (Part No. CAL2K-4-FC) was looped over the firing wire (Part No. CAL2K-4-FW) and twisted at the ends. A mass of 0.30 g of the dried biomass was weighed in a crucible and inserted into the outside electrode's crucible, ensuring that the firing cotton touches the sample. The electrode assembly was loaded into the vessel body and slightly tightened. The vessel was kept upright and filled with 3000 kPa oxygen, removed from the filling station and allowed to stabilize for 1 min prior to insertion into the calorimeter. The calorimeter was calibrated with analytical grade Benzoic acid (Part No. CAL2K-BA).

The percentage of ash in dried biomass was determined by drying at 100 °C in an oven to constant weight as previously explained. The dried biomass was ashed in an EMF 260 furnace (Kiln Contracts Pty Ltd, Cape Town, South Africa) at 550 °C for 2 h in triplicate. The fraction of oxygen was computed by difference from the total dry weight using Eq. (2.2).

CHAPTER 4

CHARACTERISATION OF THE *FUSARIUM OXYSPORUM* EKT01/02 ISOLATE

Published as: **Akinpelu, E. A.,** Adetunji, A. T., Ntwampe, S. K. O., Nchu, F. & Mekuto, L. 2017. Biochemical characteristics of a free cyanide and total nitrogen assimilating Fusarium oxysporum EKT01/02 isolate from cyanide contaminated soil. *Data in Brief,* 14, 84-87 DOI: 10.1016/j.dib.2017.07.023

Akinpelu, E.A., Adetunji, A.T, Ntwampe, S.K.O, Nchu, F & Mekuto, L. Characterisation of *Fusarium oxysporum* EKT01/02 Isolate associated with cyanide biodegradation system. Submitted to *Biology* (Manuscript ID: biology-216360)

CHAPTER 4
CHARACTERISATION OF THE *FUSARIUM OXYSPORUM* EKT01/02 ISOLATE

4.1 Introduction

Fusarium oxysporum is widely distributed in soils including plants and it is known to be phylogenetically diverse (Altınok & Can 2010). In soil, it occurs as a saprophyte, while some produce biocontrol agents (Alabouvette et al. 2009). They are best known as plant pathogens causing vascular wilts, crown including root rot diseases in several hosts (Leslie et al. 2006), and are ranked fifth as the most important plant pathogens (Dean et al. 2012). However, *F. oxysporum* has medical and/or veterinary uses, with an ability to hydrolyse starch via enzymatic biocatalysis (Pereiro Jr et al. 2001, Dogaris et al. 2009).

Fusarium oxysporum isolates consist of pathogenic members including non-pathogenic members which keeps most of the genetic diversity within the species (Bao et al. 2002). Previous studies have shown that there is a genetic connection between pathogenic and non-pathogenic *F. oxysporum* leading to evolvement of certain pathogenic isolates from non-pathogenic strains, and vice versa through the mutation of non-pathogenic and loss of virulence in pathogenic strains, respectively (Baayen et al. 2000, Skovgaard et al. 2002). DNA sequence analysis such as the translation elongation factor 1-α (TEF 1-α), amplified fragment length polymorphisms (AFLPs), internal transcribe spacer (ITS) among others, have been used to understand the phylogenetic and genetic diversity of the *Fusarium* sp. (O'Donnell et al. 2000, Bogale et al. 2005, Baysal et al. 2010, Gurjar et al. 2009). Findings have shown that *F. oxysporum f.* spp*.* could either be monophyletic such as *f.* spp*. tulipae and lilii* (Baayen et al. 2000) or polyphyletic such as *f. spp. asparagi, cubense, dianthi and vasinfectum* (O'Donnell et al. 1998, Baayen et al. 2000, Mirtalebi & Banihashemi 2014).

Additionally, several biochemical characterisation techniques have been developed for microbial species in particular bacteria; however, such techniques have been difficult for filamentous fungi, due to the varied morphology and a lack of reproducibility of research studies (Ainsworth & Sussman 2013, Murray 1968). Presently, standardised colorimetric biochemical tests have been developed that use growth-based techniques for microbial characterisation (Pincus 2006). Since, yeast has a reduced morphology, with standardised biochemical properties, it is easier to identify and characterise its biological functionality as well as properties. Such functionality would include characteristics which are useful in biodegradation.

Biodegradation processes have increasingly gained popularity due to their cost effectiveness, robustness and environmental benignity, with a large quantity of research being conducted in

this area (Hubbe et al. 2011). Besides the biological cyanide biodegradation system at the Homestake Mine, (Dakota USA), Biomin® Limited (South Africa) recently developed a biological process named the Activated Sludge Tailings Effluent Remediation (ASTER™) technology, which is being developed for the safe treatment of effluent containing CN^- and thiocyanate (SCN^-) in South Africa (Du Plessis et al. 2001, Huddy et al. 2015). These processes have been widely reported to be dominated by bacterial and fungal organisms, which facilitate the free cyanide biodegradation process. Fungal species such as *Aspergillus* sp. and *Fusarium* sp. and bacterial species such as *Bacillus* sp. and *Pseudomonas* sp., amongst others, have been found to utilise cyanide as a nitrogen source and/or carbon source, which generally results in the production of ammonium-nitrogen ($NH_4^+ - N$) (Barclay et al. 1998, Santos et al. 2013, Khamar et al. 2015, Mekuto et al. 2016b).

Therefore, in the selection of a suitable biocatalyst for a designed process, it is essential to ascertain the ability of the organism to utilise various substrates in the absence or presence of certain macro- and micronutrients including free cyanide (Hakim et al. 2013, Kitancharoen & Hatai 1998, Murray 1968). This is the case for selecting a microorganism for a CN^-/SCN^- bioremediation process. Free CN^- is a known metabolic inhibitor, as it inhibits the activity of cytochrome c oxidase, thus leading to the cessation of oxidative phosphorylation which results in oxygen utilisation impairment. This among other factors will have an effect on microbial performance and its architecture (Peiqian et al. 2014, Huddy et al. 2015).

4.2 Objectives

The objectives were to:

- Isolate and identify a cyanide degrading isolate;
- Characterise and identify biochemical properties of the isolate;
- Examine the impact of free cyanide on the architecture of the isolate; and
- Investigate the suitability of the isolate for a heavy metals and free cyanide biodegradation system.

4.3 Materials and methods

Fusarium oxysporum EKT01/02 (KU985430/KU985431) is a cyanide degrading fungal and was isolated as shown in chapter 3. Molecular characterisation procedures and extraction of EPS from the isolate, including biochemical tests and microbial growth assays are reported in section 3.2.

4.3.1 Cyanide removal and scanning electron microscopy

The isolate was inoculated into two sets of bioreactors (250 mL Erlenmeyer flasks) containing nutrient broth in a rotary shaker (ZHICHENG® model ZHWY-200D, Shanghai, China) at 25 ˚C, pH of 10 and 140 rpm. After 24 h, CN^- (KCN) was added to one of the reactors to make a 100 mg CN^-/L solution while the other set was free of CN^-. The uninoculated reactors served as a control. Samples (2 mL) were periodically withdrawn from the bioreactors and analysed for free cyanide biodegraded, residual ammonium-nitrogen and nitrate-nitrogen using Merck® cyanide (CN^-) (09701), ammonium (NH_4^+-N) (00683) and nitrate (NO_3-N) (14773) test kits respectively, in a NOVA 60 spectroquant. After 120 h, biofilms were harvested from the walls of the reactors, centrifuged at 30, 000 x g for 10 min at 4 °C in an Avanti® J-E centrifuge (Beckman Coulter, USA) which was followed by fixation in 2.5% (v/v) glutaraldehyde for 16 h at 4 °C. The fixed biomass was rinsed (n=4) with sterile distilled water (SDW), prior to dehydration in an alcohol series containing 50%, 70%, 90% and 100% (v/v) ethanol (Merck, USA). Each dehydration step was performed at 4°C for 12 to 16 h. The samples were dried using hexamethyldisilazane (HMDS), placed on a stub covered with a carbon glue. The stub was sputter coated using carbon and visualized on a scanning electron microscopy (SEM: FEI Nova NanoSEM 230) with a field emission gun (Huddy et al. 2015).

4.4 Results

4.4.1 Sequence analyses

The consensus nucleotide sequence amplicons of 703 base pairs (bp) and 465 bp were obtained for TEF 1-α and ITS genes from the isolate, respectively. The sequences were deposited in the NCBI database and assigned the following accession numbers: KU985430 for EKT01 and KU985431 for EKT02. Alignment of the nucleotide and amino acid sequences indicated similarities to other *Fusarium oxysporum* isolates (Table 4.1). Furthermore, the phylogenetic tree for individual sequences showed a high similarity and the combined tree separated the taxa analysed into different groups (Figures 4.1 & 4.2).

Table 4. 1: Nucleotide and amino acid similarity for TEF 1-α and ITS genes

Genes	Isolate	Nucleotide sequence	Amino acid sequence
TEF 1-α	F72	99%	100%
	FSY0829	99%	100%
	FSY0812	99%	100%
	FUS1	99%	100%
ITS	CCF4362	100%	93%
	WM04490	100%	93%
	48	100%	93%

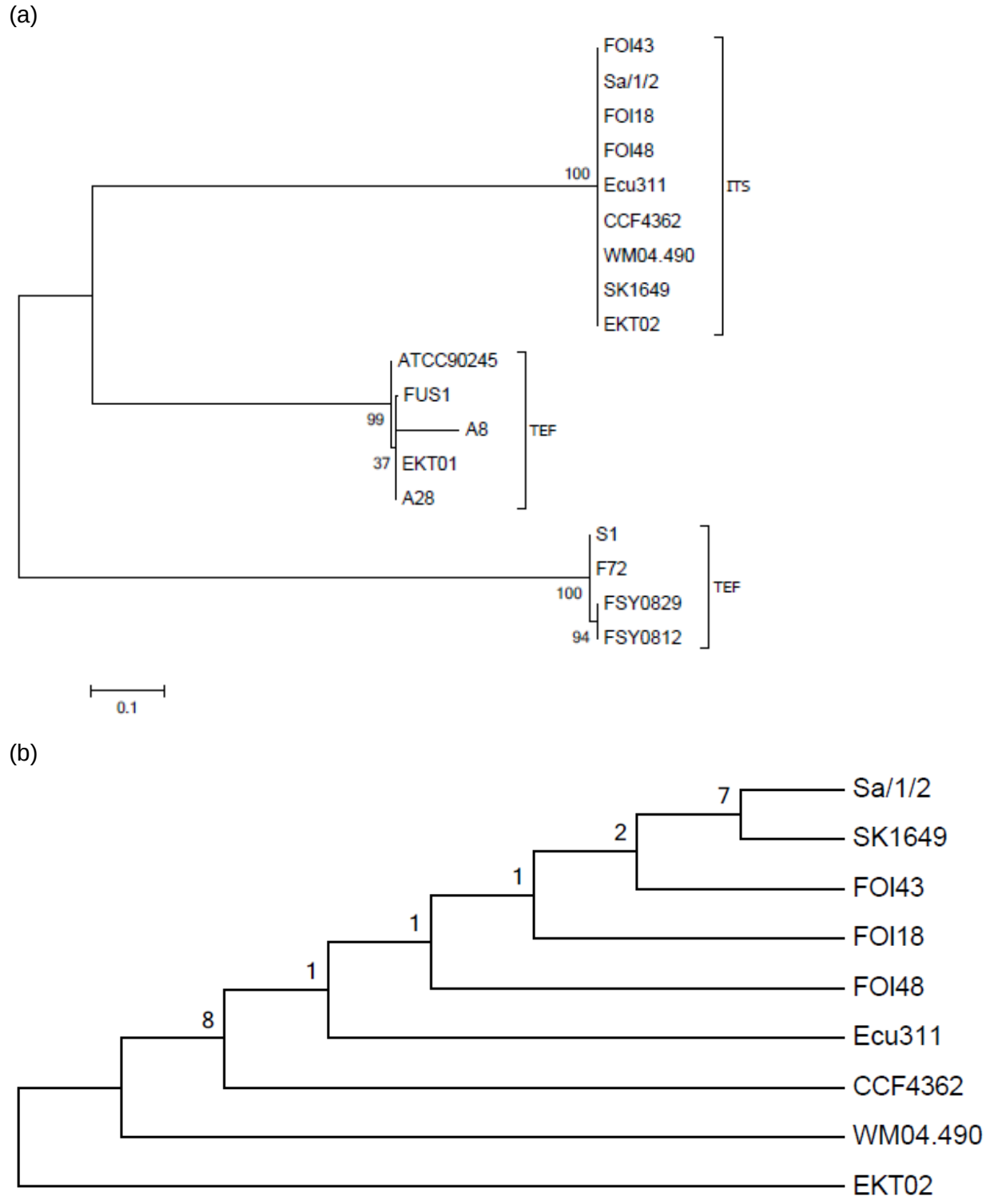

Figure 4. 1: Maximum Likelihood trees of (a) combined genes and (b) ITS genes

The tree analysis from the Maximum Parsimony Method gave the tree length as 370, a consistency index of 0.986, with a retention index of 0.995 and a composite index of 0.981 including a parsimony-informative sites of 0.981, for the EKT01. There was minimal bootstrap

support for the ITS genes while TEF 1-α genes were well supported. The sequence translation of TEF 1-α and ITS genes showed a peptide of 105 amino acids (aa) and 144 aa long, respectively (Figure 4.3). The amino acid sequence of TEF 1-α gene showed putative conserved domains. A majority of the TEF 1-α gene had an identical sequence to the isolate (KU985430/KU985431). The isolate belongs to the P-loop containing nucleoside triphosphate hydrolases (P-loop NTPase) superfamily. The actual alignment was detected with the superfamily cd01883 on NCBI's conserved domain database. However, there were no putative conserved domains in the amino acid sequence of ITS gene. The amino acid residues of the ITS are a more conservative substitution (highlighted in grey in –Figure.4.3).

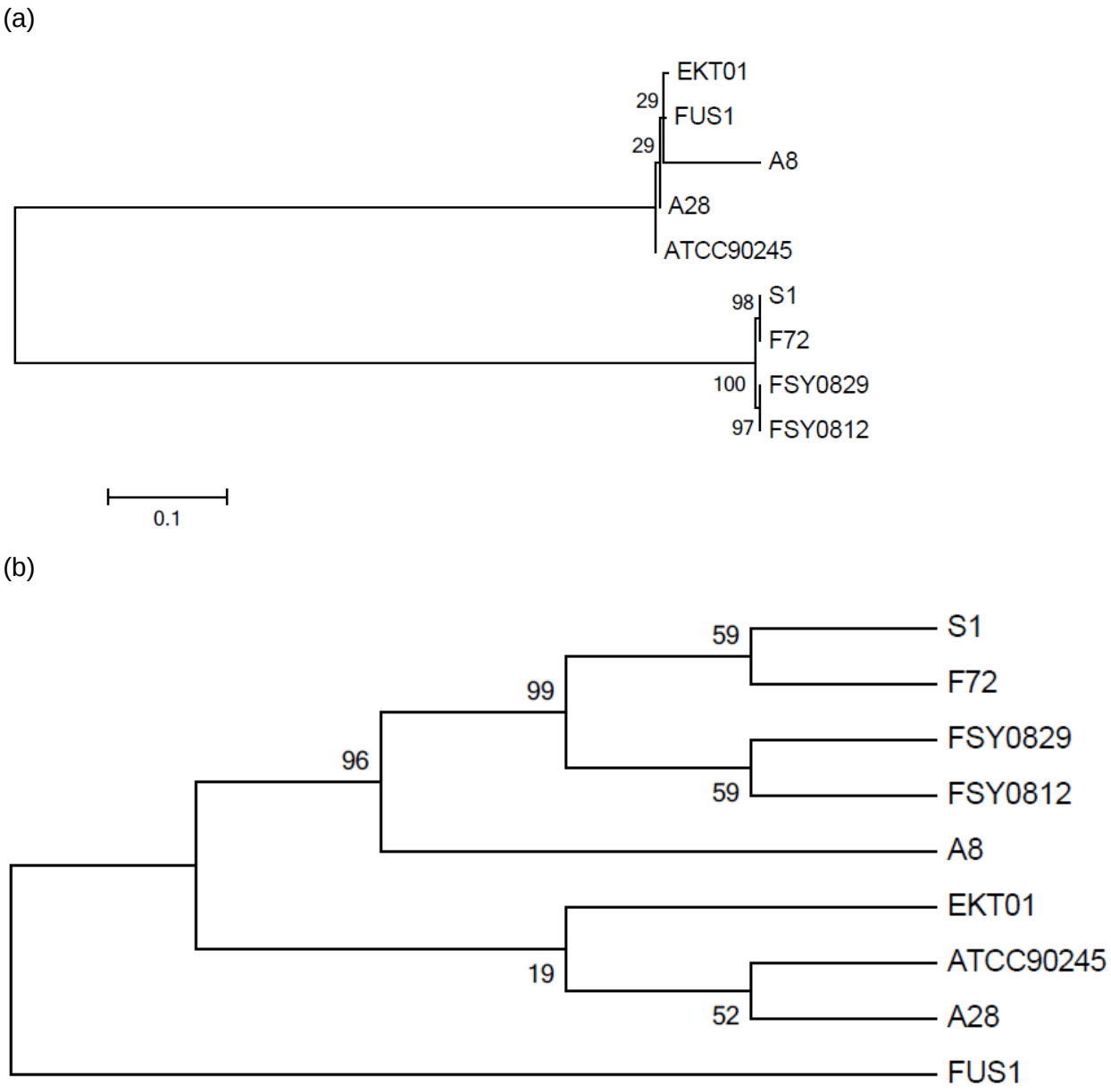

Figure 4. 2: (a) Maximum Likelihood trees of TEF 1-α genes; (b) One of 25 parsimony trees from TEF 1-α

Sequence alignment characteristics indicated that there are numerous conserved, variable and parsimony informative sites in TEF 1-α data than in ITS data. Meanwhile, there are numerous degeneratory sites (zero-fold, two-fold & four-fold) in ITS data which makes them more tolerant to point mutation by maintaining their hydrophobicity/hydrophilicity through amino acid substitution (see Table 4.2).

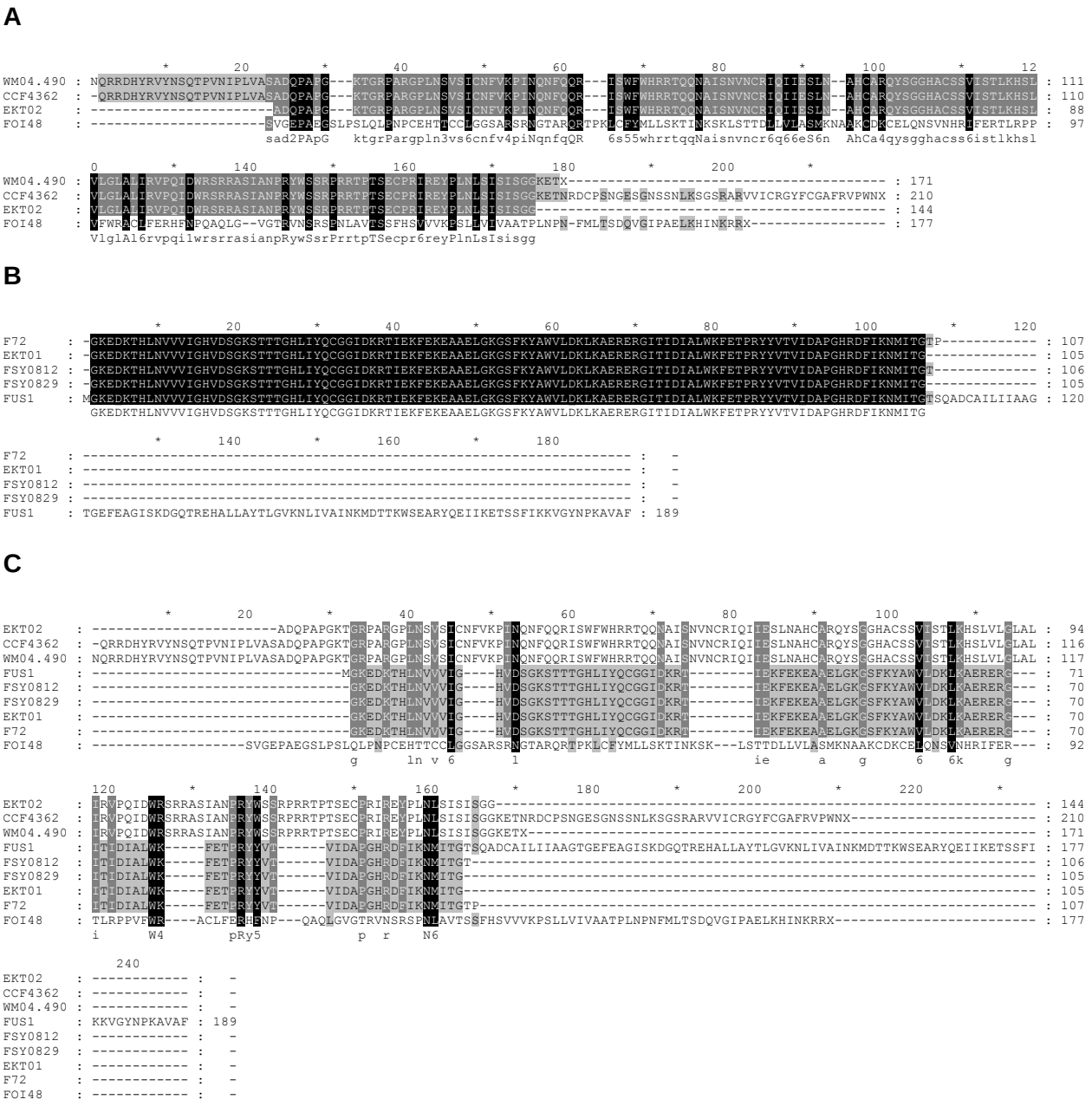

Figure 4. 3: Amino acid alignment of (a) ITS genes, (b) TEF 1-α genes and (c) Combined TEF 1-α and ITS gene.

Furthermore, an estimation of the evolutionary distance between nucleotide sequences showed the mean diversity within subpopulation as 0.292, interpopulation diversity as 0.524 and mean distance within the group for TEF 1-α and ITS as 0.573 and 0.010, respectively.

This indicated high similarities among the ITS genes. The overall average was 0.816 with a high coefficient of differentiation of 0.581 ± 0.012. The highest genetic disparity value of 2.294, which was observed from TEF 1-α gene sequences was observed between the pairs, A28/FSY0812, A28/FSY0829, EKT01/FSY0812 and EKT01/FSY0829. Similarly, most of the significant P-values are from the TEF 1-α sequence except for the pairs of EKT01/Ecu311 and Sa/1/2/A28 with values of 0.046 and 0.048, respectively, which showed that the sequences did not evolve from the same pattern of substitution. Meanwhile most of the ITS sequences evolved from the same substitution pattern –see Table A2 (Appendix).

Table 4. 2: Sequence alignment characteristics from individual TEF 1-α and ITS partitions and combined datasets

Dataset	Cons. Sites[a]	Var. Sites[b]	Pars. Info. Sites[c]	Singleton Sites[d]	0-fold Sites[e]	2-fold Sites[f]	4-fold Sites[g]
TEF 1-α	699	402	374	28	681	138	128
	54.87%	31.55%	29.36%	2.20%	53.45%	10.83%	10.05%
ITS	626	66	2	64	728	195	186
	49.14%	5.18%	0.16%	5.02%	57.14%	15.31%	14.60%
TEF 1-α +	362	763	553	208	759	106	119
ITS	28.41%	59.89%	43.41%	16.33%	59.58%	8.32%	9.34%

[a)] Number of conserved sites, [b)] Number of variable sites, [c)] Number of parsimony informative sites, [d)] Number of singleton sites, [e)] Number of zero-fold sites, [f)] Number of two-fold sites, and [g)] Number of four-fold sites.

4.4.2 Biochemical reactions

The biochemical methods of distinguishing fungi and/or pathogenic fungi functionality are slowly being developed due to varied morphology in environmental isolates. However, when yeast with a reduced morphology and standard biochemical procedure is considered, the classification is very clear; hence, the use of the VITEK® 2 Compact 30 system cards with emphasis on the YST card. The biochemical reactions ascertained the multi-enzyme capability of the isolate which was dominated by aminopeptidases. Table A3 (Appendix) indicates the assimilation of different carbohydrates such as Gentiobiose, D-Glucose, D-Maltose, L-Sorbose, L-Rhamnose, D-Turanose, D-Trehalose, L-Arabinose, Glucuronate, and nitrate by the isolate.

4.4.3 Isolate growth in heavy metals and free cyanide

The EPS recovered from isolate incubated on nutrient broth was miniscule (2 mg) compared with 40 mg from cultures supplemented with wastewater containing CN^- and heavy metals. The growth of the isolate was impaired in cultures supplemented with heavy metals, with the exception of Fe^{3+} cultures which showed to be highly tolerant of the contaminant at 1 mM. Arsenic (As) and CN^- showed a greater inhibitory effect on the microbial growth of the isolate

both with and without EPS. The supplementation of the EPS improved the growth of the isolate, see –Figure 4.4. This suggested the ability of the isolate to protect itself against variations in toxicant concentration, an admirable trait suited for mining wastewater bioremediation.

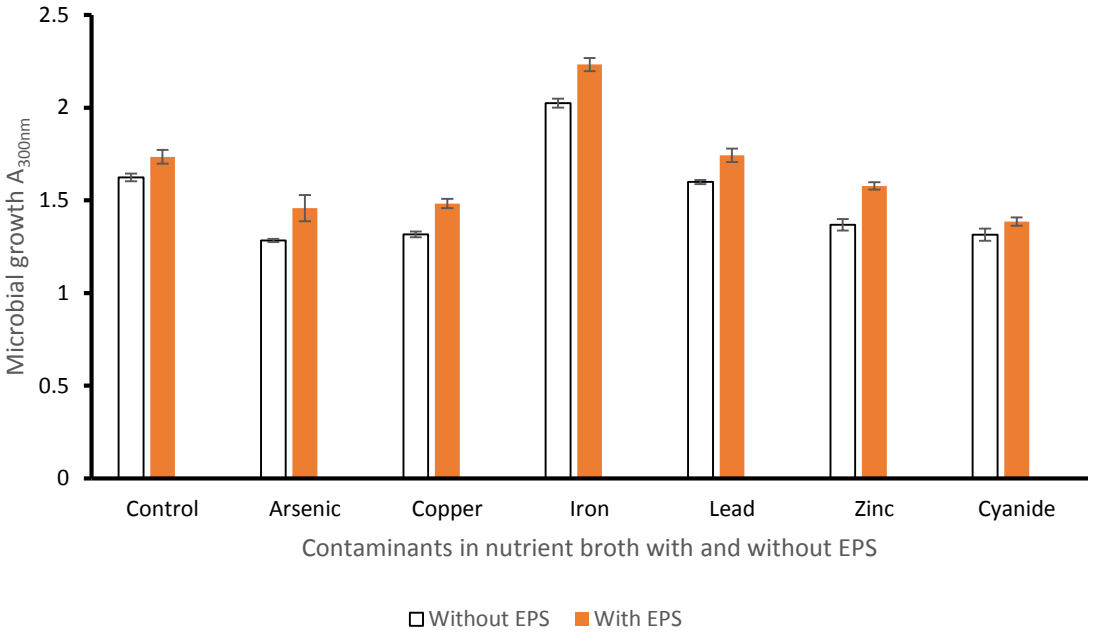

Figure 4. 4: *F.oxysporum* EKT01/02 growth in heavy metals and free cyanide

4.4.4 Free cyanide removal and scanning electron micrographs

The isolate showed degradation efficiency of 77.6% within five days from an initial free cyanide concentration of 100 mg CN^-/L (see Fig. 4.5). The free cyanide loss owing to volatilisation was less than 10% with residual ammonium-nitrogen and nitrate-nitrogen being 30.1 mg/L and 0.2 mg/L, respectively. The accumulation of ammonium suggested a hydrolytic mechanism utilisation in the cyanide biodegradation process by the isolate (Akcil 2003, Ebbs 2004). The micrographs showed that the microbial biomass is embedded in extracellular polymeric substance (EPS) which plays a major role in the structural integrity of the biofilm formed; hence, its resistance to toxicants (see –Fig. 4.6). Similarly, the biomass from the culture without CN^- appeared physically distinct from that exposed to CN^-. The solute well is bigger with more gums which improves nutrient uptake in biofilms with CN^- as the biomass adjusted to the inhibitory effect of the CN^- and heavy metals.

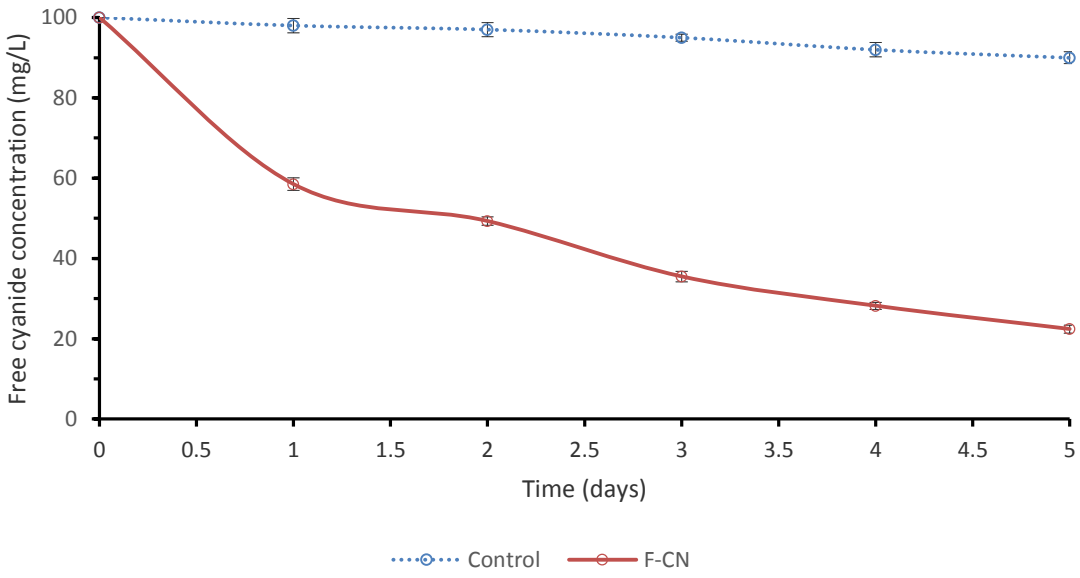

Figure 4. 5: Free cyanide degradation profile of the isolate

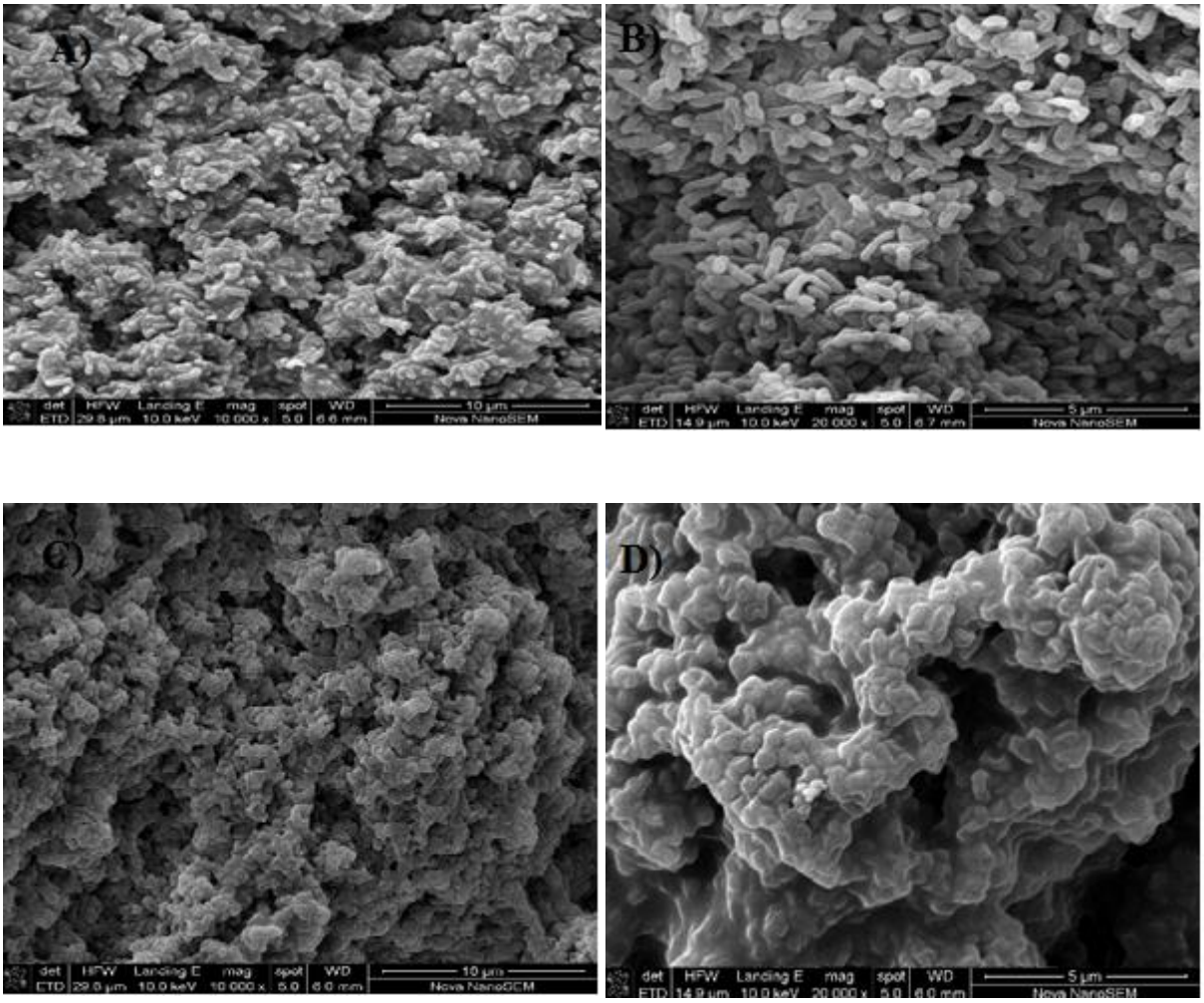

Figure 4. 6: Scanning electron micrographs of *Fusarium oxysporum* biofilm from cultures without cyanide (A-B) and those with cyanide (C-D)

4.5 Discussion

This study showed that the TEF 1-α and ITS primers can be used to elucidate the characteristic of the isolate. Previous reports on *F. oxysporum f.* sp*. cubense* showed that molecular genetic techniques could be used to determine a phylogenetic relationship (O'Donnell et al. 1998). Similarly, the phylogenetic analysis clearly distinguished the two primers used from each other. The tree analysis of TEF 1-α was very similar to that of Bogale *et al*. (Bogale et al. 2006) since we also reported a very high consistency index, retention index and a composite index which corresponded with the non-pathogenic *Fusarium oxysporum* isolate FUS1 (Taylor et al. 2016). The isolate was a part of the P-loop NTPases superfamily which are characterised by conserved nucleotide phosphate-binding motifs known as Walker A and B motifs that bind to the beta-gamma phosphate moiety of the bound nucleotide adenosine triphosphate/guanosine triphosphate (ATP or GTP) and magnesium ion (Mg^{2+}), respectively.

There are two major structural classes of P-loop NTPases that are recognised in diverse cellular functions; namely, the kinase-GTPase (KG) class, which includes Ras-like GTPases, and an additional strand catalytic E (ASCE) class, which includes ATPases associated with a wide variety of activities (Marchler-Bauer et al. 2015). Although, simple sequence repeat (SSR), amplified fragment length polymorphisms (AFLPs), mitochondrial small subunit (mtSSU), randomly amplified polymorphic DNA (RAPD) and TEF 1-α are used to characterise *Fusarium* sp. (Baysal et al. 2010, Bogale et al. 2006, O'Donnell et al. 1998, Voigt et al. 1995) which are based on pathogenicity/non-pathogenicity, only Baysal *et al*. (2010) reported a similar high coefficient of differentiation for *Fusarium oxysporum* strains using ISSR and RAPD primers. This present study is the first report that had utilised the combination of TEF 1-α and ITS primers for *F. oxysporum* characterisation.

The dominance of aminopeptidase in the biochemical test was an indication of its suitability to survive nitrogen limitation conditions as shown in Table A3 (Sala et al. 2001). For instance, Leucine arylamidase, a type of aminopeptidase produced by this fungus isolate is a cellular enzyme that is common in bacteria and yeast, which helps to liberate amino acids from high molecular compounds (Müller et al. 2004, Chróst 1992). Similarly, β-Glucosidase is known for catalysing the hydrolysis of β-linked disaccharides of glucose, carbonmethylcellulose and celluhaxaose, better substrates than alkyl glycosides (Chróst 1992). In addition, most heavy metal tolerant microorganisms have been shown to express these enzymes in their quest for survival in polluted environments (Durve et al. 2012, Gadd 2010). The aminopeptidases produced by this isolate was an indicator of a wide range of substrate utilisation capabilities. Previously, Anuradha *et al*. (2010) have established the ability of *Fusarium* sp. to utilise

numerous carbohydrates for multi-enzyme production which was validated by other researchers (Anuradha et al. 2010, Akinpelu et al. 2015, Paper et al. 2013).

Furthermore, the higher EPS recovered in cultures supplemented with CN^- and heavy metals indicated that the EPS production system was a consequence of adaptation to the toxic environment which facilitated the isolate's ability to sustain its metabolic activity. The inhibitory effect of As and CN^- may be attributed to their tendencies to impede ATP production thereby disrupting oxidative phosphorylation (Kruger et al. 2013). Generally, microorganisms have different tolerance levels for heavy metals. Previous studies have indicated *Fusarium* sp. can tolerate most of these heavy metals up to 1000 mg/L (Durve et al. 2012, Jha et al. 2014, Verma et al. 2016). The concentration of the contaminants used in this study was higher compared with the report of Acheampong et al.(2013), thus this isolate could be explored to bioremediate cyanide containing gold mine wastewater. There are limited reports on fungal biofilms besides that of *Zygomycetes* sp. (Singh et al. 2011), *Aspergillus* sp. (Seidler et al. 2008, Mowat et al. 2009) and *Fusarium* sp. (Mukherjee et al. 2012, Peiqian et al. 2014, Huddy et al. 2015) which indicated that inhibitors such as CN^-, SCN^- and fungicides have adverse effect on the architecture of the *Fusarium* sp. The bigger solute wells within the biofilms of the isolate suggested minimal impact of the CN^- on the structural characteristics of the biofilm formed by the *F. oxysporum* isolate. The presence of CN^- within the biomass walls is a key factor in cellular respiration.

4.6 Summary

This part of the study reports on a cyanide resistant and/or tolerant fungus, isolated from a cyanide - (CN^-) containing pesticide environment. The isolate was identified both morphologically and phenotypically as *Fusarium oxysporum* EKT01/EKT02 (KU985430 and KU985431). In this study, DNA sequences obtained from TEF 1-α and ITS were used to study the genetic diversity of the isolate. The phylogenetic analysis classified the genes into three major groups. TEF 1-α gene showed a high disparity among pairs with putative conservative domain in amino acid sequences while the ITS gene showed high similarities with conservative substitution. The combined datasets showed a high coefficient of differentiation of 0.581 ± 0.012 and a high tolerance for mutation. A homogeneity test indicated that the ITS data-set evolved from the same pattern of substitution. The biochemical characteristic of the isolate was dominated by aminopeptidases. The extracellular polymeric substance from the isolate increased the isolate's growth in the presence of both CN^- and heavy metals. Gelatinous biofilms with bigger solute wells showed the response of the isolate to cyanide. This study also showed that the isolate possesses a wide substrate utilisation mechanism that could be

deployed in environmental engineering applications; in particular gold mining wastewater bioremediation.

The next chapter focuses on the substrate limitation of the *F. oxysporum* EKT01/02 cultured in refined carbon source (glucose) and agro-industrial waste (*Beta vulgaris*) including the optimisation of the bioremediation process for free cyanide containing wastewater while the isolate was grown exclusively on *Beta vulgaris* (beetroot).

CHAPTER 5

OPTIMISING THE BIOREMEDIATION OF FREE CYANIDE CONTAINING WASTEWATER BY *FUSARIUM OXYSPORUM* GROWN ON *Beta vulgaris* WASTE USING RESPONSE SURFACE METHODOLOGY

Published as: **Akinpelu, E. A**., Ntwampe, S. K. O., Mekuto, L. & Itoba Tombo, E. F. Optimizing the bioremediation of free cyanide containing wastewater by *Fusarium oxysporum* grown on beetroot waste using response surface methodology. *In:* Ao, S. I., Douglas, C. & Grundfest, W. S., eds. Lecture Notes in Engineering and Computer Science: Proceedings of the World Congress on Engineering and Computer Science, ISBN: 987-988-14048-2-4, 19-21 October 2016 San Francisco, USA. Newswood Limited, 664-670.

CHAPTER 5
OPTIMISING THE BIOREMEDIATION OF FREE CYANIDE CONTAINING WASTEWATER BY *FUSARIUM OXYSPORUM* GROWN ON *Beta vulgaris* WASTE USING RESPONSE SURFACE METHODOLOGY

5.1 Introduction

Industrial discharge contains a variety of contaminants from different anthropogenic sources. In most developing countries, more than 70% of industrial wastewater are disposed into usable water bodies which does not only pollute rivers but leach into the water table resulting in groundwater deterioration (Donato et al. 2007). This may not be detected for years as monitoring programmes are non-existent in most developing countries. A majority of the toxicants in industrial wastewater are generated from mining, pharmaceutical, petrochemical industries among others. Poorly treated wastewater discharge into fresh water bodies is common in developing countries due to cost implications of operating wastewater treatment plants.

Cyanide remains the preferred reagent for metal recovery from ores despite its toxicity, thus its presence in process wastewater is unavoidable. Several CN^- chemical treatment methods such as alkaline chlorination and copper catalyzed hydrogen peroxide oxidation amongst others, are being used in the mining industry (Dash et al. 2009). However, due to different challenges associated with poor treatment performance and infrastructure, addition of hazardous chemicals to the wastewater, excess precipitate accumulation, inability to remove ammonia and chlorides, including other species, makes microbial remediation of CN^- laden wastewater, a feasible alternative (Patil & Paknikar 1999).

There are several reports on biological treatment of cyanide containing wastewater, but a few mineral processing industries have adopted this approach. In addition to the Homestake Mine, (USA), for which this process was determined to be economically viable and sustainable for the treatment of cyanide containing wastewater (Stott et al. 2001), Biomin® Limited (South Africa) has recently designed a biological process known as the Activated Sludge Tailings Effluent Remediation (ASTER™) for the safe handling of cyanide containing wastewater in South Africa (Du Plessis et al. 2001, Huddy et al. 2015). Some of the microbial remediation methods have focused on the application of bacterial strains such as *Pseudomonas* sp. and *Bacillus* sp. (Luque-Almagro et al. 2005, Potivichayanon & Kitleartpornpairoat 2010) with few studies focusing on *Aspergillus* sp. and *Fusarium* sp. (Barclay et al. 1998, Santos et al. 2013). Although, this process is environmentally friendly, the nutrient requirements for sustenance of microbial proliferation on a large-scale is a challenge. To mitigate this challenge, an alternative

strategy is to utilise agro-industrial waste. When agro-industrial waste is disposed-off on land, its leachate enters water bodies, causing changes in the ecological biodiversity of the water bodies, increasing dead zones which results in eutrophication (Glibert et al. 2008, Nyenje et al. 2010). With the enormous agro-industrial waste being generated annually, some of which contains soluble sugars, trace elements and proteins, it is appropriate to use it to sustain microbial growth in cyanide biodegradation processes, an important factor to be considered for large scale bioremediation applications (Ntwampe & Santos 2013). *Beta vulgaris* (Beetroot) has been shown to contain more soluble sugars when used raw. *Fusarium oxysporum* has also been shown to produce numerous enzymes when grown on *B. vulgaris* (Anuradha et al. 2010). The compatibility of *B. vulgaris* and *F. oxysporum* EKT01/02 in the biodegradation of free cyanide in wastewater will be significant in the development of a suitable biological process.

5.2 Objectives

The objectives of this part of the study were to:

- Assess the response of *F. oxysporum* EKT01/02 to substrate limitation; and
- Optimise the operating conditions (pH, temperature and substrate concentration) for free cyanide biodegradation grown exclusively on *B. vulgaris* agro-industrial waste.

5.3 Materials and methods

Fusarium oxysporum EKT01/02 maintained on PDA at 4 ˚C was sub-cultured and used. Inoculum preparation and substrate limiting procedures, including agro-industrial waste and bioremediation of free cyanide containing wastewater procedures are as shown in chapter 3.

5.3.1 Central composite design

A Response Surface Methodology (RSM) assesses the influence of parameters in a process that leads to optimum performance. The central composite design (CCD) of RSM was used in this study for evaluating three variables; pH, temperature and substrate concentration which gives a minimum number of experimental runs for determining the optimal operating conditions for maximum free cyanide biodegradation. The range of variables (pH and temperature) was specified based on optimum values reported for most cyanide degrading fungi (Pereira et al. 1996, Santos et al. 2013). The range of the substrate concentration was based on the attainment of an exponential phase in a substrate-limiting experiment which was carried out on the isolated *F. oxysporum* –Fig. 5.1. The Design-Expert® software version 6.0.8 (Stat-Ease

Inc., USA) was used to generate the experimental design. A set of experiments (n = 20) was carried-out consisting of six center points, eight factorial points and six axial points at five different coded levels; -α, -1, 0, +1, and +α. All experiments were in triplicate and the mean of measured values was used to generate the response (*Y*), representing the cyanide biodegraded after 72 h.

$$Y = \alpha_0 + \sum_{i=1}^{n} \alpha_i X_i + \sum_{i=1}^{n} \alpha_{ii} X_i^2 + \sum_{i=1}^{n-1} \sum_{j=i+1}^{n} \alpha_{ij} X_i X_j + \varepsilon \quad (5.1)$$

where $X_1, X_2, X_3 \ldots, X_n$ are the independent coded variables, α_0 is the offset term, α_i, α_{ii} and α_{ij} is linear, squared and interaction effects, respectively. The quantity of free cyanide degraded and volatilized was quantified using a mass balance; Eq.5.2 and Eq.5.3, respectively.

$$CN_B^- = CN_I^- - CN_R^- - CN_V^- \quad (5.2)$$

$$CN_V^- = CN_{IC}^- - CN_{FC}^- \quad (5.3)$$

where CN_B^- is the bioremediated free cyanide; CN_I^- is the initial free cyanide concentration in the culture broth; CN_V^- is the free cyanide volatilized during incubation; CN_R^- is the residual free cyanide measured after incubation; CN_{IC}^- is the initial free cyanide in the control culture; CN_{FC}^- is the final free cyanide in control cultures i.e. culture free of any inoculum. In general terms, the control cultures were prepared under the same conditions as other cultures except that it was not inoculated with *F. oxysporum* EKT01/02. The samples were analysed using the photometric procedure stated in section 3.3.1.

Table 5. 1: Experimental design variables

Variables	Codes	Units	High	Medium	Low
Temperature	A	˚C	30	25	20
pH	B	-	11	8.5	6
Substrate concentration	C	mg/L	400	300	200

5.4 Results and discussion

5.4.1 Effect of the limiting substrate on *F. oxysporum* growth rate

The isolate's growth rate increased as the substrate concentration was increased up to a maximum growth rate at which the substrate concentration was 0.3 g/L in both refined and agro-industrial waste carbon source cultures. However, the maximum growth rate on *B. vulgaris* was higher compared with the growth rate on glucose -Fig. 5.1.

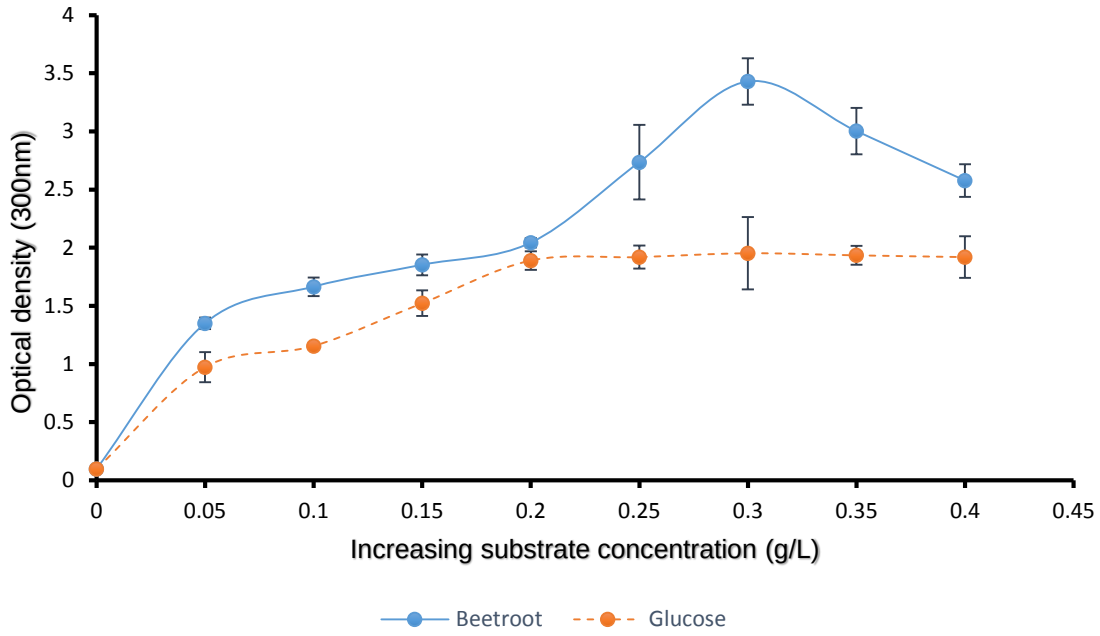

Figure 5. 1: Effect of limiting substrate concentration on the growth rate of *F. oxysporum* EKT01/02

This could be attributed to the treatment method used for the *B. vulgaris* which makes more soluble sugars available for the microbial growth as reported previously (Rodríguez-Sevilla et al. 1999, Wruss et al. 2015). Thus, the agro-industrial waste *B. vulgaris* was selected to be used for this research, as it also provided for the biphasic growth of the isolate used.

5.4.2 Central composite design response

The response of the individual and interactive effects of the three variables on free cyanide biodegradation is shown in Table 5.2. The results showed random variations in the responses measured, which suggested that the effect of operating conditions and culture components had a direct effect on the isolate's metabolic activity. The highest free cyanide degradation occurred at an axial point (Run 7); at temperature of 25°C, pH of 12.7 and a substrate concentration of 300 mg/L, where 180.90 mg CN^-/L was degraded from an initial 300 mg CN^-/L after 72 h of incubation. The center point (25°C, pH = 8.5, substrate concentration = 300 mg/L) also showed an appreciable quantity of free cyanide degradation of 166.5 mg CN^-/L corresponding to runs 3, 4, 6, 10, 16, and 17 which highly correlated (>99%) with the predicted values. Meanwhile, the lowest free cyanide biodegradation was observed at extremely low temperature, i.e. only 49.80 mg CN^-/L biodegraded at axial point (Run 20) which also recorded the highest level of free cyanide volatilization due to low temperature and a near neutral pH. The free cyanide volatilization was between 0.6 and 13 % over the period of incubation for all runs.

Furthermore, previous studies on *F. oxysporum* had reported free cyanide degradation at temperature of 25°C and pH of 8.0, with the differentiation in pH observed in these studies being attributed to the difference between the utilisation of a refined carbon source (Pereira et al. 1996, Campos et al. 2006) and the agro-industrial waste used in this study. Nonetheless, these studies all indicated that the isolate is alkaline pH tolerant thus is suitable for cyanide biodegradation. The substrate concentration corresponded to the optimum substrate concentration which can support the exponential phase growth observed in the substrate-limiting studies as shown in Fig. 5.1. This indicated the importance of sustaining microbial growth in the exponential phase for optimum biodegradation as validated by other reports (Mirizadeh et al. 2014, Mekuto et al. 2015).

In addition, factors affecting microbial free cyanide degradation besides nutrient requirements are pH and temperature. Generally, the free cyanide biodegradation was high at pH above 8.5 with the highest being at pH of 11 and 12.7; an indication of the isolate's tolerance for alkaline pH. Since free cyanide exist in the form of HCN at pH below 8, this might have impacted the level of interactions between the *F. oxysporum* and the *B. vulgaris* agro-industrial waste which invariably can affect the level of enzyme production during cyanide biodegradation (Anuradha et al. 2010; Rao et al. 2010). Similarly, the high initial free cyanide concentration also had an influence on the pH of the culture and free cyanide biodegradation. Free cyanide degradation has been found to be independent of pH at pH < 6 for initial free cyanide concentration of 26 mg CN^-/L, while between pH of 7 and 11, free cyanide biodegradation was dependent on pH (Huang et al, 1977). The impact of temperature on free cyanide biodegradation was observed to be high at > 20 ˚C. This concurred with preceding reports that free cyanide biodegradation increases with an increase in temperature for most microorganisms except for *Pseudomonas* sp. (Adams et al. 2001).

However, some runs (5, 13, 15, and 20) showed extremely low cyanide biodegradation; an indication of slow and/or minimal microbial growth resulting from low temperature and/or unsuitable pH which is known to facilitate cyanide efficacy as a metabolic inhibitor (Barclay et al. 1998, Zou et al. 2014). The residual ammonium-nitrogen and nitrate-nitrogen observed were considerably low especially at low pH and/or temperatures. It was hypothesized that the isolate was utilizing these by-products during unfavorable conditions. Based on the results in Table 5.2, it would be prudent to optimize around the center point for optimum free cyanide biodegradation, particularly when the influent quality fluctuates.

5.4.3 Statistical model analysis

The statistical model clarifies the fitness of mean and quadratic models using the Sequential Model Sum of Squares and a Lack-of-Fit Test for the responses measured after 72 h. The free cyanide response was further optimized around the center point since it gives minimal residual ammonium-nitrogen and nitrate-nitrogen. The responses were analyzed using ANOVA to assess the significance of each variables in the model –Table 5.3. A quadratic model was obtained from Eq. 5.1 that relates the free cyanide biodegraded with the independent variables.

Table 5. 2: Coded experimental design variables and responses

Runs	A	B	C	CN^- biodeg. (mg/L) Expt. Value	CN^- biodeg. (mg/L) Pred. value	Res. NH_4-N (mg/L)	Res. NO_3-N (mg/L)
1	0	0	α	94.86	100.88	36.40	2.00
2	1	-1	1	102.00	109.36	46.40	15.67
3	0	0	0	166.50	166.62	30.10	2.67
4	0	0	0	166.50	166.62	30.10	2.67
5	-1	-1	-1	76.20	86.61	54.70	2.00
6	0	0	0	166.50	166.62	30.10	2.67
7	0	α	0	180.90	166.90	32.30	36.33
8	0	0	-α	112.29	102.05	37.10	1.00
9	1	1	-1	104.94	129.14	26.10	5.33
10	0	0	0	166.50	166.62	30.10	2.67
11	0	-α	0	120.60	130.39	39.30	2.50
12	α	0	0	117.60	110.99	36.90	4.00
13	-1	1	1	90.00	103.57	65.00	3.67
14	1	-1	-1	128.10	117.51	40.10	2.67
15	-1	-1	1	93.00	71.78	74.70	2.00
16	0	0	0	166.50	166.62	30.10	2.67
17	0	0	0	166.50	166.62	30.10	2.67
18	1	1	1	150.00	142.57	38.90	12.67
19	-1	1	-1	101.19	96.81	54.30	1.00
20	-α	0	0	49.80	52.20	41.40	7.33

Table 5. 3: ANOVA for free cyanide response quadratic model

Factors	Coeff. Estim	DF	Std. error	F value	Prob>F	Significance
Intercept	166.62	1	5.84	13.51	0.0002	S
A	17.48	1	3.88	20.33	0.0011	S
B	10.85	1	3.88	7.84	0.0188	S
C	-0.35	1	3.88	0.008	0.9304	NS
A^2	-30.06	1	3.77	63.48	<0.0001	S
B^2	-6.36	1	3.77	2.84	0.1230	NS
C^2	-23.03	1	3.77	37.27	0.0001	S
AB	0.36	1	5.06	0.0049	0.9453	NS
AC	1.67	1	5.06	0.11	0.7485	NS
BC	5.40	1	5.06	1.14	0.3116	NS

S = Significant; NS = Not significant; DF = Degree of freedom; "Prob>F" less than 0.05 indicates the model is significant while values greater than 0.1 indicates the model term is insignificant

The predicted response (Y) for the free cyanide biodegradation system was:

$$Y = 166.62 + 17.48A + 10.85B - 0.35C - 30.06A^2 - 6.36B^2 - 23.03C^2 + 0.36AB + 1.67AC + 5.40BC \quad (5.4)$$

where *A*, *B*, and *C* were the coded values for temperature, pH, and substrate concentration, respectively. The coefficient of interaction was estimated from the average of the two confidence levels. ANOVA also showed that five of the ten model terms were significant, using the data in Table 5.4, the predicted coefficient of determination (Pred. R^2) was not as close to the adjusted coefficient of determination (Adj. R^2) which was an indicator of a large block effect, thus a model reduction was considered in order to improve the model which gave Eq. 5.5:

$$Y = 166.62 + 17.48A + 10.85B - 30.06A^2 - 23.03C^2 \quad (5.5)$$

Table 5. 4: ANOVA for free cyanide biodegradation in CCD

Source of variation	Sum of squares	DF	Mean square	F-value	Significance
Regression	24948.39	9	2772.04	13.51	S
Residual	2051.44	10	205.14		
Lack of Fit	2051.44	5	410.29	0.000	
Pure error	0.000	5	0.000		
Cor. Total	26999.83	19			

Std.dev. = 14.32; R^2 = 0.9240; Adj. R^2 = 0.8556; Pred. R^2 = 0.3513; Adeq. Precision = 11.325

The quadratic regression model for the free cyanide biodegradation showed that the model was significant at 99.98%; an indication that the total variance in the response could be explained with the model. The Model F-value of 13.51 also supported the significance of the model, whereby there is only a 0.02% chance that a Model F-value this large could occur due to noise.

The adequate precision ratio of 11.325 observed was within a desirable range for signal-to-noise ratio, an indication of an adequate signal which could be used to navigate the design space. The calculated value of the coefficient of determination (R^2 = 0.9240) showed that 92% of the variations in the actual and predicted values can be explained by the model, with a high degree of correlation between the experimental and predicted values. This showed the accuracy and applicability of the model for predicting free cyanide biodegradation in the system designed. The suitability of the model was also confirmed by the non-significance of the F-value for the Lack-of-Fit Test (–see Table 5.4) and normality in the error term as shown in Fig. 5.2.

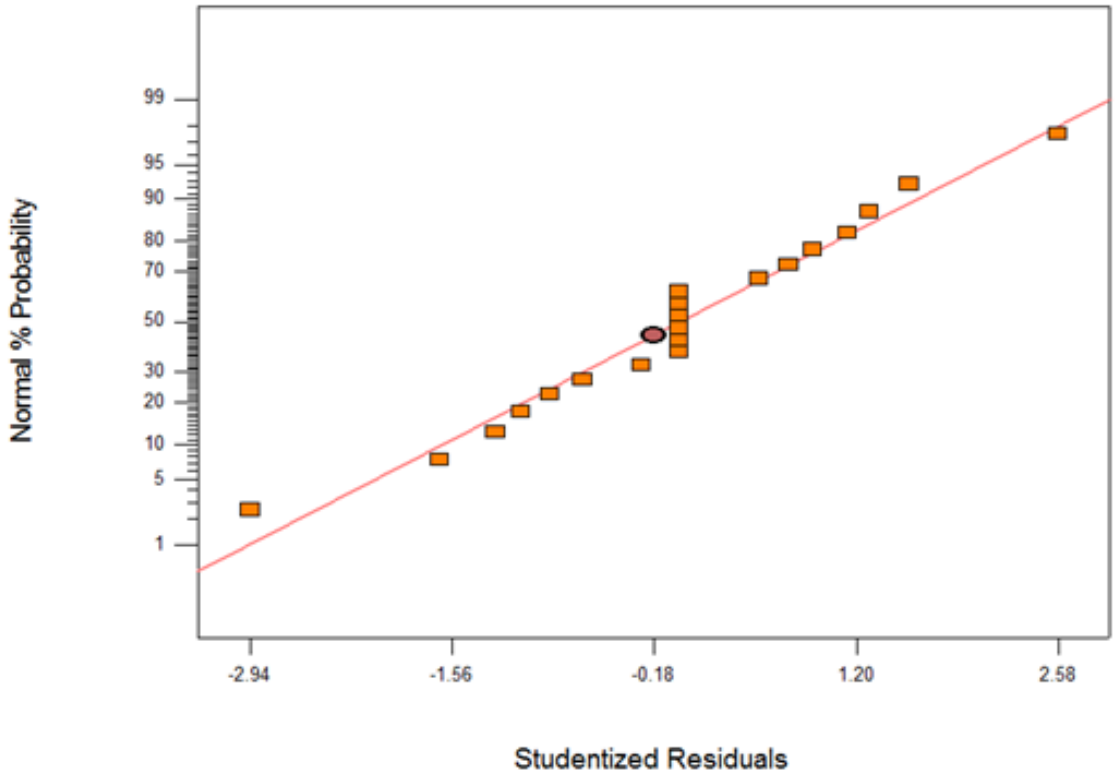

Figure 5. 2: Normal probability plot of the residuals

5.4.4 Graphical representation of the biodegradation model

The level of interaction between independent variables can be determined using 3-D and contour plots. A perfect interaction between two independent variable plots shows an elliptical contour shape while a circular contour represents a non-interactive effect on the system's response (Montgomery 2008)(Montgomery 2008)(Montgomery 2008). For easy of interpretation of experimental results and the prediction of optimum conditions, three-dimensional curves of the system's response was plotted against any two of the variables while keeping the third variable constant. This allows for the investigation of interactive effects of three independent variables on the system's response i.e. free cyanide biodegradation. The 3-D and contour plots for all the variable pairs are shown in Fig. 5.3. The center point was chosen as a constant value. The quantity of free cyanide biodegraded increased towards the center point with pH and temperature being the most important factors (Mirizadeh et al. 2014, Mekuto et al. 2015). The pair, temperature and pH at constant substrate concentration gave the highest free cyanide biodegradation.

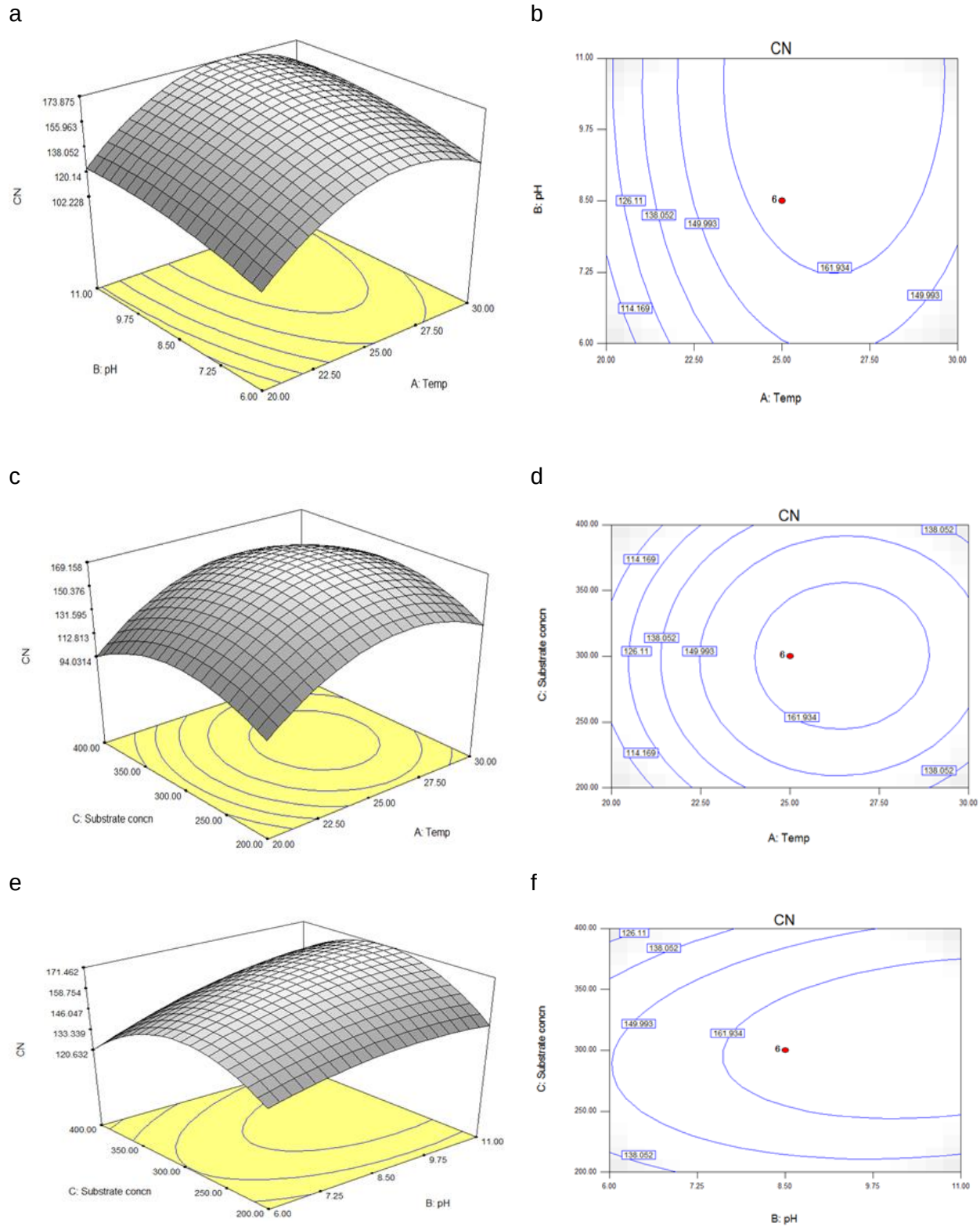

Figure 5. 3: 3-D plots a, c, and e and contour plots b, d, f showing the effect of independent variables on free cyanide biodegradation

5.4.5 Optimisation of the free cyanide biodegradation system

The optimization of the system's response was done using the numerical option of the Design-Expert® software. The input factors were combined by selecting the desired goal for each variable and the response to achieve peak process performance. In this analysis, all the independent variables, i.e. temperature, pH and substrate concentration were set within range, and the response was set at maximum since the desired optimum for the combined independent variables is the highest free cyanide biodegraded. Design-Expert® software gave a list of probable outcomes to match the criteria from the least to the most desirable. Fig. 5.4 shows the desirability ramp generated from 10 solutions through numerical optimization. The optimum point with the highest desirability was selected. Hence, the optimum point with maximum free cyanide biodegradation of 174.148 mg CN^-/L after 72 hours was found at temperature of 26.50°C, pH of 10.77 and substrate concentration of 310.89 mg/L.

Figure 5. 4: Desirability ramp for the numerical optimisation of free cyanide biodegradation

5.5 Summary

This part of the study reports the use of a cyanide resistant fungus; *Fusarium oxysporum* EKT01/02 for the bioremediation of wastewater containing free cyanide, its preference for *B. vulgaris* agro-industrial waste as the primary carbon source, and the optimisation of the free cyanide (CN^-) bioremediation conditions using statistical modelling. The *F. oxysporum* EKT01/02 growth observed on *B. vulgaris* agro-industrial waste showed the importance of mild treatment of the waste for maximum nutrient uptake for microbial growth. Higher growth rate

of *F. oxysporum* EKT01/02 was observed on *B. vulgaris* waste (OD = 3.430) compared to glucose (OD = 1.953). The cultures highest free cyanide biodegraded was 180.9 mg CN^-/L from an initial 300 mg CN^-/L after 72 h at 25°C, pH of 12.70, and a substrate concentration of 300 mg/L. The ANOVA of the quadratic model indicated the model obtained was highly significant (R^2 = 0.9240). The response from the central composite design (CCD) indicated that pH and temperature are the most significant factors affecting the CN^- biodegradation system designed. The residual ammonium-nitrogen and nitrate-nitrogen formed could serve as a nitrogen source for the isolate when operating conditions are optimised for a single stage nitrification and aerobic denitrification system since the isolate has capability for nitrate assimilation as shown in the biochemical analyses reported in chapter 4. Besides the biochemical and genetic analyses of the *F. oxysporum* EKT01/02 reported in chapter 4, there is a need for thermodynamic analysis of the process in which *F. oxysporum* EKT01/02 proliferation in cyanide containing wastewater is studied prior to the application in field-scale bioremediation. This is the focus of the next chapter (Chapter 6).

CHAPTER 6

BIOLOGICAL STOICHIOMETRY AND BIOENERGETICS OF *FUSARIUM OXYSPORUM* EKT01/02 PROLIFERATION USING DIFFERENT SUBSTRATES IN CYANIDATION WASTEWATER

Accepted as: **Akinpelu, E.A**., Ntwampe, S. K. O. & Bing-Hung, C. Biological stoichiometry and bioenergetics of *Fusarium oxysporum* EKT01/02 proliferation using different substrates in cyanidation wastewater. *The Canadian Journal of Chemical Engineering* DOI:10.1002/cjce.22935

CHAPTER 6
Biological stoichiometry and bioenergetics of *Fusarium oxysporum* EKT01/02 proliferation using different substrates in cyanidation wastewater

6.1 Introduction

Cyanidation wastewater from gold mining operations contains high concentrations of heavy metals, ammonia and cyanide. Although the wastewater can be bioremediated, few studies report on the stoichiometric and thermodynamic analysis of such processes.

Thermodynamic analysis can predict the feasibility of a metabolic reaction and suitable conditions under which such a reaction can occur, thus addressing the feasibility of the process being studied (Liu et al. 2007, Heijnen 2010). Similarly, few studies report on the stoichiometric analysis of microbial proliferation and yield in bioremediation processes, although these factors determine the effectiveness of such bioprocesses because they are dependent on the microbial metabolic functions including cellular respiration of the isolate used. Furthermore, the stoichiometric coefficients define the efficiency of a specific microbial species in a defined process. Introducing bioenergetic analysis in such processes can further elucidate the feasibility of reactions under observation.

Gibbs energy dissipation per C-mol of biomass produced has been used to determine the balance between growth efficiency and metabolic rates using different thermodynamic models of microbial growth to justify the relationship between Gibbs energy dissipation and other parameters as the driving force for microbial growth and biomass yield in the presence of toxicants (von Stockar et al. 2008, Gonzalez-Cabaleiro et al. 2015). Available literature on bioenergetics, including stoichiometric analysis of microbial growth, has largely focused on the use of refined carbon sources such as glucose, sucrose, ethanol and acetate, as substrates and/or electron donors, mostly in batch or fed-batch processes (Wlaschin & Hu 2006, Battley 2011, Watanabe & Isoda 2013, da Silva et al. 2016). Although this approach can quantify the amount of Gibbs energy required to generate suitable quantities of biomass to support bioremediation reactions by varying the carbon sources used, it does not adequately describe systems in which a green chemistry approach is advocated for, as reported in Akinpelu et al. (2016). Thus, the challenge is, to determine the energy requirements for a system in which a microorganism is grown on an agro-industrial waste in the presence of a metabolic inhibitor such as cyanide, particularly for the bioremediation of cyanidation wastewater.

There are several reports on microbial remediation of industrial wastewater with numerous species of bacteria, fungi, algae and protozoa for the treatment of cyanidation wastewater

(Kandasamy et al. 2015, Khamar et al. 2015, Mekuto et al. 2016a). Although the process is adjudged to be robust and environmentally benign, few mineral processing industries have adopted this treatment process due to the nutritional requirements essential for microbial growth on a large scale. The future of microbial remediation of wastewater depends on studies that identify renewable substrates such as agro-industrial waste for microbial growth in bioremediation systems on a large scale. With the large quantity of agro-industrial waste generated annually from processing of agricultural produce, this challenge can be mitigated (Gustavsson et al. 2011).

For bioremediation processes, agro-industrial waste can be used to provide sufficient macro- and micro-nutrient and/or carbon sources for microbial growth including biocatalytic functions to decontaminate wastewater. The presence of micro- and macro-nutrients such as proteins, soluble sugars and minerals in agro-industrial waste can replace the use of refined carbon sources (Rodríguez-Sevilla et al. 1999, Mussatto et al. 2012). Furthermore, applying bioenergetics and biological stoichiometric analyses to systems in which agro-industrial waste is used can further demonstrate the appropriateness of using suitable agro-industrial waste in large scale wastewater treatment plants.

6.2 Objectives

The objectives of this part of the study was to promote the use of renewable feedstock in the bioremediation of cyanidation wastewater by applying biological stoichiometric and bioenergetic models to determine the functionality including requirements for a *F. oxysporum* EKT01/02 previously determined to be suitable for cyanide degradation in chapter 5 by investigating the growth of *F. oxysporum* EKT01/02 on: 1) glucose with ammonia as a nitrogen source (GA); 2) *Beta vulgaris* with ammonia as a nitrogen source (BA); and 3) *Beta vulgaris* with cyanide as a nitrogen source (BCN).

6.3 Materials and methods

The agro-industrial waste (*B. vulgaris*) preparation, inoculum, and experimental culture conditions are as shown in chapter 3 (sections; 3.2.4, 3.2.5, and 3.2.8). The dry biomass elemental and combustion analysis are as described in chapter 3. All experiments were in triplicate, reproducibility was expressed as a standard deviation obtained from the data set (n = 3). Normality of sample distribution was assessed using Shapiro-Wilk's test ($p>0.05$) (Shapiro & Wilk 1965, Razali & Wah 2011) with inspection of skewness and kurtosis measures and standard errors (Cramer & Howitt 2004, Doane & Seward 2011), including visual

inspection of box plots, histograms and normal Q-Q plots. Test of equality of variances in samples (homogeneity of variance) ($p>0.05$) was done using parametric and non-parametric Levene's test for approximately normally and non-normally distributed sample data respectively (Nordstokke & Zumbo 2010, Nordstokke et al. 2011). The statistically analyses were performed in an IBM Statistical Package for the Social Sciences (SPSS) software v24.0.

6.4 Theory

6.4.1 Stoichiometric microbial analysis

Microbial growth models represent a material balance of the system in compliance with the law of conservation of mass. The overall stoichiometry of a biological reaction can be estimated using either the method of half reactions or regularities (Battley 1999b, Duboc et al. 1999a). The general form of such a biological stoichiometric reaction was described by Eq. 2.1 (Liu et al. 2007) which by sequentially decoupling the overall reaction into catabolic and anabolic reactions, we have Eq.(s) 2.16 & 2.17.

Furthermore, each empirical model was converted to a unit carbon elemental formula and the molecular weights were estimated as shown in Table 6.2. For the microbial growth model using glucose (GA cultures), the molar yield coefficient (MYC) was expressed as the ratio of molar growth yield (dry weight of biomass grown per mole of substrate utilised) to the molecular weight of biomass containing a unit carbon was 3.126 C-mol per mole of glucose. Thus, the growth equation became (Eq. 6.1):

$$C_6H_{12}O_{6(aq)} + aNH_{3(aq)} + bO_{2(aq)} \rightarrow dCO_{2(aq)} + eH_2O_{(l)} + 3.126CH_{1.167}N_{0.067}O_{0.558} \qquad (6.1)$$

The four unknown stoichiometric coefficients (*a, c, d* & *e*), were estimated from an elemental balance using the conservation of mass relationship. However, since the molecular weight of the agro-waste, i.e. *B. vulgaris* is unknown, a different approach was used. *B. vulgaris* contains about 9.56 % readily oxidisable carbohydrates (USDA 2016); hence, the general formula for a carbohydrate n(CH_2O) was used to represent the agro-waste in models used. The experimental microbial yield based on the quantity of carbon source used $\left(Y_{X/S}\right)$ determined as 0.623 and 0.425 for ammonia as the nitrogen source (BA cultures) and *B. vulgaris* agro-waste with cyanide (CN^-) as the nitrogen source (BCN cultures) experiments respectively, were used. The reciprocal of the experimental biomass yield accounts for the C-mole of n(CH_2O) consumed to produce 1 C-mole of biomass which was thus quantifiable. The stoichiometric

coefficients (*p, q, r, s, v, w, x*, & *y*) in Eq.(s) 6.2, & 6.3 were thus stoichiometrically balanced using an elemental analysis approach.

$$1.605CH_2O_{(aq)} + pNH_{3(aq)} + qO_{2(aq)} \rightarrow rCO_{2(aq)} + sH_2O_{(l)} + CH_{2.377}N_{0.091}O_{1.093}(cells) \quad (6.2)$$

$$2.353CH_2O_{(aq)} + vCN^-_{(aq)} + wO_{2(aq)} \rightarrow xCO_{2(aq)} + yH_2O_{(l)} + CH_{1.82}N_{0.027}O_{0.804}(cells) \quad (6.3)$$

6.4.2 Energy balances for biological systems

The biological stoichiometry of a defined process is incomplete without the exploratory analysis of an energy balance. The standard enthalpy of formation (ΔH_f^O) and Gibbs energy (ΔG_f^O) values (at pH = 7, 1 atm and 298 K) available in literature -Table 6.1, were used for bioenergetic models taking into account the stoichiometric coefficients from the microbial models to determine the heat of reaction(ΔH_{RX}^O). Furthermore, to determine experimental values for biomass enthalpy of formation (ΔH_f^{cell}), including heat of combustion (ΔH_c^{cell}) were obtained as described in chapter 2, from which a model representing the combustion of a unit mass of biomass can be derived. The biomass enthalpy of formation was calculated for an ion containing carbon mole (ICC/mole) by multiplying the heat of combustion of the dry biomass with the mass of 1 C-mole biomass as shown in Eq. 6.4:

$$\Delta H_f^{cell}\left(\frac{kJ}{mol}\right) = \Delta H_c^{cell}\left(\frac{kJ}{g}\right).M_X \quad (6.4)$$

where M_X is the mass of 1 C-mole of the dry biomass. The heat of reaction evolved in the synthesis of 1 C-mole of biomass was calculated using Hess's Law (Eq. 2.10)

Table 6. 1: Thermodynamic properties of compounds used at 298.15 K and 1 atm (Battley 1999b)

Substance	Formula	ΔH_f^O (kJ/mol)
Glucose	$C_6H_{12}O_{6(aq)}$	-1263.07
Ammonia	$NH_{3(aq)}$	-80.29
Oxygen	$O_{2(aq)}$	-12.09
Water	$H_2O_{(l)}$	-285.83
[a]Cyanide ion	$CN^-_{(aq)}$	140.3

[a]The data was adapted from (Finch et al. 1993)

Moreover, from the second law of thermodynamics, an increase in temperature result in an increase in the random molecular energy within a substance, thus its entropy. Therefore, the change in the entropy during microbial growth can be determined by quantifying the thermal energy of a known mass of dry biomass using a low temperature calorimeter. For a biological process, the temperature is usually from absolute zero to 298.15 K as represented in Eq.2.12.

This entropy of reaction can then be used with the enthalpy of reaction above to calculate the Gibbs free energy of the biomass and subsequently, result in the resolution of the model in Eq. 2.15.

Once the bioenergetic properties of the inputs and outputs are known, values of $\Delta G, \Delta H,$ and ΔS can be estimated for microbial growth models. The quantity of Gibbs energy needed to synthesise 1 C-mole of microbial biomass has been previously modelled by Heijnen and van Dijken (1992 & 1993) using an empirical correlation. Their findings indicated Gibbs energy of a reaction $\left(\Delta G_{RX}^{O}\right)$ for synthesizing 1 C-mole of biomass depends majorly on the degree of reduction (γ_s) of the carbon donor and the number of carbon atoms as expressed in the model -Eq. 2.19 (Heijnen & Van Dijken 1992, Heijnen & van Dijken 1993).

6.4.3 Quantifying microbial growth and bioenergetic kinetic parameters

The Gibbs energy dissipation for biomass growth and maintenance $(1/Y_{GX})$ was estimated – Eq.6.5 Heijnen (2002):

$$\frac{1}{Y_{GX}} = \frac{1}{Y_{GX}^{max}} + \frac{m_G}{\mu} \tag{6.5}$$

where $1/Y_{GX}^{max}$ was the Gibbs energy requirement for synthesising a unit C-mole of biomass as defined in Eq. 2.19, with m_G being the maintenance Gibbs energy, approximated to 4.5 kJ C-mol^{-1} h^{-1} at 298K. The specific microbial growth rate (μ) was estimated using Eq. 6.6:

$$\mu = \frac{1}{t_n - t_{n-1}} \ln\left(\frac{X_n}{X_{n-1}}\right) \tag{6.6}$$

where X_n and X_{n-1}were biomass concentrations (g dry biomass weight/L) at times $t_n \; and \; t_{n-1}$ (h), respectively.

6.5 Results and discussion

6.5.1 Elemental analysis

Elemental analysis of the biomass (Table 6.2) showed the percentages of ash, *C, H*, *N* and *O* are similar for all cultures studied. The mass fraction of sulphur, potassium, phosphorus and other ions was not considered. Previous studies have shown that these constituents only

contribute minorly to the empirical formula as their inclusion only affects the composition associated with the oxygen fraction of the biomass (Duboc et al 1999, Battley 2009). The hydrogen and carbon fractions of the *F. oxysporum* biomass grown on BA and BCN was determined to be relatively constant (6.22% and 36.07%, respectively) by dry weight. In contrast, the nitrogen content differed for cultures grown on BA and grown on BCN, which was attributed to the different nitrogen source (ammonia and cyanide). The nitrogen content of the dry biomass for GA and BA cultures was statistically similar (average = 3.47%). The ash content for cultures grown on *B. vulgaris* (average = 10.46%) differed from those that were grown on glucose (12.98%). Although, the average values of ash and hydrogen in BA and BCN differ, the t-test showed that the results in Table 6.2 were statistically indifferent. Comparing with similar filamentous fungi in Table 6, the percent fractions of *C, H, N* and ash constituents of *F. oxysporum* concurred with Duboc et al report even with the *B. vulgaris* agro-industrial waste (Duboc et al. 1999a).

Table 6. 2: Elemental analysis of dry biomass as a mass fraction (g per 100 g dry biomass) measured in triplicate. The standard deviation is indicated in the parenthesis

Substrate	f_{ash}	f_C	f_H	f_N
GA	12.98 (±0.04)	45.24 (±0.03)	4.40 (±0.06)	3.53 (±0.03)
BA	10.73 (±0.02)	32.33 (±0.02)	6.41 (±0.01)	3.42 (±0.01)
BCN	10.19 (±0.02)	39.82 (±0.03)	6.04 (±0.03)	1.24 (±0.03)
[b]*A. niger*	8.77(±0.05)	46.18(±0.30)	6.17(±0.13)	5.16(±0.25)
[b]*Mucor rouxii*	9.57(±0.01)	50.35(±0.21)	7.52(±0.06)	3.91(±0.05)
[b]*P. chrysogenum*	21.13(±0.90)	51.14(±0.13)	7.95(±0.02)	4.78(±0.05)
[b]*N. crassa*	8.48(±0.02)	48.17(±0.07)	7.22(±0.02)	7.14(±0.03)

[b]Adapted from Duboc et al. (1999)

The mass of 1 C-mole of biomass and the elemental formula were quantified to be within the range of previous research –Table 6.3. The higher C-molar mass (33.14 g C-mole) observed when cultures were grown on agro-industrial waste can be attributed to the excess macro- and micro nutrients available within *B. vulgaris* which were not present in the refined carbon source used and/or the rigidification of the fungal cell membranes including accumulations of extracellular polymeric substances, as the biomass strived to protect itself from cyanide toxicity. The degree of reduction indicates there are more available electrons during cyanide biodegradation which may be linked to the constituents available in *B. vulgaris* (Pavan Kumar et al. 2015). The degree of reduction on agro-waste (BA) is similar to cultures in which glucose was used, an indication that use of using agro-industrial waste as a carbon source has minimal impact on the performance of the cultures. The degree of reduction and dry biomass weight of various filamentous fungi from Duboc et al (1999) corresponds with the results of this study in Table 6.3.

Table 6. 3: Elemental formula of filamentous fungi with mass of 1 C-mole for dry biomass (M_X) and the degree of reduction (γ). The standard deviation is indicated in parenthesis

Fungi	Carbon source	Elemental formula	M_X	γ
[a]*F. oxysporum*	Refined (GA)	$CH_{1.167}N_{0.067}O_{0.558}$	23.03 (±0.12)	3.850 (±0.05)
[a]*F. oxysporum*	Agro-waste (BA)	$CH_{2.377}N_{0.091}O_{1.093}$	33.14 (±0.31)	3.918 (±0.04)
[a]*F. oxysporum*	Agro-waste (BCN)	$CH_{1.82}N_{0.027}O_{0.804}$	27.06 (±0.28)	4.131 (±0.06)
[b]*N. crassa*	Refined	$CH_{1.80}N_{0.13}O_{0.45}$	24.91	4.52
[b]*P. chrysogenum*	Refined	$CH_{1.87}N_{0.08}O_{0.22}$	23.47	5.18
[b]*M. rouxii*	Refined	$CH_{1.79}N_{0.07}O_{0.43}$	23.83	4.74
[b]*A. niger*	Refined	$CH_{1.60}N_{0.10}O_{0.55}$	25.98	4.22

[a]This study, [b]adapted from Duboc et al. (1999)

6.5.2 Microbial growth model

The microbial growth models used to represent the aerobic growth of *F. oxysporum* on GA, BA, and BCN are shown in Table 6.4. They are organized into catabolic, anabolic and overall metabolic stoichiometric reactions. The catabolic equations represent the oxidation of the carbon source (glucose or *B. vulgaris*). The nitrogen source (ammonia or cyanide) reacts with the catabolic products to produce biomass as shown in the anabolic equations. In reality, catabolic and anabolic processes are interdependent during growth, although they are theoretically constructed independently to elucidate the metabolism process. The overall metabolic description of a process is required to describe the actual biomass generated even for bioremediation studies.

Table 6. 4: Microbial growth equations for aerobic growth of *F. oxysporum* on GA, BA, and BCN based on suggested model equations 2.18 and 2.19

Growth on GA
Catabolism:
$C_6H_{12}O_{6(aq)} + 6O_{2(aq)} \rightarrow 6H_2O_{(l)} + 6CO_{2(aq)}$
Anabolism:
$1.511H_2O_{(l)} + 3.126CO_{2(aq)} + 0.209NH_{3(aq)} \rightarrow 3.126CH_{1.167}N_{0.067}O_{0.558}(cells) + 3.009O_{2(aq)}$
Metabolism:
$C_6H_{12}O_{6(aq)} + 0.209NH_{3(aq)} + 2.991O_{2(aq)} \rightarrow$
$2.874CO_{2(aq)} + 4.489H_2O_{(l)} + 3.126CH_{1.167}N_{0.067}O_{0.558}(cells)$
Growth on BA
Catabolism:
$CH_2O_{(aq)} + O_{2(aq)} \rightarrow H_2O_{(l)} + CO_{2(aq)}$
Anabolism:
$0.655H_2O_{(l)} + 0.623CO_{2(aq)} + 0.057NH_{3(aq)} \rightarrow 0.623CH_{2.377}N_{0.091}O_{1.093}(cells) + 0.61O_{2(aq)}$
Metabolism:
$CH_2O_{(aq)} + 0.057NH_{3(aq)} + 0.390O_{2(aq)} \rightarrow$
$0.377CO_{2(aq)} + 0.345H_2O_{(l)} + 0.623CH_{2.377}N_{0.091}O_{1.093}(cells)$
Growth on BCN
Catabolism:
$CH_2O_{(aq)} + O_{2(aq)} \rightarrow H_2O_{(l)} + CO_{2(aq)}$
Anabolism:
$0.387H_2O_{(l)} + 0.414CO_{2(aq)} + 0.011CN^-_{(aq)} \rightarrow 0.425CH_{1.82}N_{0.027}O_{0.804}(cells) + 0.436O_{2(aq)}$
Metabolism:
$CH_2O_{(aq)} + 0.011CN^-_{(aq)} + 0.564O_{2(aq)} \rightarrow$
$0.586CO_{2(aq)} + 0.613H_2O_{(l)} + 0.425CH_{1.82}N_{0.027}O_{0.804}(cells)$

During catabolism, the oxidised carbon source provides for ATP required to catalyse the anabolic reaction. In turn the anabolism conserves the chemical energy contained within the carbon source. Therefore, metabolism can be said to be an energy conservation process i.e. all the non-thermal energy remaining within the carbon source for microbial growth processes (Battley 2013). Meanwhile, for complete aerobic oxidation of the substrate, a non-conservative process is followed with minimal non-thermal energy being required for the conservation of energy within biomass. The growth efficiency can be estimated as a quantifiable ratio between available electrons (AE) in conserved biomass to those that are available in the non-conservative reactions. The AE can be classified as a degree of reduction for a unit carbon atom. For growth on BCN, cyanide can be converted to cyanate by cyanide monoxygenase, followed by conversion of cyanate to ammonia and carbon dioxide with cyanate as catalyst. Alternatively, cyanide can be oxidised directly using cyanide dioxygenase to produce ammonia and carbon dioxide as shown in Equation 6.7 (Ebbs 2004, Ibrahim et al. 2016).

$$HCN_{(aq)} + O_{2(aq)} + 2H^{+}_{(aq)} + NAD(P)H \xrightarrow{cyanide\ dioxygenase} CO_{2(aq)} + NH_{3(aq)} + NAD(P)^{+} \qquad (6.7)$$

The ammonia by-product can be consumed with other by-products to generate biomass including the carbon dioxide from cyanide biocatalytic decomposition which accounts for the higher molar production of carbon dioxide observed in BCN cultures compared with those grown in BA. This contributes to the higher AE observed in the BCN cultures.

6.5.3 Bioenergetic parameters

In addition, changes in thermodynamic properties can be calculated although not precisely, by using the microbial growth models and known thermodynamic properties of reactants and products except for biomass for which a true standard state is unknown. The ΔH_c^{cell} determinations as described earlier in a bomb calorimeter were -12.23 ± 0.03, -13.15 ± 0.02, -15.54 ± 0.04 kJ/g for biomass obtained from GA, BA, and BCN cultures, respectively. The experimental enthalpy of combustion for *B. vulgaris* waste was -431.1 ± 0.3 kJ C-mol^{-1} (n = 6). Generally, Thornton's rule (Thornton, 1917) can be used for estimating heat of combustion of organic substances, as for many organic substances, their heat of combustion is directly proportional to the number of atoms of oxygen consumed during combustion, as described by Equation 2.10 was estimated as -435.96 kJ C-mol^{-1} which correlated to the experimental value (-431.1 kJ C-mol^{-1}) obtained while the equivalent electron transferred to oxygen using calorimetric value was 3.95.

The experimental values from bomb calorimetric combustion with the available thermodynamic properties listed in Table 6.1 were used to determine the changes in bioenergetic parameters accompanying the aerobic growth of the *F. oxysporum* isolate used as shown in Table 6.5. The more exothermic ΔH_f^{cell} calculated using Eq.6.4 indicated higher values for growth on *B. vulgaris* than on glucose as previously observed. The accuracy of these values is a function of the validity of the molecular formula of the carbohydrate used to represent the *B. vulgaris* agro-waste which has a direct influence on the accuracy of the bioenergetic parameter determinations.

Table 6. 5: Thermodynamic parameters of *F. oxysporum* growth in different substrates at 298.15 K and 1 atm.

Substrate	ΔH_f^{cell} (kJ C-mol^{-1})	ΔH_{RX}^{O} (kJ C-mol^{-1})	ΔG_{RX}^{O} (kJ C-mol^{-1})	ΔS_{RX}^{O} (kJ K^{-1} C-mol^{-1})
GA	-281.69 (±0.47)	-652.55 (±0.21)	-432.11 (±0.05)	-0.74 (±0.02)
BA	-435.78 (±1.04)	-132.59 (±0.14)	-471.19 (±0.03)	1.14 (±0.03)
BCN	-420.54 (±1.76)	-370.34 (±0.18)	-225.35 (±0.05)	-0.48 (±0.01)

The thermal energy change (ΔH_{RX}^{O}) representing the heat of reaction and the Gibbs energy change (ΔG_{RX}^{O}) shown in Table 6.4, is an indication of spontaneous metabolic processes in both refined and agro-industrial waste carbon source. Furthermore, from bioenergetic analysis, the growth on BA was hypothetically spontaneous at varying temperature due to negative enthalpy and positive entropy changes for such a system. This may be directly linked to other added nutritional value components such as proteins, vitamins, and other minerals besides the available carbohydrates which are available in the agro-industrial waste used thus can dissociate at different rates depending on the culture temperature. The estimated change in entropy values in all cases was determined to be weak, therefore, the growth processes were observed to be enthalpically driven which is similar to most previous reports (Duboc et al. 1999a, von Stockar et al. 2006, Battley 2013).

Table 6. 6: Kinetic parameters of *F. oxysporum* on glucose with ammonia (GA), *Beta vulgaris* with ammonia (BA) and *Beta vulgaris* with cyanide (BCN)

Substrate	$Y_{X/S}$ (g dry cell/g substrate)	Y_{X/O_2} (g dry cell/g O_2)	μ_{max} (h^{-1})	[a]R.Q
GA	0.39 (±0.01)	0.75 (±0.11)	0.0076	0.96
BA	0.69 (±0.03)	1.65 (±0.31)	0.0642	0.97
BCN	0.38 (±0.02)	0.64 (±0.05)	0.0089	1.04

[a]R.Q = respiratory quotient

The results in Fig. 6.1, show a gradual increase in the total Gibbs energy dissipated over time. Previous reports indicated that the Gibbs energy dissipation for biomass growth including maintenance $(1/Y_{GX})$ increases gradually in batch cultures (Soletto et al. 2005, da Silva et al. 2016), achieving increasing metabolic rates although resulting in low biomass yield. The

microbial growth model showed highest biomass yield based on substrate and oxygen in BA cultures – Table 6.6. The results in Table 6.6 and Fig. 6.1 concur with observations in previous studies that showed an increase in energy requirements is largely due to constraints in synthesising biomass from a carbon and/or an energy source which causes reduction in specific growth rate as the process approaches the stationary phase (Heijnen 2010, da Silva et al 2016).

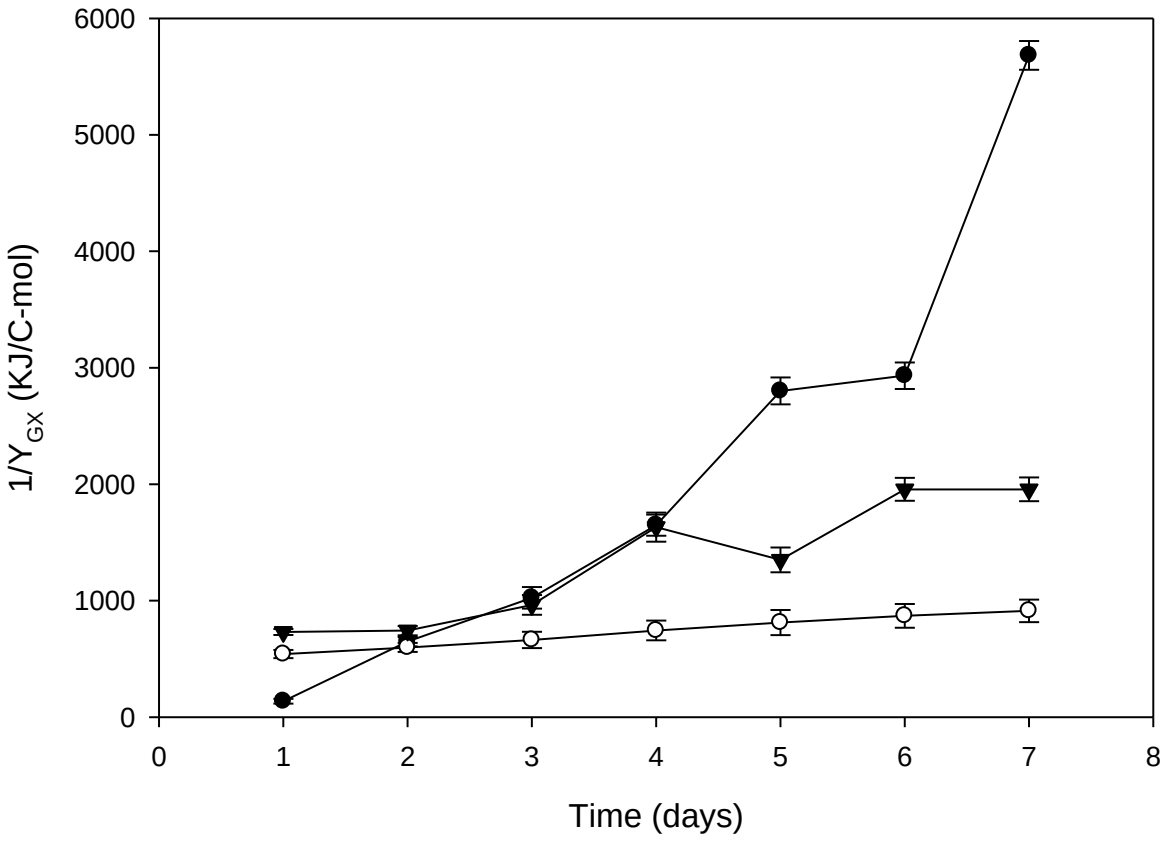

Figure 6. 1: Time behaviour of total Gibbs energy of biomass $(1/Y_{GX})$ during *F. oxysporum* growth in (—●—) glucose (GA), in (···○···) *Beta vulgaris* with ammonia (BA), and in (- -▼- -) *Beta vulgaris* with cyanide (BCN)

By comparison, the growth on BA showed the lowest energy requirements for microbial growth with the highest dry biomass yield and maximum specific growth rate as shown in Table 6.6, while the Gibbs energy dissipated on GA was quantifiably large resulting in a lower maximum specific growth rate and dry biomass yield. The increase in energy requirements occurred at a specific growth rate of 0.0008 h^{-1} after 6 days on GA, meanwhile, prior to that, i.e. after 4 days, there was a decrease in energy requirements on cultures grown in BCN due to an increase in

the specific growth rate from 0.0032 to 0.004 h^{-1} prior to cultures reaching the stationary phase. The relatively high biomass yield in BCN compared to GA may be due to the combined effect of an elongated catabolic pathway, presence of stored mucilage in the cells and the requirements to assimilate micro- and macro-nutrients available in *B. vulgaris* (Mussatto et al 2012, Gonzalez-Cabaleiro et al 2015). The biomass yield based on oxygen consumption varied but the respiratory quotient (R.Q) was similar for the isolate in all cultures studied, an indication that the metabolic performance of the isolate was largely identical irrespective of the substrate used.

6.6 Summary

Clearly, the biological stoichiometry of microbial growth on agro-waste is as feasible as growth on glucose. The bioenergetic parameters even in the presence of an inhibitor, i.e. CN^-, support this claim. The agro-industrial waste used proved to be as efficient as glucose with biomass yield and energy requirements. The respiratory quotient showed the metabolism of the *F. oxysporum* EKT01/02 was not affected by the different carbon sources used. This study revealed that the use of *B. vulgaris* agro-industrial waste for the bioremediation of cyanidation wastewater is feasible and could engender sustainability of gold mining wastewater treatment processes. However, there is a need to validate Heijnens' model used to estimate the Gibbs free energy of the growth process equation by determining the heat capacity of dry biomass at low temperature. This forms the basis for the next chapter (Chapter 7).

CHAPTER 7

Heat capacity measurements of lyophilised biomass of *Fusarium oxysporum* EKT01/02 at temperatures 130 to 305 K using modulated Differential Scanning Calorimeter

Akinpelu, E.A., Ntwampe, S.K.O, Mekuto, L & Ojumu T.V. Heat capacity measurements of lyophilised biomass of *Fusarium oxysporum* associated with cyanidation wastewater from temperatures 130 to 305 K. Submitted to *Chemical Engineering and Technology* (Manuscript ID: ceat.201700359)

Akinpelu, E.A., Ntwampe, S.K.O., Mekuto, L & Ojumu, T.V. Thermodynamic data of Fusarium oxysporum using different substrates in gold mine wastewater. Submitted to *Data* (Manuscript ID: data-214190)

CHAPTER 7
Heat capacity measurements of lyophilised biomass of *Fusarium oxysporum* EKT01/02 at temperatures 130 to 305 K using modulated Differential Scanning Calorimeter

7.1 Introduction

Thermodynamic properties of a material are an essential tool for predicting the feasibility of any chemical and biological reaction including processes such as the microbial growth process and the biomass conversion of nutrient media to useful products. Among these thermodynamic properties, heat capacity of biological molecules such as starch, glucose, proteins and amino acids reportedly measured based on rudimentary heat capacity quantifications can be used to estimate entropy increments and/or changes at low temperatures (0 to 298.15 K); however, the high uncertainty associated with this estimate is disadvantageous (Boerio-Goates 1991). Recently, some researchers have reported on the use of an adiabatic calorimeter for measuring heat capacity of biological materials at low temperature; based on the application of the third law of thermodynamics, for which incremental entropy and/or absolute entropy can be estimated (Pyda 2001, Kabo et al. 2013). Nevertheless, the results were determined to be unreproducible because there was no reference material used and that each researcher had to fabricate their own calorimeter. This maybe the reason for Pyda's (2001) preference for Differential Scanning Calorimeter (DSC) measurements over adiabatic calorimeter measurements. Overall, there is only one report on heat capacity of microbial dried biomass thus far (Battley et al 1997) which reported on the use of an adiabatic calorimeter for quantifying the heat capacity of lyophilised cells of *Saccharomyces cerevisiae,* subsequent to the estimation of entropy changes as a function of temperature based on the third law of thermodynamics.

From the second law of thermodynamics, the heat capacity of any material can be estimated/quantified using heat flow curves obtained from DSC generated profiles of the sample being studied. A DSC provides a more reliable, accurate and reproducible results because it is often calibrated with a standard reference and/or material such as a sapphire, which is used to ascertain and/or detect any error with the equipment, a parametric requirement not available with an adiabatic calorimeter. Nevertheless, it is often difficult to interpret the heat flow data from DSC experiments when multiple processes are involved over a similar temperature range with overlapping of transitions different compounds in a multicomponent material, being problematic. Besides, the heat capacity of a material cannot be determined directly from DSC data, it requires multiple experiments including data interpretation to ascertain or determine the heat capacity (Verdonck et al. 1999, Brantley et al. 2003, Xie et al. 2010, Magoń & Pyda 2013).

Furthermore, a modulated DSC (MDSC™) overcomes these drawbacks and thus provide an insight into the thermal properties of materials being studied. MDSC™ uses a modulated temperature input signal to provide information on the heat capacity, both under isothermal and non-isothermal conditions. Further details on theory, principles, application and instrumentation requirements of the MDSC™ can be found in Vendonck (1999) and Knopp (2016).

7.2 Objective

The objective of this part of the study was to determine the effect of free cyanide on the heat capacity and changes in entropy for lyophilised biomass of *Fusarium oxysporum* using a modulated DSC (MDSC™). This is necessary for the assessment of impact of free cyanide on the physical properties (such as melting point, glass transition temperature etc.) of the lyophilised biomass of *F. oxysporum*.

7.3 Materials and methods

Samples were prepared as stated in chapter 3 (section 3.2.11). *F. oxysporum* growth on glucose, *Beta vulgaris* with ammonia and *Beta vulgaris* with cyanide are presented as GA, BA and BCN samples, respectively. The molecular weight of the lyophilised biomass were 23.03, 33.14 and 27.06 g/C-mol for GA, BA and BCN samples, respectively as previously highlighted in Table 6.3.

The MDSC™ uses both the linear heating rate as well as a modulated (sinusoidal) heating rate to determine the total heat flow rate, see Eq. 7.1. The linear heating rate provides information on the total heat rate while the sinusoidal heating rate provides the heat capacity information from a fraction of the heat flow (Stark et al. 2013).

$$\frac{dQ}{dt} = C_P\beta + f(T,t) \tag{7.1}$$

Where (dQ/dt) is the total heat flow due to the linear heating rate (equivalent of standard DSC), C_P is the heat capacity component calculated from the heat flow due to the sinusoidal heating rate, β is the heating rate of the sample, $C_P\beta$ is the reversing heat flow while $f(T,t)$ is the kinetic component of total heat flow known as the non-reversing heat flow which can be calculated from the difference between the heat capacity and total heat signal component.

Entropy of the lyophilised biomass was estimated by integrating C_{pm}/T with an independent variable (T) – see Eq. 7.2 (Leyx et al. 2005).

$$\Delta S = \int_{T_1}^{T_2} \frac{C_{Pm}}{T}\, dT \qquad (7.2)$$

Where C_{pm} is the molar heat capacity of the lyophilised biomass.

In this part of the study, thermal analyses were done on a Discovery DSC® (TA Instruments, Inc. New Castle, DE, USA) equipped with a modulated Differential Scanning Calorimeter (MDSC™) software using a Liquid Nitrogen Cooling Accessory (LNCA). For the purge, helium gas was used at a flow rate of 50 mL/min. The MDSC™ equilibrated at a temperature of 123 K and the scans were performed at an underlying heating rate of 3 K/min up to a temperature of 373 K. An amplitude of 1 K and a modulation period of 60 s were used for the sample mass of 2 mg – dry biomass weight, with isothermal measurements being quantified at 5 min intervals. Temperature and specific heat calibrations were performed with a MDSC™ certified Indium reference material (Part No. 915061.901) and a sapphire for the specific heat capacity determinations (Part No. 9703790.901), respectively. The data were analysed using a TRIOS software v4.1.1.33073 (TA Instruments Inc. USA). All procedures were done in triplicate.

7.4 Results and discussion

7.4.1 Phase transition

MDSC™ allows for separation and evaluation of thermodynamic and kinetic processes within the regions of glass and melting transitions as shown in Eq. 7.1. Below the glass and melting transitions, heat capacity is caused by vibrational motion and above it, the vibrational motion changes to the conformational motion (Pyda & Wunderlich 2005). Within the glass transition range, endothermic or exothermic enthalpy relaxation may occur owing to changes in the temperature of the sample. The experimental MDSC™ results presented in Fig. 7.1 and Fig. 7.2 illustrates the total heat flow, reversible heat flow and non-reversible heat flow profiles. No glass transition was observed on total heat flow and non-reversible heat flow profiles for all biomass samples tested. This included GA samples for which reversible heat flow profiles were assessed. However, there was glass transition (T_g) at a temperature of 239 K and the enthalpy change of 12.586 J/g with an endothermic peak temperature of 292.333 K for BA sample, and a T_g of 211 K, an enthalpy change of 22.096 J/g at an endothermic peak temperature of 287 K for BCN samples on the reversible heat flow profiles which was an indication of a structural transformation of the samples studied, i.e. BA and BCN samples; that is reversible with any temperature changes (Lai & Lii 1999, Tan et al. 2004). The lower T_g for BCN samples indicated a rapid breakdown of aromatic constituents in *Beta vulgaris* supplemented biomass owning to

the residual free cyanide within the synthetic wastewater used, thereby enhancing microbial growth during the free cyanide biodegradation process.

Furthermore, the melting transition (T_m) was observed for all samples studied, i.e. as obtained from the reversing heat flow profiles – see Table 7.1. Microbial degradation is directly affected by T_m, i.e. the lower the T_m, the higher the biodegradation of a toxicant such as free cyanide (Herzog et al. 2006, Mueller 2006, Kasuya et al. 2009). *Beta vulgaris* as mentioned earlier (section 6.4.1), consist of 9.56 % carbohydrates, with betalains, phenolic compounds, including trace elements and minerals accounting for a larger percentage (Wruss et al. 2015, USDA 2016). The presence of betalains and phenolic compounds definitely affected the microbial growth in BA samples since they degrade under different bioreactor operating conditions (Herbach et al. 2006) from that of free cyanide, resulting in a slightly higher molecular weight of the *F. oxysporum* and thus, a higher T_m for BA samples. Similarly, interactions of molecular chains affect the change of enthalpy (ΔH) in melting with the internal energy accounting for the flexibility or otherwise of the samples studied, thus affecting the change of entropy (ΔS) in melting (Tokiwa et al. 2009). The highest ΔH in melting for BCN samples was an indication of highest molecular interactions during free cyanide biodegradation.

Table 7. 1: Effect of melting temperature on the samples

Samples	T_m (onset) (K)	T_m (peak) (K)	ΔH (J/g)
GA	218.72	277.113	17.476
BA	212.311	292.333	12.586
BCN	127.341	287.729	22.096

Several theories have been proposed for the glass transition of granular samples (Lai & Lii 1999, Tan et al. 2004, Liu & Shi 2006). Tan et al. (2004) found glass transition on reversible heat flow profile of MDSC™ occurred after the onset temperature which overlapped with the peak temperature. It was presumed that this was due to changes in the state of the starch molecules i.e. from being highly confined within the granular packing, to being disentangled as the order in which the molecules are arranged changed as the transition occured. According to Liu & Shi (2006), glass transition occurs when the rigid amorphous regions of starch granules are re-arranged and it does not occur until the melting of the crystallites commences. As such, a glass transition below 273 K can occur partly due to the mobility of the amorphous fractions in the granular starch, i.e. as they re-arranged. Battley (1997) reported this was due to structural transitions of cellular materials at temperatures below freezing point of pure water including the influence of the underlying heating rate, modulation period and amplitude (Stark et al. 2013).

In this part of the study, it was evident that the substrate from which the biomass materials were formed, played a major role in the phase transition as can be seen that only cultures grown on *Beta vulgaris* (BA and BCN), had a glass transition. Phase transitions are associated with sudden increases in entropy with a high degree of freedom (Otto et al. 2013). Within the region of melting transition, BCN samples recorded the highest change of entropy from 0.147 to 0.526 J K^{-1} g^{-1}. This showed the impact of the free cyanide on the lyophilised biomass of *F. oxysporum* during the biodegradation process.

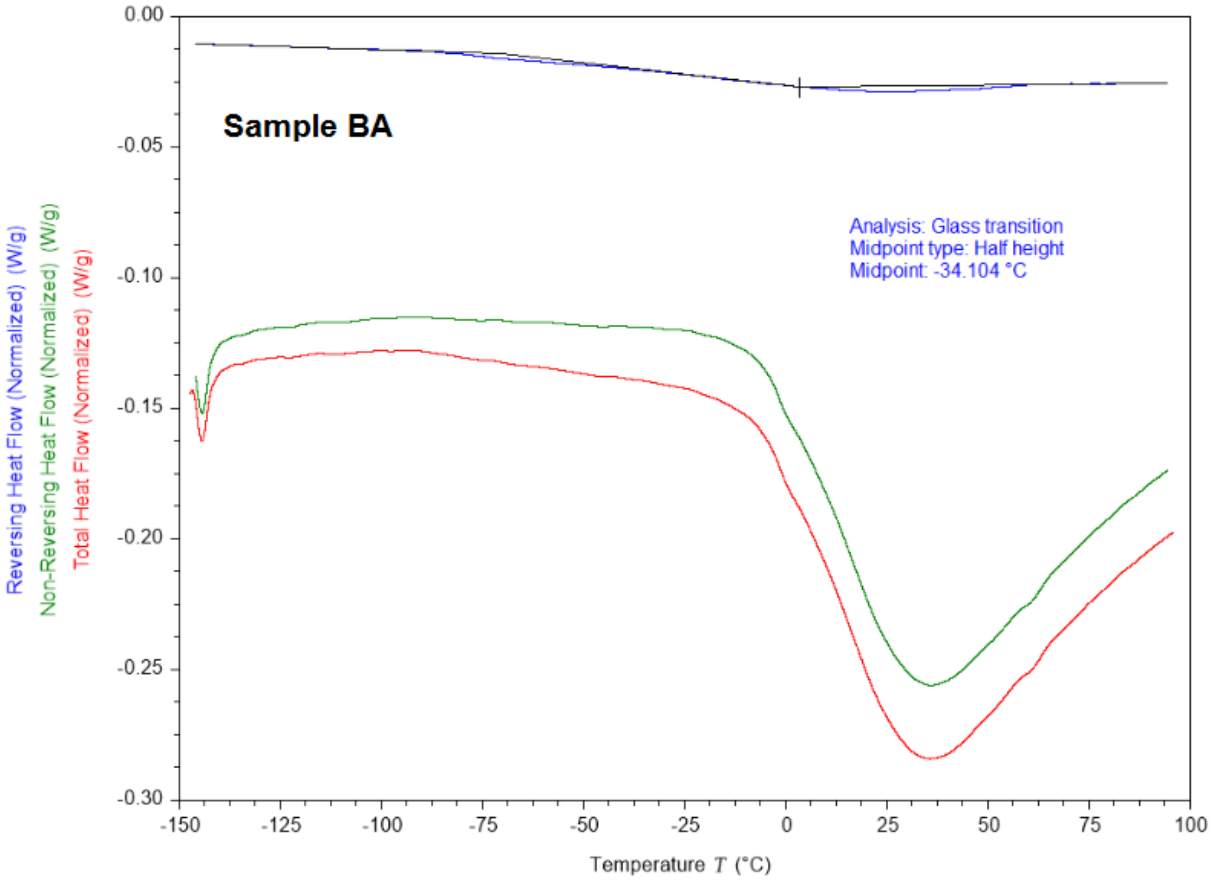

Figure 7. 1: MDSC result of sample BA showing total, reversible and non-reversible heat flow with glass transition

a)

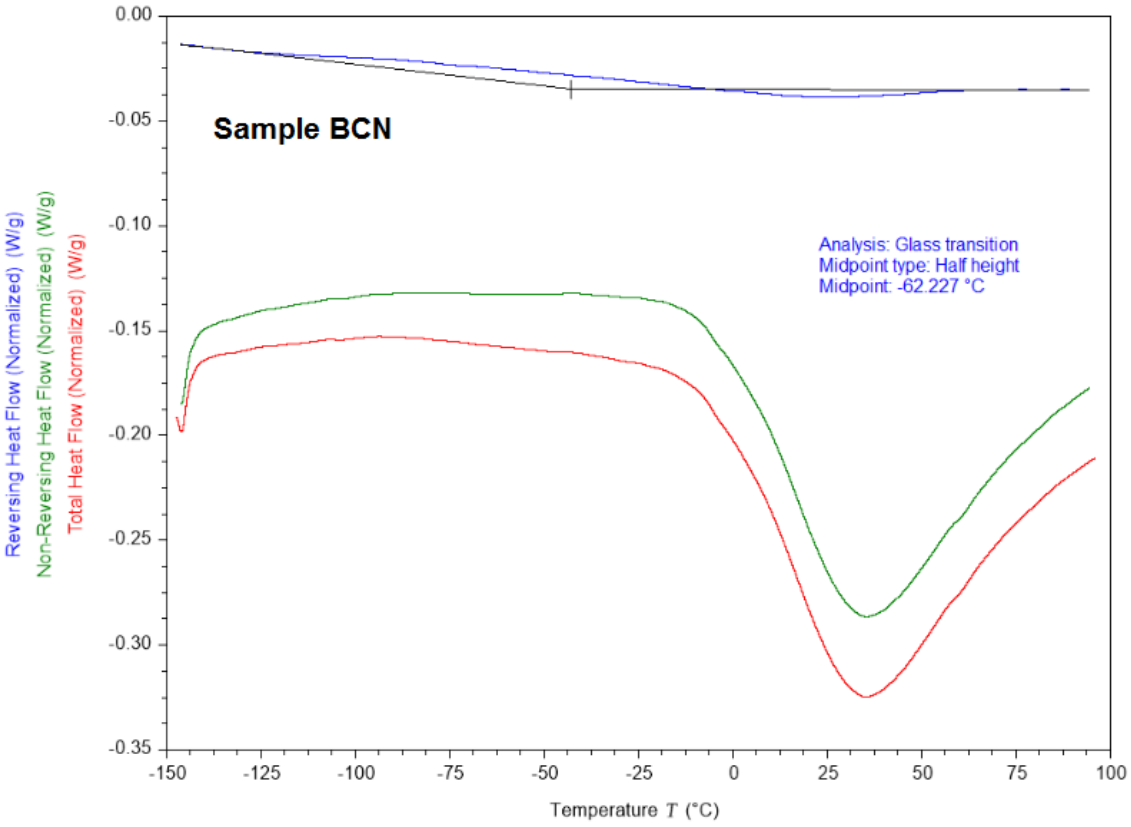

b)

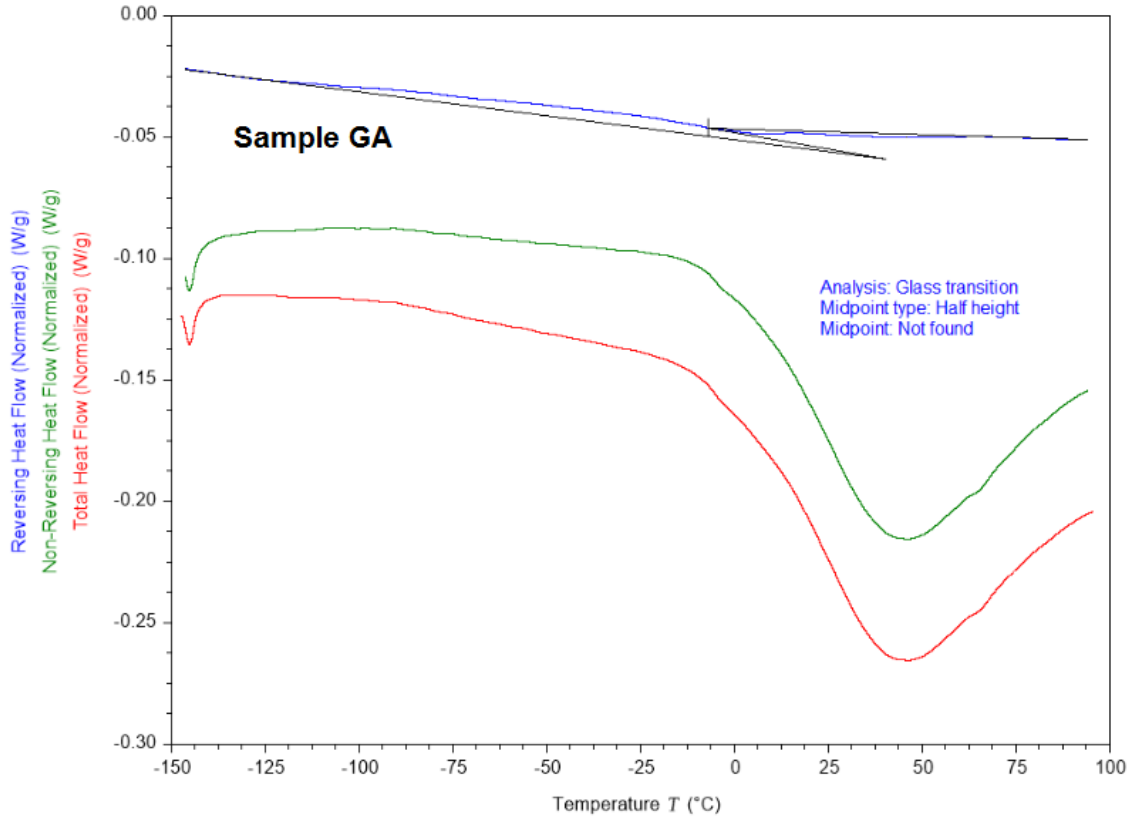

Figure 7. 2: MDSC results of sample BCN (a) and GA (b) showing total, reversible and non-reversible heat flow with glass transition

7.4.2 Heat capacity measurements and entropy of the samples

Heat capacity measurements were obtained from 123 K to 373 K. The experimental specific heat capacity of lyophilised cells of *F. oxysporum* samples in the temperature range of 130 to 305 K are presented in Fig. 7.3, including entropy in Table 7.2.

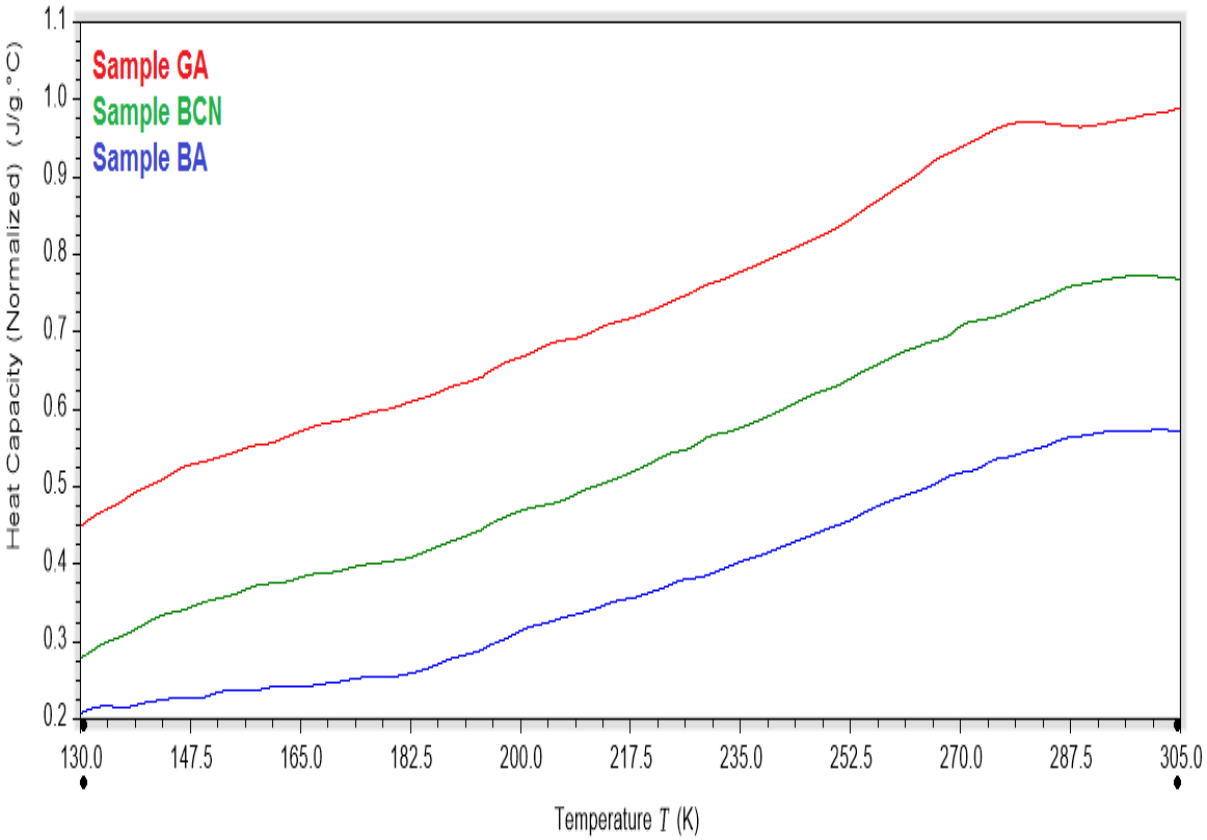

Figure 7. 3: Heat capacity of samples BA, BCN and GA as a function of temperature

Although there is no general statements on heat capacity changes, the heat capacity of the samples increased steadily with rise in temperature. Anomalies were observed in the heat capacity in the region 282 to 294 K for GA, and 300 to 305 K for BCN sample owning to the phase transitions observed. This confirmed the phenomenon observed with *Saccharomyces cerevisiae* biomass by Battley (1997) i.e. molecules are known to undergo several internal vibrations, which is dependent on their internal degree of freedom – internal entropy. This shift in heat capacity had been ascribed to interactions between the modulation period and the underlying heating rate, including relaxation enthalpy on both heating and cooling cycles especially for an amorphous samples such as *F. oxysporum* biomass (Pyda & Wunderlich 2005).

Table 7. 2: Heat capacity and change of entropy in lyophilised biomass of *F. oxysporum* from different substrates

T (K)	BA		BCN		GA	
	C_p $(J\,K^{-1}\,g^{-1})$	ΔS $(J\,K^{-1}g^{-1})$	C_p $(J\,K^{-1}\,g^{-1})$	ΔS $(J\,K^{-1}g^{-1})$	C_p $(J\,K^{-1}\,g^{-1})$	ΔS $(J\,K^{-1}g^{-1})$
133	0.216	0.108	0.295	0.147	0.466	0.233
143	0.224	0.124	0.334	0.170	0.510	0.268
153	0.237	0.139	0.358	0.194	0.541	0.304
163	0.241	0.155	0.378	0.217	0.565	0.339
173	0.251	0.169	0.396	0.240	0.589	0.373
183	0.260	0.184	0.410	0.263	0.611	0.407
193	0.287	0.198	0.442	0.285	0.640	0.440
200	0.314	0.209	0.469	0.301	0.667	0.463
220	0.362	0.241	0.528	0.349	0.725	0.530
230	0.387	0.258	0.565	0.373	0.762	0.563
250	0.449	0.292	0.629	0.423	0.834	0.629
273	0.518	0.335	0.708	0.482	0.939	0.707
273.15	0.525	0.335	0.715	0.482	0.951	0.707
280	0.545	0.348	0.734	0.500	0.971	0.731
290	0.567	0.368	0.763	0.526	0.965	0.765
298.15	**0.572**	**0.384**	**0.772**	**0.547**	**0.978**	**0.792**
300	0.573	0.387	0.772	0.552	0.981	0.798
303	0.573	0.393	0.770	0.560	0.985	0.808

The heat capacity of GA samples was shown to be the highest. The low heat capacity observed for BCN samples maybe due to the stress imposed by the free cyanide during microbial proliferation which in turn affected the biomass structural integrity as shown in Figure 4.6 achieving lower entropy changes compared to GA samples. Furthermore, BA samples recorded the lowest heat capacity when compared with all other samples studied. This was expected since *Beta vulgaris* contains approximately 9.56 % carbohydrate that served as an energy and/or carbon source for the *F. oxysporum* used (Wruss et al. 2015, USDA 2016*)*. The higher values of heat capacity and entropy in BCN samples when compared to BA samples, could be directly related to the microorganism's ability to utilise cyanide as a carbon source to supplement carbohydrates in *B. vulgaris* agro-industrial waste. Since there is no other reports on heat capacities of microbial dried biomass in literature particularly for fungi, comparing the heat capacity of yeast-like *Fusarium oxysporum* with *Saccharomyces cerevisiae* showed that from the results obtained, GA samples were comparatively similar to those reported by Battley (1997). Although, Battley (1997) acknowledged that the results are not reproducible, due to the use of an adiabatic calorimeter. However, the results reported herein; i.e. from a MDSC™ are generally deemed reliable thus reproducible. Albeit, if sufficient quantities of *B. vulgaris* and/or further pre-treatment of agro-industrial waste besides pulverising were used, better biodegradation and substrate utilisation performance could have been observed, as this influence the integrity and the quality of the biomass being generated thus bioreactor

performance. As such, it is feasible to suggest that a highly stressful environment culminates in poorly structured cells, which can impede the ability of such cells to detoxify a highly contaminated environment.

The empirical formula of the biomass containing a unit carbon for BA, BCN and GA samples are $CH_{2.377}N_{0.091}O_{1.093}$, $CH_{1.82}N_{0.027}O_{0.804}$, and $CH_{1.167}N_{0.067}O_{0.558}$, with molecular weight of 33.14, 27.06 and 23.03 g/C-mol, respectively as shown in Table 6.3. The molecular weight of unit carbon mole times the entropy in gram gives the entropy in unit carbon mole. The values 0.384, 0.547 and 0.792 J K^{-1} g^{-1} were measured for the entropy of the samples BA, BCN and GA at 298.15 K and 1 atm.- see Table 7.2. The entropy of dried *F. oxysporum* biomass samples at 298.15 K can be calculated using the chemical composition analysis given above as 12.72, 14.80, and 18.24 J K^{-1} C-mol^{-1} for samples BA, BCN and GA, respectively. Based on the analysis above, entropy of formation of biomass can be calculated using Battley's model (1997).

$$\Delta S_f = S - 5.74nC - 65.34nH - 102.57nO - 95.81nN \qquad (7.3)$$

Where *S* is the entropy at 298.15 K of a unit mole of dried biomass and n is the quantity of each atom in the formula. The constant 5.74 is the molar entropy of solid graphite, 65.34, 102.57, and 95.81 are one-half of the molar entropies of $H_{2(g)}$, $O_{2(g)}$, and $N_{2(g)}$, respectively. All at 298.15 K and 1 atm. with dimensions of J K^{-1} mol^{-1} (Wagman et al. 1982).

Using Eq. 2, ΔS_f for the samples BA, BCN and GA are -269.16, -194.91, and -127.40 J K^{-1} C-mol^{-1}, respectively.

Furthermore, Table 7.3 shows the changes of entropy in some selected molecules of biological importance during phase changes. The data ranges from a low 0.003 J K^{-1} g^{-1} for thiosemicarbazide to a high 1.151 J K^{-1} g^{-1} for ethylene. The change of entropy in lyophilised biomass for all samples were within the range of change of entropy in a number of biological molecules (Domalski & Hearing 1990). In particular, the change of entropy for BCN samples at 298.15 K is similar to the values of cyanamide and urea. This showed that the higher entropy change observed in BCN compared to BA samples must arise from molecular disorder caused by free cyanide on mycelia constituting the biomass which is essential for the spontaneity of the biodegradation process.

Table 7. 3: Change of entropies in selected biological molecules at phase transition (Domalski & Hearing 1990)

Compound name	Molecular formula	$\Delta S\ (J\ K^{-1}\ g^{-1})$
Thiosemicarbazide	CH_5N_3S	0.003
Sodium acetate	$C_2H_3NaO_2$	0.152
Trichloroacetic acid	$C_2HCl_3O_2$	0.109
Sodium formate	$CHNaO_2$	0.491
Cyanamide	CH_2N_2	0.543
Urea	CH_4N_2O	0.571
Polyethylene	$(CH_2)n$	0.668
Formamide	CH_3NO	0.699
Acetamide	C_2H_5NO	0.747
Ethylene	C_2H_4	1.151

7.5 Summary

The results presented herein showed that the substrate used for microbial growth can affect the determination of the heat capacity as well as entropy changes of biological samples. Although the MDSC™ operations (tests) are lengthy, its accuracy, including the direct determination of the heat capacity, revealing hidden and/or complex transitions which might have not been noticed using a conventional DSC or an adiabatic calorimeter, is advantageous. The determination of such heat capacity of a material as a function of the structure of the material can assist in agro-industrial waste selection for cyanidation wastewater treatment. The impairment caused by free cyanide also reflected on the heat capacity and change of entropy quantification of the biomass assessed. The toxicity by free cyanide reduces the biomass molecular degree of freedom (entropy); hence, the biomass does not store sufficient thermal energy as most energy resources are dedicated for cellular maintenance. Generally, cellular materials are known for poor thermal relaxation; however, the heat capacity and entropy presented herein, including the reproducibility of its determination (3.5% uncertainty) can be used to further elucidate the capabilities associated with the novel biocatalyst chosen for the bioremediation of cyanidation wastewater.

CHAPTER 8

SUMMARY AND CONCLUSIONS

Chapter 8
Summary and conclusions

8.1 Summary and conclusions

Water is fundamental to all facets of life. Since the beginning of 21st century, the world has started facing water crisis owing to industrialisation, population growth, deficient water management practices and policies. Access to safe drinking water is considered a human right but the right to pollute and release wastewater back into the environment without treatment is not. Hence, the need for efficient wastewater management especially industrial discharge. Mining activity is one of the biggest generators of toxic industrial wastewater. In most cases, industrial wastewater is discharged directly into fresh water bodies and could leach into the water table resulting in groundwater contamination.

Free cyanide is one of the extremely toxic contaminants prevalent in mining wastewater which causes environmental deterioration affecting both flora and fauna. Several chemical treatment methods such as copper catalysed hydrogen peroxide oxidation and alkaline chlorination are being used in the mining industry for cyanide degradation in wastewater. However, owing to different constraints associated with poor treatment performance, high cost of reagents, failure to remove ammonia, including oxidation by-products and chloride, amongst others, makes microbial remediation of free cyanide in wastewater a viable option.

There are several studies for which microbial treatment of wastewater is supported using refined carbon sources on a laboratory scale with systems which cannot be duplicated at an industrial scale. Furthermore, despite the adaptable nature of microbial species and the environmentally benignity of the designed processes, their industrial application on a large-scale has not been progressively adopted due to concerns about the sustainability of nutrient requirements to support such processes. Bioprocesses using agro-industrial waste has been shown to have the capability to replace conventional methods used in wastewater treatment with several reports indicated their potential to support diverse enzymatic pathways providing nutritional value for microbial growth. However, there are no reports of any industrial applications, even at the Homestake Mine (USA) and Biomin® (South Africa) that uses biological processes for treatment of wastewater containing free cyanide; processes which still use refined carbon for microbial growth. Therefore, to better understand the process, a thermodynamic study of the biodegradation of free cyanide in wastewater supported using agro-industrial waste (*Beta vulgaris*) was undertaken.

Thermodynamic analysis is a suitable approach which can be used to determine the feasibility of these biological processes on a large-scale, including those in which agro-industrial waste

is used, in order to assess influential conditions under which such processes can be efficient. Thermodynamic properties such as the heat of combustion, heat capacity, entropy, Gibbs free energy, including the stoichiometry of microbial proliferation in cyanidation wastewater treatment using agro-industrial waste as a nutrient source were analysed. The success of such bioremediation depends on the biomass yield including the bioenergetics of the system designed since it determines overall microbial performance.

This study began with the isolation of *Fusarium oxysporum* EKT01/02 (KU985430/KU985431) from the rhizosphere of *Zea mays* contaminated with a cyanide-based pesticide in South Africa. The isolate was characterised using molecular biology, biochemical and bioinformatic methods. Also, the effect of free cyanide and heavy metals on the growth of the isolate in a synthetic gold mine wastewater was examined. The molecular analyses showed the fungus belongs to *Fusarium* species. The biochemical analyses indicated the isolate has aminopeptidases including nitrate assimilation potential. The isolate had a free cyanide degradation efficiency of 77.6% 100 mg CN^-/L, although greater growth impairment were observed in cultures containing Arsenic (optical density 1.28 and 1.458) and free cyanide (optical density 1.315 and 1.385), with higher microbial growth in all cultures supplemented with extracellular polymeric substance (EPS) produced by the isolate – chapter 4.

Furthermore, under substrate limitations, the *F. oxysporum* showed preference for *B. vulgaris* agro-industrial waste as the primary carbon source. In addition, the operating conditions for the bioremediation of free cyanide containing wastewater by the cyanide resistant fungus *F. oxysporum* grown on *B. vulgaris* were optimised using the numerical optimisation option of the response surface methodology (RSM). The optimum was found to be at a temperature of 26.50 °C, pH 10.77, and a agro-industrial waste concentration of 310.89 mg/L. The response surface plots identified temperature and substrate concentration as the significant factors affecting free cyanide biodegradation – chapter 5. The fungus growth on agro-industrial waste would ensure economic sustainability of the free cyanide biodegradation system in environmental engineering applications, on an industrial scale.

Aerobic growth of *F. oxysporum* EKT01/02 in synthetic gold mine wastewater under different substrates in batch systems showed that the bioenergetics and stoichiometry of the microorganism's growth on agro-industrial waste was achievable even in the presence of free cyanide. The molecular weight of the dry biomass obtained were 23.03 g/C-mol, 33.14 g C-mol^{-1}, and 27.06 g/C-mol in synthetic media (wastewater) containing glucose with ammonia (GA), *Beta vulgaris* with ammonia (BA) and *B. vulgaris* with cyanide (BCN) cultures, respectively. The microbial growth model showed a higher biomass yield of 0.69 g dry cell/g

substrate in BA cultures. The heat of reaction (ΔH_{RX}^{O}) and Gibbs energy dissipation per mole of biomass formed (ΔG_{RX}^{O}) were -652.55/-432.11 kJ/C-mol, -132.59/-471.19 kJ/C-mol, and -370.34/-225.35 kJ/C-mol for GA, BA, and BCN cultures, respectively. The total Gibbs energy dissipated increased steadily over time and the metabolic rate of the *F. oxysporum* used was adversely affected minimally by the cyanidation wastewater as shown by the degree of reduction, including the respiratory quotient quantified. The *F. oxysporum* proliferation was observed to be enthalpically driven in all the cultures studied (chapter 6). In addition, the heat capacity and change of entropy for *F. oxysporum* grown in cyanide containing wastewater were 0.772 J K^{-1} g^{-1} and 0.547 J K^{-1} g^{-1}, respectively at 298.15 K (Chapter 7) –an indication that the isolate has an in-built resistance mechanism to store enough thermal energy in the bioremediation of wastewater containing free cyanide.

In conclusion, this study revealed that the use of *B. vulgaris* agro-industrial waste for the bioremediation of cyanidation wastewater is feasible and could engender sustainability of gold mining wastewater treatment processes; thereby providing a basis for further investigation on the likelihood of a large-scale application of agro-industrial waste in environmental engineering.

Therefore, scientific advancement from this study are as follows:

- Application of agro-industrial waste as sole carbon source for microbial growth at optimum operating conditions is effective for free cyanide bioremediation. This could enhance economic viability of bioremediation processes,
- This is the first report on the development of stoichiometry including bioenergetics of microbial proliferation on agro-industrial waste in the presence of an inhibitor – free cyanide. This proved to be as effective as glucose,
- The first reported on the heat capacity and change of entropy for a fungal isolate at 298.15 K which indicated that the biomass generated do not have the same heat capacity, as it is a function of the substrate (materials) from which they were formed.

8.2 Recommendations

Although this thesis report the successful bioenergetics and stoichiometry of bioremediation of wastewater containing free cyanide, there were challenges arising from this work. As reported in chapter 4, cyanidation wastewater is complex with three different forms in gold mine wastewater based on their solubility and stability which were not covered in this thesis. Furthermore, the study of thermodynamics for the biodegradation of metal-cyanide complexes is needed. Similarly, cellular materials are known for poor thermal relaxation, thus further studies on the limits of cellular materials thermal limitations in a bioremediation process would

be advantageous. A scale-up design to pilot plant for applicability and economic feasibility of the agro-industrial waste/wastewater systems could be investigated.

REFERENCES

References

Acheampong, M. A., Meulepas, R. J. & Lens, P. N. 2010. Removal of heavy metals and cyanide from gold mine wastewater. *Journal of Chemical Technology and Biotechnology,* 85**,** 590-613.

Acheampong, M. A., Paksirajan, K. & Lens, P. N. L. 2013. Assessment of the effluent quality from a gold mining industry in Ghana. *Environmental Science and Pollution Research,* 20**,** 3799-3811.

Ahluwalia, S. S. & Goyal, D. 2007. Microbial and plant derived biomass for removal of heavy metals from wastewater. *Bioresource Technology,* 98**,** 2243-2257.

Ainsworth, G. C. & Sussman, A. S. 2013. *The Fungal Population: An Advanced Treatise*, Elsevier.

Ajay Kumar, G. 2014. *Colletotrichum gloeosporioides*: Biology, Pathogenicity and management in India. *Journal of Plant Physiology and Pathology* 2**,** 2-11.

Akcil, A. 2003. Destruction of cyanide in gold mill effluents: biological versus chemical treatments. *Biotechnol Adv,* 21.

Akinpelu, E. A., Amodu, O. S., Mpongwana, N., Ntwampe, S. K. O. & Ojumu, T. V. 2015. Utilization of *Beta vulgaris* Agrowaste in Biodegradation of Cyanide Contaminated Wastewater. *In:* Ekinci, D. (ed.) *Biotechnology.* Croatia: INTECH.59-75

Akinpelu, E. A., Ntwampe, S. K., Mpongwana, N., Nchu, F. & Ojumu, T. V. 2016. Biodegradation Kinetics of Free Cyanide in *Fusarium oxysporum-Beta vulgaris* Waste-metal (As, Cu, Fe, Pb, Zn) Cultures under Alkaline Conditions. *BioResources,* 11**,** 2470-2482.

Alabouvette, C., Olivain, C., Migheli, Q. & Steinberg, C. 2009. Microbiological control of soil-borne phytopathogenic fungi with special emphasis on wilt-inducing *Fusarium oxysporum*. *New Phytologist,* 184**,** 529 -544

Altınok, H. H. & Can, C. 2010. Characterization of *Fusarium oxysporum f. sp. melongenae* isolates from eggplant in Turkey by pathogenicity, VCG and RAPD analysis. *Phytoparasitica,* 38**,** 149-157.

Amodu, O. S., Ntwampe, S. K. & Ojumu, T. V. 2014. Optimization of biosurfactant production by *Bacillus licheniformis* STK 01 grown exclusively on *Beta vulgaris* waste using response surface methodology. *BioResources,* 9**,** 5045-5065.

Anuradha, K., Padma, P. N., Venkateshwar, S. & Reddy, G. 2010. Fungal isolates from natural pectic substrates for polygalacturonase and multienzyme production. *Indian Journal of Microbiology,* 50**,** 339-344.

Anwar, Z., Gulfraz, M. & Irshad, M. 2014. Agro-industrial lignocellulosic biomass a key to unlock the future bio-energy: A brief review. *Journal of Radiation Research and Applied Sciences,* 7**,** 163-173.

Atkinson, B. & Mavituna, F. 1983. *Biochemical engineering and biotechnology handbook,* New York, Nature Press.

Avalos Ramirez, A., Bénard, S., Giroir-Fendler, A., Jones, J. P. & Heitz, M. 2008. Kinetics of microbial growth and biodegradation of methanol and toluene in biofilters and an analysis of the energetic indicators. *Journal of Biotechnology,* 138**,** 88-95.

Azcón, R., Medina, A., Roldán, A., Biró, B. & Vivas, A. 2009. Significance of treated agrowaste residue and autochthonous inoculates (*Arbuscular mycorrhizal* fungi and *Bacillus cereus*) on bacterial community structure and phytoextraction to remediate soils contaminated with heavy metals. *Chemosphere,* 75**,** 327-334.

Baayen, R. P., O'Donnell, K., Bonants, P. J., Cigelnik, E., Kroon, L. P., Roebroeck, E. J. & Waalwijk, C. 2000. Gene genealogies and AFLP analyses in the *Fusarium oxysporum* complex identify monophyletic and nonmonophyletic formae speciales causing wilt and rot disease. *Phytopathology,* 90**,** 891-900.

Bao, J. R., Fravel, D. R., O'Neill, N. R., Lazarovits, G. & Berkum, P. v. 2002. Genetic analysis of pathogenic and nonpathogenic *Fusarium oxysporum* from tomato plants. *Canadian Journal of Botany,* 80**,** 271-279.

Barclay, M., Tett, V. A. & Knowles, C. J. 1998. Metabolism and enzymology of cyanide/metallocyanide biodegradation by *Fusarium solan*i under neutral and acidic conditions. *Enzyme and Microbial Technology,* 23**,** 321-330.

Battley, E. H. 1995a. The advantages and disadvantages of direct and indirect calorimetry. *Thermochimica Acta,* 250**,** 337-352.

Battley, E. H. 1995b. An apparent anomaly in the calculation of ash-free dry weights for the determination of cellular yields. *Applied and environmental microbiology,* 61**,** 1655-1657.

Battley, E. H. 1998. The development of direct and indirect methods for the study of the thermodynamics of microbial growth. *Thermochimica Acta,* 309**,** 17-37.

Battley, E. H. 1999a. On entropy and absorbed thermal energy in biomass; a biologist's perspective. *Thermochimica Acta,* 331**,** 1-12.

Battley, E. H. 1999b. The thermodynamics of microbial growth. *In:* Kemp, R. B. (ed.) *Handbook of thermal analysis and calorimetry.* Amsterdam: Elsevier.219-266

Battley, E. H. 2011. A comparison of energy changes accompanying growth processes by Saccharomyces cerevisiae. *Journal of Thermal Analysis and Calorimetry,* 104**,** 193-200.

Battley, E. H. 2013. A theoretical study of the thermodynamics of microbial growth using Saccharomyces cerevisiae and a different free energy equation. *The Quarterly review of biology,* 88**,** 69-96.

Battley, E. H., Putnam, R. L. & Boerio-Goates, J. 1997. Heat capacity measurements from 10 to 300 K and derived thermodynamic functions of lyophilized cells of Saccharomyces cerevisiae including the absolute entropy and the entropy of formation at 298.15 K. *Thermochimica Acta,* 298**,** 37-46.

Battley, E. H. & Stone, J. R. 2000. A comparison of values for the entropy and the entropy of formation of selected organic substances of biological importance in the solid state, as determined experimentally or calculated empirically. *Thermochimica Acta,* 349**,** 153-161.

Baysal, Ö., Siragusa, M., Gümrükcü, E., Zengin, S., Carimi, F., Sajeva, M. & Da Silva, J. A. T. 2010. Molecular characterization of *Fusarium oxysporum f. melongenae* by ISSR and RAPD markers on eggplant. *Biochemical genetics,* 48**,** 524-537.

Behera, S., Mohanty, R. C. & Ray, R. C. 2011. Ethanol production from mahula (*Madhuca latifolia* L.) flowers with immobilized cells of *Saccharomyces cerevisiae* in Luffa cylindrica L. sponge discs. *Applied Energy,* 88**,** 212-215.

Boerio-Goates, J. 1991. Heat-capacity measurements and thermodynamic functions of crystalline α-D-glucose at temperatures from 10 K to 340 K. *The Journal of Chemical Thermodynamics,* 23**,** 403-409.

Bogale, M., Wingfield, B., Wingfield, M. & Steenkamp, E. 2005. Simple sequence repeat markers for species in the *Fusarium oxysporum* complex. *Molecular Ecology Notes,* 5**,** 622-624.

Bogale, M., Wingfield, B. D., Wingfield, M. J. & Steenkamp, E. T. 2006. Characterization of *Fusarium oxysporum* isolates from Ethiopia using AFLP, SSR and DNA sequence analyses. *Fungal Diversity,* 23**,** 51-66.

Braissant, O., Bonkat, G., Wirz, D. & Bachmann, A. 2013. Microbial growth and isothermal microcalorimetry: Growth models and their application to microcalorimetric data. *Thermochimica Acta,* 555**,** 64-71.

Brantley, W. A., Iijima, M. & Grentzer, T. H. 2003. Temperature-modulated DSC provides new insight about nickel-titanium wire transformations. *American Journal of Orthodontics and Dentofacial Orthopedics,* 124**,** 387-394.

Brebu, M. & Vasile, C. 2010. Thermal degradation of lignin—a review. *Cellulose Chemistry & Technology,* 44**,** 353.

Brunner, P. H. & Rechberger, H. 2015. Waste to energy – key element for sustainable waste management. *Waste Management,* 37**,** 3-12.

Buyukkileci, A. O., Lahore, M. F. & Tari, C. 2015. Utilization of orange peel, a food industrial waste, in the production of exo-polygalacturonase by pellet forming Aspergillus sojae. *Bioprocess and biosystems engineering,* 38**,** 749-760.

Chen, L., Yang, X., Raza, W., Luo, J., Zhang, F. & Shen, Q. 2011. Solid-state fermentation of agro-industrial wastes to produce bioorganic fertilizer for the biocontrol of Fusarium wilt of cucumber in continuously cropped soil. *Bioresource Technology,* 102**,** 3900-3910.

Chróst, R. J. 1992. Significance of bacterial ectoenzymes in aquatic environments. *In:* Ilmavirta, V. & Jones, R. I. (eds.) *The Dynamics and Use of Lacustrine Ecosystems: Proceedings of the 40-Year Jubilee Symposium of the Finnish Limnological Society, held in Helsinki, Finland, 6–10 August 1990.* Dordrecht: Springer Netherlands.61-70

Corcoran, E. 2010. *Sick water?: the central role of wastewater management in sustainable development: a rapid response assessment*, UNEP/Earthprint.

Cordier, J.-L., Butsch, B. M., Birou, B. & Stockar, U. 1987. The relationship between elemental composition and heat of combustion of microbial biomass. *Applied Microbiology and Biotechnology,* 25**,** 305-312.

Cramer, D. & Howitt, D. L. 2004. *The Sage dictionary of statistics: a practical resource for students in the social sciences*, Sage.

da Silva, M. F., Casazza, A. A., Ferrari, P. F., Perego, P., Bezerra, R. P., Converti, A. & Porto, A. L. F. 2016. A new bioenergetic and thermodynamic approach to batch photoautotrophic growth of Arthrospira (Spirulina) platensis in different photobioreactors and under different light conditions. *Bioresource Technology,* 207**,** 220-228.

Dash, R. R., Gaur, A. & Balomajumder, C. 2009. Cyanide in industrial wastewaters and its removal: A review on biotreatment. *Journal of Hazardous Materials,* 163**,** 1-11.

Dean, R., Van Kan, J. A. L., Pretorius, Z. A., Hammond-Kosack, K. E., Di Pietro, A., Spanu, P. D., Rudd, J. J., Dickman, M., Kahmann, R., Ellis, J. & Foster, G. D. 2012. The Top 10 fungal pathogens in molecular plant pathology. *Molecular Plant Pathology,* 13**,** 414-430.

Demirel, Y. & Sandler, S. I. 2002. Thermodynamics and bioenergetics. *Biophysical Chemistry,* 97**,** 87-111.

Dhillon, G. S., Brar, S. K., Kaur, S. & Verma, M. 2013. Bioproduction and extraction optimization of citric acid from Aspergillus niger by rotating drum type solid-state bioreactor. *Industrial Crops and Products,* 41**,** 78-84.

Dias, A. A., Freitas, G. S., Marques, G. S. M., Sampaio, A., Fraga, I. S., Rodrigues, M. A. M., Evtuguin, D. V. & Bezerra, R. M. F. 2010. Enzymatic saccharification of biologically pre-treated wheat straw with white-rot fungi. *Bioresource Technology,* 101**,** 6045-6050.

Dlangamandla, C., Dyantyi, S., Mpentshu, Y., Ntwampe, S. & Basitere, M. 2016. Optimisation of bioflocculant production by a biofilm forming microorganism from poultry slaughterhouse wastewater for use in poultry wastewater treatment. *Water Science and Technology,* 73**,** 1963-1968.

Doane, D. P. & Seward, L. E. 2011. Measuring skewness: a forgotten statistic. *Journal of Statistics Education,* 19**,** 1-18.

Dogaris, I., Karapati, S., Mamma, D., Kalogeris, E. & Kekos, D. 2009. Hydrothermal processing and enzymatic hydrolysis of sorghum bagasse for fermentable carbohydrates production. *Bioresource technology,* 100**,** 6543-6549.

Domalski, E. S. & Hearing, E. D. 1990. Heat Capacities and Entropies of Organic Compounds in the Condensed Phase Volume II. *Journal of Physical and Chemical Reference Data,* 19**,** 881-1047.

Donato, D. B., Nichols, O., Possingham, H., Moore, M., Ricci, P. F. & Noller, B. N. 2007. A critical review of the effects of gold cyanide-bearing tailings solutions on wildlife. *Environment International,* 33**,** 974-984.

dos Santos, T. C., Gomes, D. P. P., Bonomo, R. C. F. & Franco, M. 2012. Optimisation of solid state fermentation of potato peel for the production of cellulolytic enzymes. *Food Chemistry,* 133**,** 1299-1304.

Dourado, M. N., Martins, P. F., Quecine, M. C., Piotto, F. A., Souza, L. A., Franco, M. R., Tezotto, T. & Azevedo, R. A. 2013. *Burkholderia sp*. SCMS54 reduces cadmium toxicity and promotes growth in tomato. *Annals of Applied Biology,* 163**,** 494-507.

Du Plessis, C., Barnard, P., Muhlbauer, R. & Naldrett, K. 2001. Empirical model for the autotrophic biodegradation of thiocyanate in an activated sludge reactor. *Letters in Applied Microbiology,* 32**,** 103-107.

Duboc, P., Marison, I. & Von Stockar, U. 1999a. Quantitative calorimetry and biochemical engineering. *In:* Kemp, R. B. (ed.) *Handbook of thermal analysis and calorimetry.* Amsterdam: Elsevier.267-365

Duboc, P., Marison, I. W. & Von Stockar, U. 1999b. Quantitative calorimetry and biochemical engineering. *In:* Kemp, R. B. (ed.) *Handbook of thermal analysis and calorimetry: from macromolecule to man.* Elsevier.

Durve, A., Naphade, S., Bhot, M., Varghese, J. & Chandra, N. 2012. Characterisation of metal and xenobiotic resistance in bacteria isolated from textile effluent. *Advances in Applied Science Research,* 3**,** 2801-2806.

Ebbs, S. 2004. Biological degradation of cyanide compounds. *Current Opinion in Biotechnology,* 15**,** 231-236.

ElMekawy, A., Srikanth, S., Bajracharya, S., Hegab, H. M., Nigam, P. S., Singh, A., Mohan, S. V. & Pant, D. 2015. Food and agricultural wastes as substrates for bioelectrochemical system (BES): The synchronized recovery of sustainable energy and waste treatment. *Food Research International,* 73**,** 213-225.

Felsenstein, J. 1985. Confidence limits on phylogenies: an approach using the bootstrap. *Evolution,* 39**,** 783-791.

Finch, A., Gardner, P. J., Head, A. J., Xiaoping, W., Yefimov, M. E. & Furkaluk, M. U. 1993. The standard enthalpy of formation of the aqueous cyanide ion. *The Journal of Chemical Thermodynamics,* 25**,** 1385-1390.

Finley, S. D., Broadbelt, L. J. & Hatzimanikatis, V. 2009. Thermodynamic analysis of biodegradation pathways. *Biotechnology and bioengineering,* 103**,** 532.

Gadd, G. M. 2010. Metals, minerals and microbes: geomicrobiology and bioremediation. *Microbiology,* 156**,** 609-643.

Geddes, C. C., Mullinnix, M. T., Nieves, I. U., Peterson, J. J., Hoffman, R. W., York, S. W., Yomano, L. P., Miller, E. N., Shanmugam, K. T. & Ingram, L. O. 2011. Simplified process for ethanol production from sugarcane bagasse using hydrolysate-resistant *Escherichia coli* strain MM160. *Bioresource Technology,* 102**,** 2702-2711.

Glibert, P. M., Mayorga, E. & Seitzinger, S. 2008. Prorocentrum minimum tracks anthropogenic nitrogen and phosphorus inputs on a global basis: application of spatially explicit nutrient export models. *Harmful Algae,* 8**,** 33-38.

Gonzalez-Cabaleiro, R., Ofiteru, I. D., Lema, J. M. & Rodriguez, J. 2015. Microbial catabolic activities are naturally selected by metabolic energy harvest rate. *ISME J,* 9**,** 2630-2641.

Guimarães, L. H. S., Somera, A. F., Terenzi, H. F., Polizeli, M. d. L. T. d. M. & Jorge, J. A. 2009. Production of β-fructofuranosidases by *Aspergillus niveus* using agroindustrial residues as carbon sources: Characterization of an intracellular enzyme accumulated in the presence of glucose. *Process Biochemistry,* 44**,** 237-241.

Gupta, N., Balomajumder, C. & Agarwal, V. K. 2010. Enzymatic mechanism and biochemistry for cyanide degradation: A review. *Journal of Hazardous Materials,* 176**,** 1-13.

Gurjar, G., Barve, M., Giri, A. & Gupta, V. 2009. Identification of Indian pathogenic races of *Fusarium oxysporum f. sp. ciceris* with gene specific, ITS and random markers. *Mycologia,* 101**,** 484-495.

Gustavsson, J., Cederberg, C., Sonesson, U., Van Otterdijk, R. & Meybeck, A. 2011. *Global food losses and food waste - Extent, causes and prevention,* Rome, FAO.

Hakim, A., Azza, S. & Rasha, M. 2013. Isolation, Biochemical Identification and Molecular Detection of Yeasts from Kareish Cheese. *International Journal of Microbiological Research,* 4**,** 95-100.

Heijnen, J. J. 2002. Bioenergetics of Microbial Growth. *Encyclopedia of Bioprocess Technology.* John Wiley & Sons, Inc.

Heijnen, J. J. 2010. Impact of Thermodynamic Principles in Systems Biology. *In:* Wittmann, C. & Krull, R. (eds.) *Biosystems Engineering II: Linking Cellular Networks and Bioprocesses.* Berlin, Heidelberg: Springer Berlin Heidelberg.139-162

Heijnen, J. J. & Van Dijken, J. P. 1992. In search of a thermodynamic description of biomass yields for the chemotrophic growth of microorganisms. *Biotechnology and Bioengineering,* 39**,** 833-858.

Heijnen, J. J. & van Dijken, J. P. 1993. Response to comments on “in search of a thermodynamic description of biomass yields for the chemotropic growth of microorganisms”. *Biotechnology and Bioengineering,* 42**,** 1127-1130.

Herbach, K. M., Stintzing, F. C. & Carle, R. 2006. Betalain Stability and Degradation—Structural and Chromatic Aspects. *Journal of Food Science,* 71**,** R41-R50.

Herzog, K., Müller, R. J. & Deckwer, W. D. 2006. Mechanism and kinetics of the enzymatic hydrolysis of polyester nanoparticles by lipases. *Polymer Degradation and Stability,* 91**,** 2486-2498.

Hubbe, M. A., Hasan, S. H. & Ducoste, J. J. 2011. Cellulosic substrates for removal of pollutants from aqueous systems: A review. 1. Metals. *BioResources,* 6**,** 2161-2287.

Huddy, R. J., van Zyl, A. W., van Hille, R. P. & Harrison, S. T. L. 2015. Characterisation of the complex microbial community associated with the ASTER™ thiocyanate biodegradation system. *Minerals Engineering,* 76**,** 65-71.

Ibrahim, K. K., Syed, M. A., Shukor, M. Y. & Ahmad, S. A. 2016. Biological Remediation of Cyanide: A Review. *BIOTROPIA-The Southeast Asian Journal of Tropical Biology,* 22**,** 151-163.

Itoba Tombo, E. F., Waxa, A. & Ntwampe, S. K. O. 2015. Isolation of an endophytic cyanide resistant fungus *Cunninghamella bertholletiae* from (*Manihot esculenta*) and cassava cultivated soil for environmental engineering applications. 7th International Conference on Latest Trends in Engineering and Technology 2015 Pretoria, South Africa. South Africa: IIE, 150-153.

Jangbua, P., Laoteng, K., Kitsubun, P., Nopharatana, M. & Tongta, A. 2009. Gamma-linolenic acid production of *Mucor rouxii* by solid-state fermentation using agricultural by-products. *Letters in applied microbiology,* 49**,** 91-97.

Jha, S., Chauhan, R. & Dikshit, S. 2014. Fungal Biomass as Biosorbent for Removal of Heavy Metal from Industrial Wastewater Effluent. *Asian Journal of Plant Sciences,* 13**,** 93.

Jiménez-Fernández, D., Montes-Borrego, M., Navas-Cortés, J. A., Jiménez-Díaz, R. M. & Landa, B. B. 2010. Identification and quantification of *Fusarium oxysporum* in planta and soil by means of an improved specific and quantitative PCR assay. *Applied Soil Ecology,* 46**,** 372-382.

Jin, A. X., Ren, J. L., Peng, F., Xu, F., Zhou, G. Y., Sun, R. C. & Kennedy, J. F. 2009. Comparative characterization of degraded and non-degradative hemicelluloses from barley straw and maize stems: Composition, structure, and thermal properties. *Carbohydrate Polymers,* 78**,** 609-619.

Joshi, C., Mathur, P. & Khare, S. K. 2011. Degradation of phorbol esters by *Pseudomonas aeruginosa* PseA during solid-state fermentation of deoiled Jatropha curcas seed cake. *Bioresource Technology,* 102**,** 4815-4819.

Kabanova, N., Kazarjan, A., Stulova, I. & Vilu, R. 2009. Microcalorimetric study of growth of *Lactococcus lactis* IL1403 at different glucose concentrations in broth. *Thermochimica Acta,* 496**,** 87-92.

Kabo, G. J., Voitkevich, O. V., Blokhin, A. V., Kohut, S. V., Stepurko, E. N. & Paulechka, Y. U. 2013. Thermodynamic properties of starch and glucose. *The Journal of Chemical Thermodynamics,* 59**,** 87-93.

Kandasamy, S., Dananjeyan, B., Krishnamurthy, K. & Benckiser, G. 2015. Aerobic cyanide degradation by bacterial isolates from cassava factory wastewater. *Brazilian Journal of Microbiology,* 46**,** 659-666.

Karatay, S. E. & Dönmez, G. 2010. Improving the lipid accumulation properties of the yeast cells for biodiesel production using molasses. *Bioresource Technology,* 101**,** 7988-7990.

Kasuya, K.-i., Ishii, N., Inoue, Y., Yazawa, K., Tagaya, T., Yotsumoto, T., Kazahaya, J.-i. & Nagai, D. 2009. Characterization of a mesophilic aliphatic–aromatic copolyester-degrading fungus. *Polymer Degradation and Stability,* 94**,** 1190-1196.

Khamar, Z., Makhdoumi-Kakhki, A. & Mahmudy Gharaie, M. H. 2015. Remediation of cyanide from the gold mine tailing pond by a novel bacterial co-culture. *International Biodeterioration & Biodegradation,* 99**,** 123-128.

Kimura, M. 1980. A simple method for estimating evolutionary rates of base substitutions through comparative studies of nucleotide sequences. *Journal of Molecular Evolution,* 16**,** 111-120.

Kitancharoen, N. & Hatai, K. 1998. Some biochemical characteristics of fungi isolated from salmonid eggs. *Mycoscience,* 39**,** 249-255.

Koutinas, M., Patsalou, M., Stavrinou, S. & Vyrides, I. 2016. High temperature alcoholic fermentation of orange peel by the newly isolated thermotolerant Pichia kudriavzevii KVMP10. *Letters in Applied Microbiology,* 62**,** 75-83.

Kruger, M. C., Bertin, P. N., Heipieper, H. J. & Arsène-Ploetze, F. 2013. Bacterial metabolism of environmental arsenic—mechanisms and biotechnological applications. *Applied Microbiology and Biotechnology,* 97**,** 3827-3841.

Kumar, S. & Gadagkar, S. R. 2001. Disparity index: a simple statistic to measure and test the homogeneity of substitution patterns between molecular sequences. *Genetics,* 158**,** 1321-1327.

Kumar, Y. S., Varakumar, S. & Reddy, O. 2010. Production and optimization of polygalacturonase from mango (*Mangifera indica L.)* peel using *Fusarium moniliforme* in solid state fermentation. *World Journal of Microbiology and Biotechnology,* 26**,** 1973-1980.

Kurniawan, T. A., Chan, G. Y., Lo, W.-H. & Babel, S. 2006. Physico–chemical treatment techniques for wastewater laden with heavy metals. *Chemical engineering journal,* 118**,** 83-98.

Lai, V.-F. & Lii, C.-Y. 1999. Effects of modulated differential scanning calorimetry (MDSC) variables on thermodynamic and kinetic characteristics during gelatinization of waxy rice starch. *Cereal chemistry,* 76**,** 519-525.

Lambert, J. L., Ramasamy, J. & Paukstelis, J. V. 1975. Stable reagents for the colorimetric determination of cyanide by modified König reactions. *Analytical Chemistry,* 47**,** 916-918.

Larsson, C. & Gustafsson, L. 1999. Calorimetry of microbial processes. *In:* Kemp, R. B. (ed.) *Handbook of thermal analysis and calorimetry.* Amsterdam: Elsevier.367-404

Lazaridis, N. K., Hourzemanoglou, A. & Matis, K. A. 2002. Flotation of metal-loaded clay anion exchangers. Part II: the case of arsenates. *Chemosphere,* 47**,** 319-324.

Leiva-Candia, D. E., Pinzi, S., Redel-Macías, M. D., Koutinas, A., Webb, C. & Dorado, M. P. 2014. The potential for agro-industrial waste utilization using oleaginous yeast for the production of biodiesel. *Fuel,* 123**,** 33-42.

Leslie, J. F., Summerell, B. A. & Bullock, S. 2006. *The Fusarium laboratory manual*, Wiley Online Library.

Leyx, C., Van Miltenburg, J. C., Chopin, C. & Cemič, L. 2005. Heat-capacity measurements and absolute entropy of ε-Mg_2PO_4OH. *Physics and chemistry of minerals,* 32**,** 13-18.

Li, J., Gellerstedt, G. & Toven, K. 2009. Steam explosion lignins; their extraction, structure and potential as feedstock for biodiesel and chemicals. *Bioresource Technology,* 100**,** 2556-2561.

Liang, S., Gliniewicz, K., Gerritsen, A. T. & McDonald, A. G. 2016. Analysis of microbial community variation during the mixed culture fermentation of agricultural peel wastes to produce lactic acid. *Bioresource Technology,* 208**,** 7-12.

Liu, J. S., Vojinović, V., Patiño, R., Maskow, T. & von Stockar, U. 2007. A comparison of various Gibbs energy dissipation correlations for predicting microbial growth yields. *Thermochimica Acta,* 458**,** 38-46.

Liu, W., Wang, Y., Yu, Z. & Bao, J. 2012. Simultaneous saccharification and microbial lipid fermentation of corn stover by oleaginous yeast Trichosporon cutaneum. *Bioresource Technology,* 118**,** 13-18.

Liu, X., Jiang, Y., Shen, S., Luo, Y. & Gao, L. 2015. Comparison of Arrhenius model and artificial neuronal network for the quality prediction of rainbow trout (Oncorhynchus mykiss) fillets during storage at different temperatures. *LWT - Food Science and Technology,* 60**,** 142-147.

Liu, Y. & Shi, Y.-C. 2006. Phase and State Transitions in Granular Starches Studied by Dynamic Differential Scanning Calorimetry. *Starch - Stärke,* 58**,** 433-442.

Luque-Almagro, V., Blasco, R., Huertas, M., Martínez-Luque, M., Moreno-Vivián, C., Castillo, F. & Roldán, M. 2005. Alkaline cyanide biodegradation by *Pseudomonas pseudoalcaligenes* CECT5344. *Biochemical Society Transactions,* 33**,** 168-169.

Magoń, A. & Pyda, M. 2013. Apparent heat capacity measurements and thermodynamic functions of d(−)-fructose by standard and temperature-modulated calorimetry. *The Journal of Chemical Thermodynamics,* 56**,** 67-82.

Maniyam, M. N., Sjahrir, F., Ibrahim, A. L. & Cass, A. E. 2013. Biodegradation of cyanide by Rhodococcus UKMP-5M. *Biologia,* 68**,** 177-185.

Marchler-Bauer, A., Derbyshire, M. K., Gonzales, N. R., Lu, S., Chitsaz, F., Geer, L. Y., Geer, R. C., He, J., Gwadz, M., Hurwitz, D. I., Lanczycki, C. J., Lu, F., Marchler, G. H., Song, J. S., Thanki, N., Wang, Z., Yamashita, R. A., Zhang, D., Zheng, C. & Bryant, S. H. 2015. CDD: NCBI's conserved domain database. *Nucleic Acids Research,* 43**,** D222-D226.

McCarty, P. L. 2007. Thermodynamic electron equivalents model for bacterial yield prediction: modifications and comparative evaluations. *Biotechnology and bioengineering,* 97**,** 377-388.

Medina, A., Vassilev, N., Barea, J. M. & Azcón, R. 2005. Application of *Aspergillus niger*-treated agrowaste residue and *Glomus mosseae* for improving growth and nutrition of *Trifolium repens* in a Cd-contaminated soil. *Journal of Biotechnology,* 116**,** 369-378.

Medina, A., Vassileva, M., Barea, J.-M. & Azcón, R. 2006. The growth-enhancement of clover by Aspergillus-treated sugar beet waste and Glomus mosseae inoculation in Zn contaminated soil. *Applied Soil Ecology,* 33**,** 87-98.

Meena, P., Tripathi, A. D., Srivastava, S. K. & Jha, A. 2013. Utilization of agro-industrial waste (wheat bran) for alkaline protease production by *Pseudomonas aeruginosa* in SSF using Taguchi (DOE) methodology. *Biocatalysis and Agricultural Biotechnology,* 2**,** 210-216.

Meier, S., Cornejo, P., Cartes, P., Borie, F., Medina, J. & Azcón, R. 2015. Interactive effect between Cu-adapted arbuscular mycorrhizal fungi and biotreated agrowaste residue to improve the nutritional status of *Oenothera picensis* growing in Cu-polluted soils. *Journal of Plant Nutrition and Soil Science,* 178**,** 126-135.

Mekuto, L., Alegbeleye, O. O., Ntwampe, S. K. O., Ngongang, M. M., Mudumbi, J. B. & Akinpelu, E. A. 2016a. Co-metabolism of thiocyanate and free cyanide by *Exiguobacterium acetylicum* and *Bacillus marisflavi* under alkaline conditions. *3 Biotech,* 6**,** 1-11.

Mekuto, L., Jackson, V. A. & Ntwampe, S. K. O. 2013. Biodegradation of free cyanide using Bacillus sp. consortium dominated by *Bacillus safensis, Lichenformis* and *Tequilensis* strains: A bioprocess supported solely with whey. *Journal of Bioremediation & Biodegradation,* S18.

Mekuto, L., Ntwampe, S. & Jackson, V. 2015. Biodegradation of free cyanide and subsequent utilisation of biodegradation by-products by Bacillus consortia: optimisation using response surface methodology. *Environmental Science and Pollution Research,* 22**,** 10434-10443.

Mekuto, L., Ntwampe, S. K. O., Kena, M., Golela, M. T. & Amodu, O. S. 2016b. Free cyanide and thiocyanate biodegradation by *Pseudomonas aeruginosa* STK 03 capable of heterotrophic nitrification under alkaline conditions. *3 Biotech,* 6**,** 1-7.

Menon, V. & Rao, M. 2012. Trends in bioconversion of lignocellulose: Biofuels, platform chemicals & biorefinery concept. *Progress in Energy and Combustion Science,* 38**,** 522-550.

Mirizadeh, S., Yaghmaei, S. & Ghobadi Nejad, Z. 2014. Biodegradation of cyanide by a new isolated strain under alkaline conditions and optimization by response surface methodology (RSM). *Journal of Environmental Health Science and Engineering,* 12**,** 1-9.

Mirtalebi, M. & Banihashemi, Z. 2014. Genetic Relationship among *Fusarium oxysporum f. sp. melonis* Vegetative Compatibility Groups and Their Relatedness to Other *F. oxysporum* formae speciales. *Journal of Agricultural Science and Technology,* 16**,** 931-943.

Montgomery, D. C. 2008. *Design and analysis of experiments*, John Wiley & Sons.

Mowat, E., Williams, C., Jones, B., Mcchlery, S. & Ramage, G. 2009. The characteristics of *Aspergillus fumigatus mycetoma* development: is this a biofilm? *Medical mycology,* 47**,** S120-S126.

Mueller, R.-J. 2006. Biological degradation of synthetic polyesters—Enzymes as potential catalysts for polyester recycling. *Process Biochemistry,* 41**,** 2124-2128.

Mukherjee, P. K., Chandra, J., Yu, C., Sun, Y., Pearlman, E. & Ghannoum, M. A. 2012. Characterization of *Fusarium* Keratitis Outbreak Isolates: Contribution of Biofilms to Antimicrobial Resistance and PathogenesisBiofilm Formation Mediates *Fusarium* Pathogenesis. *Investigative ophthalmology & visual science,* 53**,** 4450-4457.

Müller, T., Müller, M. & Behrendt, U. 2004. Leucine arylamidase activity in the phyllosphere and the litter layer of a Scots pine forest. *FEMS microbiology ecology,* 47**,** 153-159.

Murray, I. 1968. Some aspects of the biochemical differentiation of pathogenic fungi: a review. *Microbiology,* 52**,** 213-221.

Mussatto, S. I., Teixeira, J. A., Ballesteros, L. F. & Martins, S. 2012. Use of agro-industrial wastes in solid-state fermentation processes. *In:* Show, K.-Y. (ed.) *Industrial Waste.* Croatia: InTech.121-140

Nordstokke, D. W. & Zumbo, B. D. 2010. A new nonparametric Levene test for equal variances. *Psicologica: International Journal of Methodology and Experimental Psychology,* 31**,** 401-430.

Nordstokke, D. W., Zumbo, B. D., Cairns, S. L. & Saklofske, D. H. 2011. The operating characteristics of the nonparametric Levene test for equal variances with assessment and evaluation data. *Practical Assessment, Research & Evaluation,* 16**,** 1-8.

Ntwampe, S. K. & Santos, B. A. 2013. Potential of agro-waste extracts as supplements for the continuous bioremediation of free cyanide contaminated wastewater. *International Journal of Agricultural, Biosystems Science and Engineering,* 7**,** 285-289.

Nyenje, P., Foppen, J., Uhlenbrook, S., Kulabako, R. & Muwanga, A. 2010. Eutrophication and nutrient release in urban areas of sub-Saharan Africa—a review. *Science of the Total Environment,* 408**,** 447-455.

O'Donnell, K., Kistler, H. C., Tacke, B. K. & Casper, H. H. 2000. Gene genealogies reveal global phylogeographic structure and reproductive isolation among lineages of *Fusarium graminearum*, the fungus causing wheat scab. *Proceedings of the National Academy of Sciences,* 97**,** 7905-7910.

O'Donnell, K., Kistler, H. C., Cigelnik, E. & Ploetz, R. C. 1998. Multiple evolutionary origins of the fungus causing Panama disease of banana: concordant evidence from nuclear and mitochondrial gene genealogies. *Proceedings of the National Academy of Sciences,* 95**,** 2044-2049.

Oelofse, S. H. & Nahman, A. 2013. Estimating the magnitude of food waste generated in South Africa. *Waste Management & Research,* 31**,** 80-86.

Oja, V. & Suuberg, E. M. 1999. Vapor Pressures and Enthalpies of Sublimation of d-Glucose, d-Xylose, Cellobiose, and Levoglucosan. *Journal of Chemical & Engineering Data,* 44**,** 26-29.

Orozco, A. L., Pérez, M. I., Guevara, O., Rodríguez, J., Hernández, M., González-Vila, F. J., Polvillo, O. & Arias, M. E. 2008. Biotechnological enhancement of coffee pulp residues by solid-state fermentation with *Streptomyces*. Py–GC/MS analysis. *Journal of Analytical and Applied Pyrolysis,* 81**,** 247-252.

Oso, B., Olagunji, M. & Okiki, P. 2015. Lead tolerance and bioadsorption potentials of indigenous soil fungi in Ado Ekiti, Nigeria. *European Journal of Experimental Biology,* 5**,** 15-19.

Otto, F., Yang, Y., Bei, H. & George, E. P. 2013. Relative effects of enthalpy and entropy on the phase stability of equiatomic high-entropy alloys. *Acta Materialia,* 61**,** 2628-2638.

Paper, J. M., Scott-Craig, J. S., Cavalier, D., Faik, A., Wiemels, R. E., Borrusch, M. S., Bongers, M. & Walton, J. D. 2013. α-Fucosidases with different substrate specificities from two species of *Fusarium*. *Applied Microbiology and Biotechnology,* 97**,** 5371-5380.

Pappenhagen, J. 1958. Colorimetric Determination of Nitrates. *Analytical Chemistry,* 30**,** 282-284.

Parolini, D. & Carcano, S. 2010. A model for cell growth in batch bioreactors. Master Thesis, Polytechnic University of Milan, Milan, Italy.

Patil, Y. B. & Paknikar, K. M. 1999. Removal and recovery of metal cyanides using a combination of biosorption and biodegradation processes. *Biotechnology Letters,* 21**,** 913-919.

Patton, C. J. & Crouch, S. 1977. Spectrophotometric and kinetics investigation of the Berthelot reaction for the determination of ammonia. *Analytical chemistry,* 49**,** 464-469.

Pavan Kumar, M. A., Suresh, D., Nagabhushana, H. & Sharma, S. C. 2015. *Beta vulgaris* aided green synthesis of ZnO nanoparticles and their luminescence, photocatalytic and antioxidant properties. *The European Physical Journal Plus,* 130**,** 109.

Peiqian, L., Xiaoming, P., Huifang, S., Jingxin, Z., Ning, H. & Birun, L. 2014. Biofilm formation by *Fusarium oxysporum f. sp. cucumerinum* and susceptibility to environmental stress. *FEMS microbiology letters,* 350**,** 138-145.

Pereira, P. T., Arrabaça, J. D. & Amaral-Collaço, M. T. 1996. Isolation, selection and characterization of a cyanide-degrading fungus from an industrial effluent. *International Biodeterioration & Biodegradation,* 37**,** 45-52.

Pereiro Jr, M., Abalde, M., Zulaica, A., Caeiro, J., Flórez, A., Peteiro, C. & Toribio, J. 2001. Chronic infection due to *Fusarium oxysporum* mimicking *Lupus vulgaris*: case report and review of cutaneous involvement in Fusariosis. *Acta dermato-venereologica,* 81**,** 51-53.

Pham, T. P. T., Kaushik, R., Parshetti, G. K., Mahmood, R. & Balasubramanian, R. 2015. Food waste-to-energy conversion technologies: Current status and future directions. *Waste Management,* 38**,** 399-408.

Pincus, D. H. 2006. Microbial identification using the bioMérieux Vitek 2 system. *In:* Miller, M. J. (ed.) *Encyclopedia of Rapid Microbiological Methods.* USA: DHI.

Potivichayanon, S. & Kitleartpornpairoat, R. 2010. Biodegradation of cyanide by a novel cyanide degrading bacterium. *World Acad Sci Eng Technol,* 42**,** 1362-1365.

Purdom Jr, P. W., Bradford, P. G., Tamura, K. & Kumar, S. 2000. Single column discrepancy and dynamic max-mini optimizations for quickly finding the most parsimonious evolutionary trees. *Bioinformatics,* 16**,** 140-151.

Pyda, M. 2001. Conformational contribution to the heat capacity of the starch and water system. *Journal of Polymer Science Part B: Polymer Physics,* 39**,** 3038-3054.

Pyda, M. 2005. Quantitative thermal analysis of carbohydrate-water systems. *In:* Lörinczy, D. (ed.) *The Nature of Biological Systems as Revealed by Thermal Methods.* Dordrecht: Springer Netherlands.307-332

Pyda, M. & Wunderlich, B. 2005. Reversing and Nonreversing Heat Capacity of Poly(lactic acid) in the Glass Transition Region by TMDSC. *Macromolecules,* 38**,** 10472-10479.

Razali, N. M. & Wah, Y. B. 2011. Power comparisons of shapiro-wilk, kolmogorov-smirnov, lilliefors and anderson-darling tests. *Journal of statistical modeling and analytics,* 2**,** 21-33.

Rodríguez-Sevilla, M. D., Villanueva-Suárez, M. J. & Redondo-Cuenca, A. 1999. Effects of processing conditions on soluble sugars content of carrot, beetroot and turnip. *Food Chemistry,* 66**,** 81-85.

Russell, J. B. & Cook, G. M. 1995. Energetics of bacterial growth: balance of anabolic and catabolic reactions. *Microbiological reviews,* 59**,** 48-62.

Saenge, C., Cheirsilp, B., Suksaroge, T. T. & Bourtoom, T. 2011. Efficient concomitant production of lipids and carotenoids by oleaginous red yeast *Rhodotorula glutinis* cultured in palm oil mill effluent and application of lipids for biodiesel production. *Biotechnology and Bioprocess Engineering,* 16**,** 23-33.

Sala, M., Karner, M., Arin, L. & Marrasé, C. 2001. Measurement of ectoenzyme activities as an indication of inorganic nutrient imbalance in microbial communities. *Aquatic Microbial Ecology,* 23**,** 301-311.

Santos, B. A. Q., Ntwampe, S. K. O., Hamuel, J. & Muchatibaya, G. 2013. Application of *Citrus sinensis* solid waste as a pseudo-catalyst for free cyanide conversion under alkaline conditions. *BioResources,* 8**,** 3461-3467.

Seidler, M. J., Salvenmoser, S. & Müller, F.-M. C. 2008. *Aspergillus fumigatus* forms biofilms with reduced antifungal drug susceptibility on bronchial epithelial cells. *Antimicrobial agents and chemotherapy,* 52**,** 4130-4136.

Shapiro, S. S. & Wilk, M. B. 1965. An analysis of variance test for normality (complete samples). *Biometrika,* 52**,** 591-611.

Shashidhar, R., Swathi, A., Vasista, K. & Reshma, S. Optimization of cellulase yield from Areca husk and Areca sheath using *Pseudomonas fluorescens*. Global Humanitarian Technology Conference: South Asia Satellite (GHTC-SAS), 2013 IEEE, 2013. IEEE, 21-26.

Singh, N. & Balomajumder, C. 2016a. Equilibrium isotherm and kinetic studies for the simultaneous removal of phenol and cyanide by use of *S. odorifera* (MTCC 5700) immobilized on coconut shell activated carbon. *Applied Water Science***,** 1-15.

Singh, N. & Balomajumder, C. 2016b. Simultaneous treatment of phenol and cyanide containing synthetic/simulated wastewater using mixed culture immobilized on coconut shell activated carbon biomass in a packed bed bio-column reactor. *Journal of Integrated Science and Technology,* 5**,** 9-14.

Singh nee' Nigam, P., Gupta, N. & Anthwal, A. 2009. Pre-treatment of Agro-Industrial Residues. *In:* Singh nee' Nigam, P. & Pandey, A. (eds.) *Biotechnology for Agro-Industrial Residues Utilisation.* Springer Netherlands.13-33

Singh, R., Shivaprakash, M. & Chakrabarti, A. 2011. Biofilm formation by zygomycetes: quantification, structure and matrix composition. *Microbiology,* 157**,** 2611-2618.

Skovgaard, K., Bødker, L. & Rosendahl, S. 2002. Population structure and pathogenicity of members of the *Fusarium oxysporum* complex isolated from soil and root necrosis of pea (*Pisum sativum L.*). *FEMS Microbiology Ecology,* 42**,** 367-374.

Soletto, D., Binaghi, L., Lodi, A., Carvalho, J. C. M. & Converti, A. 2005. Batch and fed-batch cultivations of *Spirulina platensis* using ammonium sulphate and urea as nitrogen sources. *Aquaculture,* 243**,** 217-224.

Srilekha Yadav, K., Naseeruddin, S., Sai Prashanthi, G., Sateesh, L. & Venkateswar Rao, L. 2011. Bioethanol fermentation of concentrated rice straw hydrolysate using co-culture of *Saccharomyces cerevisiae* and *Pichia stipitis*. *Bioresource Technology,* 102**,** 6473-6478.

Srivastava, S., Bharti, R. K. & Thakur, I. S. 2015. Characterization of bacteria isolated from palaeoproterozoic metasediments for sequestration of carbon dioxide and formation of calcium carbonate. *Environmental Science and Pollution Research,* 22**,** 1499-1511.

Stark, W., Jaunich, M. & McHugh, J. 2013. Cure state detection for pre-cured carbon-fibre epoxy prepreg (CFC) using Temperature-Modulated Differential Scanning Calorimetry (TMDSC). *Polymer Testing,* 32**,** 1261-1272.

Stott, M., Franzmann, P., Zappia, L., Watling, H., Quan, L., Clark, B., Houchin, M., Miller, P. & Williams, T. 2001. Thiocyanate removal from saline CIP process water by a rotating biological contactor, with reuse of the water for bioleaching. *Hydrometallurgy,* 62**,** 93-105.

Takakuwa, N. & Saito, K. 2010. Conversion of beet molasses and cheese whey into fatty acid methyl esters by the yeast *Cryptococcus curvatus*. *Journal of oleo science,* 59**,** 255-260.

Tamura, K., Stecher, G., Peterson, D., Filipski, A. & Kumar, S. 2013. MEGA6: Molecular Evolutionary Genetics Analysis version 6.0. *Molecular biology and evolution*.

Tan, I., Wee, C. C., Sopade, P. A. & Halley, P. J. 2004. Investigation of the starch gelatinisation phenomena in water–glycerol systems: application of modulated temperature differential scanning calorimetry. *Carbohydrate Polymers,* 58**,** 191-204.

Tang, B., Xu, H., Xu, Z., Xu, C., Xu, Z., Lei, P., Qiu, Y., Liang, J. & Feng, X. 2015. Conversion of agroindustrial residues for high poly(γ-glutamic acid) production by *Bacillus subtilis* NX-2 via solid-state fermentation. *Bioresource Technology,* 181**,** 351-354.

Taylor, A., Vágány, V., Jackson, A. C., Harrison, R. J., Rainoni, A. & Clarkson, J. P. 2016. Identification of pathogenicity-related genes in *Fusarium oxysporum* f. sp. cepae. *Molecular Plant Pathology,* 17**,** 1032-1047.

Thornton, W. M. 1917. XV. The relation of oxygen to the heat of combustion of organic compounds. *Philosophical Magazine Series 6,* 33**,** 196-203.

Tijhuis, L., Van Loosdrecht, M. C. M. & Heijnen, J. J. 1993. A thermodynamically based correlation for maintenance gibbs energy requirements in aerobic and anaerobic chemotrophic growth. *Biotechnology and Bioengineering,* 42**,** 509-519.

Tokiwa, Y., Calabia, B., Ugwu, C. & Aiba, S. 2009. Biodegradability of Plastics. *International Journal of Molecular Sciences,* 10**,** 3722.

Uçkun Kiran, E., Trzcinski, A. P., Ng, W. J. & Liu, Y. 2014. Bioconversion of food waste to energy: A review. *Fuel,* 134**,** 389-399.

USDA 2016. USDA National Nutrient Database for Standard Reference Release 28. September, 2015 ed. USA: USDA.

VanBriesen, J. M. 2001. Thermodynamic yield predictions for biodegradation through oxygenase activation reactions. *Biodegradation,* 12**,** 263-279.

Vargas-García, M. d. C., López, M. J., Suárez-Estrella, F. & Moreno, J. 2012. Compost as a source of microbial isolates for the bioremediation of heavy metals: In vitro selection. *Science of The Total Environment,* 431**,** 62-67.

Verdonck, E., Schaap, K. & Thomas, L. C. 1999. A discussion of the principles and applications of Modulated Temperature DSC (MTDSC). *International Journal of Pharmaceutics,* 192**,** 3-20.

Verma, P., Singh, S. & Verma, R. 2016. Heavy Metal Biosorption by *Fusarium* strains Isolated from Iron Ore Mines Overburden Soil. *International Journal of Environmental Science and Toxicology Research,* 4**,** 61-69.

Vijayaraghavan, K. & Yun, Y.-S. 2008. Bacterial biosorbents and biosorption. *Biotechnology Advances,* 26**,** 266-291.

Voigt, K., Schleier, S. & Brückner, B. 1995. Genetic variability in *Gibberella fujikuroi* and some related species of the genus *Fusarium* based on random amplification of polymorphic DNA (RAPD). *Current Genetics,* 27**,** 528-535.

von Stockar, U. 2010. Biothermodynamics of live cells: a tool for biotechnology and biochemical engineering. *Journal of Non-Equilibrium Thermodynamics,* 35**,** 415-475.

von Stockar, U. & Liu, J. S. 1999. Does microbial life always feed on negative entropy? Thermodynamic analysis of microbial growth. *Biochimica et Biophysica Acta (BBA) - Bioenergetics,* 1412**,** 191-211.

von Stockar, U., Maskow, T., Liu, J., Marison, I. W. & Patiño, R. 2006. Thermodynamics of microbial growth and metabolism: An analysis of the current situation. *Journal of Biotechnology,* 121**,** 517-533.

von Stockar, U. & van der Wielen, L. A. M. 2003. Back to Basics: Thermodynamics in Biochemical Engineering. *In:* von Stockar, U., van der Wielen, L. A. M., Bruggink, A., Cabral, J. M. S., Enfors, S. O., Fernandes, P., Jenne, M., Mauch, K., Prazeres, D. M. F., Reuss, M., Schmalzriedt, S., Stark, D., von Stockar, U., Straathof, A. J. J. & van der Wielen, L. A. M. (eds.) *Process Integration in Biochemical Engineering.* Berlin, Heidelberg: Springer Berlin Heidelberg.1-17

von Stockar, U., Vojinović, V., Maskow, T. & Liu, J. 2008. Can microbial growth yield be estimated using simple thermodynamic analogies to technical processes? *Chemical Engineering and Processing: Process Intensification,* 47**,** 980-990.

Wadsö, L., Li, Y. & Bjurman, J. 2004. Measurements on two mould fungi with a calorespirometric method. *Thermochimica Acta,* 422**,** 63-68.

Wagman, D. D., Evans, W. H., Parker, V. B., Schumm, R. H. & Halow, I. 1982. The NBS tables of chemical thermodynamic properties. Selected values for inorganic and C1 and C2 organic substances in SI units. National Standard Reference Data System.

Wang, L., Wei, W., Tian, X., Shi, K. & Wu, Z. 2016. Improving bioactivities of polyphenol extracts from Psidium guajava L. leaves through co-fermentation of Monascus anka GIM 3.592 and Saccharomyces cerevisiae GIM 2.139. *Industrial Crops and Products,* 94**,** 206-215.

Watanabe, O. & Isoda, S. 2013. Quantitative analysis of microbial biomass yield in aerobic bioreactor. *Journal of Environmental Sciences,* 25**,** S155-S160.

Wlaschin, K. F. & Hu, W.-S. 2006. Fedbatch culture and dynamic nutrient feeding. *Cell Culture Engineering.* Springer.43-74

Wolski, E., Menusi, E., Remonatto, D., Vardanega, R., Arbter, F., Rigo, E., Ninow, J., Mazutti, M. A., Di Luccio, M., de Oliveira, D. & Treichel, H. 2009. Partial characterization of lipases produced by a newly isolated *Penicillium sp*. in solid state and submerged fermentation: A comparative study. *LWT - Food Science and Technology,* 42**,** 1557-1560.

Wruss, J., Waldenberger, G., Huemer, S., Uygun, P., Lanzerstorfer, P., Müller, U., Höglinger, O. & Weghuber, J. 2015. Compositional characteristics of commercial beetroot products and beetroot juice prepared from seven beetroot varieties grown in Upper Austria. *Journal of Food Composition and Analysis,* 42**,** 46-55.

Xiao, J. & VanBriesen, J. M. 2006. Expanded thermodynamic model for microbial true yield prediction. *Biotechnology and bioengineering,* 93**,** 110-121.

Xiao, J. & VanBriesen, J. M. 2008. Expanded thermodynamic true yield prediction model: adjustments and limitations. *Biodegradation,* 19**,** 99-127.

Xie, F., Liu, W.-C., Liu, P., Wang, J., Halley, P. J. & Yu, L. 2010. Starch thermal transitions comparatively studied by DSC and MTDSC. *Starch - Stärke,* 62**,** 350-357.

Yeddou, A. R., Nadjemi, B., Halet, F., Ould-Dris, A. & Capart, R. 2010. Removal of cyanide in aqueous solution by oxidation with hydrogen peroxide in presence of activated carbon prepared from olive stones. *Minerals Engineering,* 23**,** 32-39.

Yu, J., XuZhang & Tan, T. 2008. Ethanol production by solid state fermentation of sweet sorghum using thermotolerant yeast strain. *Fuel Processing Technology,* 89**,** 1056-1059.

Zhu, Z., Zhang, F., Wei, Z., Ran, W. & Shen, Q. 2013. The usage of rice straw as a major substrate for the production of surfactin by *Bacillus amyloliquefaciens* XZ-173 in solid-state fermentation. *Journal of Environmental Management,* 127**,** 96-102.

Appendices

Table A 1: Consensus sequences of the isolate

Fusarium oxysporum EKT01 KU985430
TEF 1-alpha gene
Cds: 1-44, 100-238, 471-533, 635-703

ACCAGTGATCATGTTCTTGATGAAATCACGGTGACCGGGAGCGTCTGAGTGATATGTT
AGTACGAAGAGAAGTAGAATGAAGCATGAGCGACAACATACCAATGACGGTGACATA
GTAGCGAGGAGTCTCGAACTTCCAGAGAGCAATATCGATGGTGATACCACGCTCACG
CTCGGCCTTGAGCTTGTCAAGAACCCAGGCGTACTTGAAGGAACCCTTACCGAGCTA
GCGGCTTCCTATTGTTGAATGGTTAGTGACTGCTTGACACGTGACGACGCACTCATTG
AGGTTGTGAGAATGGTAAGAGGGCAAACGCTCCCGTCGCTCAAGTGGCGGGGTAAG
TGCCCCACCAAAAAAATTACGGTCATATTGCAAAATTTTTGGTCTCGAGCGGGGTAGC
GGGCACGTTTCGAGTCGTAGGGGAAATCGATGGGCAAAGGACGCGCGATTGAAGGG
AAAGTGACTAACCTTCTCGAACTTCTCGATGGTTCGCTTGTCGATACCACCGCACTGG
TAGATCAAGTGACCGGTCTGTGAAACGATGTCAGTATGTTGACTTTGAGAAATACCCC
GCCAGGTCTTGGTCGGGATTGACGATGGCAGATATGCTCATTGTCGAGGAGAGTACT
CACAGTGGTCGACTTGCCAGAGTCGACGTGGCCGATGACGACGACGTTAAGGTGAG
TCTTGTCCTCCTTACC

Fusarium oxysporum EKT02 KU985431
ITS gene

GCGGATCAGCCCGCTCCCGGTAAAACGGGACGGCCCGCCAGAGGACCCCTAAACTC
TGTTTCTATATGTAACTTCTGAGTAAAACCATAAATAAATCAAAACTTTCAACAACGGAT
CTCTTGGTTCTGGCATCGATGAAGAACGCAGCAAAATGCGATAAGTAATGTGAATTGC
AGAATTCAGTGAATCATCGAATCTTTGAACGCACATTGCGCCCGCCAGTATTCTGGCG
GGCATGCCTGTTCGAGCGTCATTTCAACCCTCAAGCACAGCTTGGTGTTGGGACTCG
CGTTAATTCGCGTTCCCCAAATTGATTGGCGGTCACGTCGAGCTTCCATAGCGTAGTA
GTAAAACCCTCGTTACTGGTAATCGTCGCGGCCACGCCGTTAAACCCCAACTTCTGAA
TGTTGACCTCGGATCAGGTAGGAATACCCGCTGAACTTAAGCATATCAATAAGCGGA
GGG

Table A 2: Homogeneity of substitution pattern between TEF 1-α and ITS nucleotide sequences

	A28	A8	ATCC90245	CCF4362	Ecu311	EKT01	EKT02	F72	FOI18	FOI43	FOI48	FSY0812	FSY0829	FUS1	S1	Sa/1/2	SK1649	WM04.490
A28	-	0.000	0.000	0.783	0.783	0.000	0.783	2.286	0.783	0.783	0.783	2.294	2.294	0.000	2.286	0.783	0.783	0.783
A8	1.000	-	0.000	0.579	0.579	0.000	0.579	1.960	0.579	0.579	0.579	1.963	1.963	0.000	1.960	0.579	0.579	0.579
ATCC90245	1.000	1.000	-	0.685	0.685	0.000	0.685	2.188	0.685	0.685	0.685	2.201	2.201	0.000	2.188	0.685	0.685	0.685
CCF4362	0.050	0.094	0.092	-	0.000	0.783	0.000	0.310	0.000	0.000	0.000	0.339	0.339	0.704	0.310	0.000	0.000	0.000
Ecu311	0.054	0.112	0.084	1.000	-	0.783	0.000	0.310	0.000	0.000	0.000	0.339	0.339	0.704	0.301	0.000	0.000	0.000
EKT01	1.000	1.000	1.000	0.054	**0.046**	-	0.783	2.286	0.783	0.783	0.783	2.294	2.294	0.000	2.286	0.783	0.783	0.783
EKT02	0.068	0.084	0.064	1.000	1.000	0.064	-	0.310	0.000	0.000	0.000	0.339	0.339	0.704	0.310	0.000	0.000	0.000
F72	**0.006**	**0.006**	**0.002**	0.212	0.222	**0.002**	0.224	-	0.310	0.310	0.310	0.000	0.000	2.241	0.000	0.310	0.310	0.310
FOI18	0.060	0.132	0.094	1.000	1.000	0.060	1.000	0.214	-	0.000	0.000	0.339	0.339	0.704	0.310	0.000	0.000	0.000
FOI43	0.060	0.111	0.114	1.000	1.000	0.050	1.000	0.198	1.000	-	0.000	0.339	0.339	0.704	0.310	0.000	0.000	0.000
FOI48	0.062	0.098	0.084	1.000	1.000	0.062	1.000	0.218	1.000	1.000	-	0.339	0.339	0.704	0.310	0.000	0.000	0.000
FSY0812	**0.002**	**0.004**	**0.004**	0.178	0.198	**0.002**	0.198	1.000	0.202	0.200	0.192	-	0.000	2.246	0.000	0.339	0.339	0.339
FSY0829	**0.004**	**0.002**	**0.004**	0.192	0.200	**0.002**	0.198	1.000	0.204	0.200	0.204	1.000	-	2.246	0.000	0.339	0.339	0.339
FUS1	1.000	1.000	1.000	0.102	0.076	1.000	0.086	**0.006**	0.070	0.112	0.064	**0.004**	**0.002**	-	2.241	0.704	0.704	0.704
S1	**0.000**	**0.008**	**0.002**	0.204	0.214	**0.000**	0.212	1.000	0.216	0.222	0.200	1.000	1.000	**0.008**	-	0.310	0.310	0.310
Sa/1/2	**0.048**	0.094	0.074	1.000	1.000	0.064	1.000	0.210	1.000	1.000	1.000	0.204	0.198	0.068	0.228	-	0.000	0.000
SK1649	0.070	0.108	0.100	1.000	1.000	0.054	1.000	0.208	1.000	1.000	1.000	0.232	0.188	0.056	0.230	1.000	-	0.000
WM04.490	0.070	0.120	0.070	1.000	1.000	0.076	1.000	0.220	1.000	1.000	1.000	0.182	0.196	0.070	0.190	1.000	1.000	-

Above the diagonal: genetic disparity. Below the diagonal: P-values. Bold: significant P-values i.e. P<0.05

Table A 3: Biochemical reaction details

Test	Result	Test	Result
Ala-Phe-Pro arylamidase	+	D-Amygdalin	-
Adonitol	-	Phosphatidylinositol phospholipase C	-
L-Pyrrolydonyl-arylamidase	-	D-Xylose	-
L-Arabitol	-	Arginine dihydrolase 1	-
D-Cellobiose	-	Cyclodextrin	-
β-galactosidase	-	L-Aspartate arylamidase	-
Hydrogen sulphide production	-	β-Galactopyranosidase	-
β-N-Acetyl-glucosaminidase	-	α-Mannosidase	-
Glutamyl arylamidase pNA	-	Leucine arylamidase	+
D-Glucose	-	β Glucuronidase	-
Fermentation/Glucose	-	L-Pyrrolidonyl-arylamidase	-
β-glucosidase	+	β-Glucuronidase	-
D-Maltose	-	Alanine arylamidase	+
D-Mannitol	-	D-Galactose	-
D-Mannose	-	D-Ribose	-
β-Xylosidase	-	Lactose	-
β-Alanine arylamidase	-	N-Acetyl-D-Glucosamine	-
L-Proline arylamidase	+	Growth in 6.5% NaCl	-
Lipase	-	Methyl-B-D-Glucopyranoside	-
Palatinose	-	Pullulan	-
Tyrosine arylamidase	+	D-Raffinose	-
D-Sorbitol	-	Salicin	-
Saccharose/Sucrose	-	Arginine dihydrolase 2	-
D-Tagatose	-	L-Lysine-arylamidase	+
D-Trehalose	-	Leucine-arylamidase	+
Citrate (Sodium)	-	Phenylalanine arylamidase	+
Malonate	-	L-Proline armylamidase	+
5-keto-D-Gluconate	-	Glycogen	-
L-lactate alkalinisation	-	myo-Inositol	-
Succinate alkalinisation	-	Methyl-A-D-Glucopyranoside acidification	-
β-N-Acetyl galactosaminidase	-	Methyl-D-Xyloside	-
α-galactosidase	-	Maltotriose	-

Phosphatase	-	Glycine arylamidase	+
Arginine GP	+	Acetate assimilation	+
Erythritol assimilation	+	Citrate (Sodium) assimilation	-
Glycerol assimilation	(+)	Glucuronate assimilation	+
Arbutin assimilation	-	L-Proline assimilation	-
Amygdalin assimilation	(-)	2-Keto-D-Gluconate assimilation	-
D-Galactose assimilation	(+)	N-Acetyl-Glucosamine assimilation	-
Gentiobiose assimilation	+	D-Gluconate assimilation	-
D-Glucose assimilation	+	Ornithine decarboxylase	-
Lactose assimilation	-	Lysine decarboxylase	-
Methyl-A-D-Glucopyranoside assimilation	-	L-Histidine assimilation	-
D-Cellobiose assimilation	-	Coumarate	-
Ɣ-Glutamyl-transferase	+	β-Glucoronidase	-
D-Maltose assimilation	+	O/129 resistance (comp. vibrio.)	-
D-Raffinise assimilation	-	Glu-Gly-Arg-Arylamidase	-
PNP-N-acetyl-BD-galactosaminidase 1	-	L-malate assimilation	-
D-Mannose assimilation	-	Ellman	-
D-Melibiose assimilation	(+)	L-Lactate assimilation	-
D-Melezitose assimilation	-	D-Melezitose	-
L-Sorbose assimilation	+	L-Rhanose	-
L-Rhamnose assimilation	+	β-Mannosidase	-
Xylitol assimilation	-	Phosphoryl Chlorine	(+)
D-Sorbitol assimilation	-	Pyruvate	-
Saccharose/Sucrose assimilation	-	Inulin	-
Urease	+	Putrescine assimilation	-
α-Glucosidase	+	Esculin hydrolysis	+
D-Turanose assimilation	+	Tetrazolium red	-
D-Trehalose assimilation	+	Polymixin B resistance	-
Nitrate assimilation	+	Bacitracin resistance	-
L-Arabinose assimilation	+	Novobiocin resistance	-
D-Galacturonate assimilation	(-)	Optochin resistance	-
L-Glutamate assimilation	-	Kanamycin resistance	+
D-Xylose assimilation	-	Oleandomycin resistance	-
DL-Lactate assimilation	-	Polymixin_B resistance	-